TELOMERE LENGTH STUDIES IN HUMAN CANCER CELLS

APPROVED BY SUPERVISORY COMMITTEE

Jerry W. Shay, Ph.D.
Professor of Cell Biology

Woodring E. Wright, M.D., Ph.D.
Professor of Cell Biology

Hongtao Yu, Ph.D.
Professor of Pharmacology

David Chen, Ph.D.
Professor of Radiation Oncology

DEDICATION

Dedicated to my large Kansas family, who made it all possible,
and to my little Texas family, who make it all worthwhile.

TELOMERE LENGTH STUDIES IN HUMAN CANCER CELLS

by

CHRISTEN MARIE BUSEMAN

DISSERTATION

Presented to the Faculty of the Graduate School of Biomedical Sciences

The University of Texas Southwestern Medical Center at Dallas

In Partial Fulfillment of the Requirements

For the Degree of

DOCTOR OF PHILOSOPHY

The University of Texas Southwestern Medical Center at Dallas

Dallas, Texas

April 2011

ACKNOWLEDGEMENTS

My deepest gratitude goes to my mentors, Jerry and Woody, who have given me so many opportunities to learn and grow. I have been inspired by Jerry's enthusiasm for science since the first time we met, and will forever remember to find the best scientific story and to always tell it well. Woody has shown me how creativity and critical thinking work hand in hand to devise new ways to do things that people thought could never be done. Thanks for teaching me how to do great science, and for being there through lots of life as well.

A big thanks to my committee members, Dr. Matt Porteus, Dr. Hongtao Yu and Dr. David Chen for all of your guidance and support over the years. I would also like to acknowledge the Cancer Biology program at UT Southwestern Division of Basic Science – it was an honor to be a member of the first class of students to join the program, and to see it grow from a training track to a program of its own.

After six years in the lab there have been so many people that I have grown to know and love. Nothing could happen in our lab without Kevin Kennon, who seems to effortlessly take care of everyone and everything. Dr. Yong Zhao has been like another mentor whose insight and help with experiments have been instrumental to my growth in the lab. Special acknowledgment to my roommate/labmate Tracy, who has shared what seems like every minute of grad school with me. Wallace, Agnel, Greg, Melissa, Christy, Guido, Shobhana, Shalmica, Chun Hong, Oliver, Hiro, Jun, Lou, Phil, Nuno, Calin, David, Jesper, Gail, Calin, JY, Andres, Jennifer, Erin, Ugur, Aric, Sabrina, Steven, Kim, Suzie, Richard, Crystal, Troy, Jerome, Sebastien, Hua, Peter, Aadil, Brody, Mandy, Martin, SB……and many more: thank you to everyone for being such good friends and colleagues.

Most importantly I must thank my family for all of their love, support and friendship. My parents always told me that I could do anything I wanted, and have always helped me figure out what that was. I can always count on my wonderful sisters to make me smile when I need it. My husband Ethan has been with me every step of the way, through the highs and the lows, and when we are old we will still laugh as we remember surviving school together. Finally, someday I hope that my beautiful Evelyn Rose is inspired by her mommy earning her Ph.D. May you grow up to make big plans and work harder than you ever thought possible so that you can see them come true!

TELOMERE LENGTH STUDIES IN HUMAN CANCER CELLS

Christen M. Buseman, Ph.D.

The University of Texas Southwestern Medical Center at Dallas, 2011

Supervising Professor: Jerry W. Shay, Ph.D.

Telomeres consist of repetitive DNA sequences and their associated binding proteins, and serve to protect linear chromosome ends from being recognized as double stranded breaks in need of repair. The telomeres of most normal diploid cells shorten with every cell division until they reach a critically short length, at which time the cells undergo senescence or apoptosis. Cancer cells which have the ability to divide indefinitely must prevent their telomeres from becoming critically short, and the majority of cancer cells achieve this by upregulating telomerase. Maintaining

telomere length involves regulating the dynamic between telomere shortening and telomere elongation. However, there are still many aspects of this dynamic regulatory process that are unknown. Many methods of telomere length assessment have been developed that utilize a variety of molecular techniques, but a major shortcoming of these methods is that they lack the ability to detect single short telomeres that are thought to trigger replicative senescence. Thus, the objective of this work was to develop an assay, named Universal STELA, which can generate an accurate distribution of telomere lengths on all chromosomes and allow for the study of the shortest telomeres in experimental settings.

Universal STELA was first used to determine if cancer stem cells are susceptible to telomerase inhibition therapy because they have a larger fraction of shorter telomeres than non cancer stem cells. Cancer stem cells are thought to contribute to cancer metastasis and recurrence, and therapies like telomerase inhibition that target cancer stem cells may lead to more durable treatment outcomes. Universal STELA was next used to investigate regulation of telomerase action. C- and G-STELA were used to determine that telomerase activity is coupled to telomere replication, while C-strand fill-in is delayed until S/G2. Universal STELA was used to compare the rate of elongation of short, average and long telomeres when telomeres are shorter than their maintenance length.

TABLE OF CONTENTS

PRIOR PUBLICATIONS

Buseman, C.M., Wright, W.E., Shay, J.W. (2011) Is telomerase a viable target in cancer? Mutation Research. *In press*.

Joseph, I., Tressler, R., Bassett, E., Harley, C., **Buseman, C.M**., Pattamatta, P., Wright, W.E., Shay, J.W., and Go, N.F. (2010). The telomerase inhibitor imetelstat depletes cancer stem cells in breast and pancreatic cancer cell lines. Cancer Res 70, 9494-9504.

Zhao, Y., Sfeir, A.J., Zou, Y., **Buseman, C.M**., Chow, T.T., Shay, J.W., and Wright, W.E. (2009). Telomere extension occurs at most chromosome ends and is uncoupled from fill-in in human cancer cells. Cell 138, 463-475.

Buseman, C.M., Tamura, P., Sparks, A.A., Baughman, E.J., Maatta, S., Zhao, J., Roth, M.R., Esch, S.W., Shah, J., Williams, T.D., et al. (2006). Wounding stimulates the accumulation of glycerolipids containing oxophytodienoic acid and dinor-oxophytodienoic acid in Arabidopsis leaves. Plant Physiol 142, 28-39.

Nandi, A., Krothapalli, K., **Buseman, C.M**., Li, M., Welti, R., Enyedi, A., and Shah, J. (2003). Arabidopsis sfd mutants affect plastidic lipid composition and suppress dwarfing, cell death, and the enhanced disease resistance phenotypes resulting from the deficiency of a fatty acid desaturase. Plant Cell 15, 2383-2398.

LIST OF FIGURES

LIST OF TABLES

LIST OF ABBREVIATIONS

ALT	Alternative Lengthening of Telomeres
CSC	Cancer Stem Cells
FISH	Flourescent in situ hybridization
HPA	Hybridization Protection Assay
M1/M2	Mortality Stage ½
MRN	Mre11/Rad50/Nbs1 complex
PRINS	Primed *In Situ* Hybridization
PCR	Polymerase Chain Reaction
Q-PCR	**Q**uantitative Polymerase Chain Reaction
STELA	Single Telomere Length Analysis
TIF	Telomere Induced Foci
T-SCE	Telomere Sister Chromatin Exchange
TRAP	Telomere Repeat Amplification Protocol
TRF	Terminal Restriction Fragment

CHAPTER ONE

GENERAL INTRODUCTION AND LITERATURE REVIEW

I. THE BEGINNING OF THE ENDS:

A BRIEF HISTORY OF TELOMERE BIOLOGY

As all lines have a beginning and an end, all linear chromosomes must be flanked by two free ends. These ends, called "telomeres" or "end parts," have proven to be intricately involved in such pivotal processes as the protection of genetic material, the regulation of cellular aging, and the protection against abnormal cellular growth. As these mechanisms have become established, the consequences of telomere dysfunction have revealed a variety of disease states ranging from pulmonary fibrosis and dyskeratosis congenita, to more than 90% of human cancers. An integral stage in the understanding of the regulation of telomeres came with the recognition of a reverse transcriptase holoenzyme named "telomerase" due to its catalytic extension of telomere ends. The study of the role of telomerase in cancer and stem cells has propelled the field into the multidirectional study of the impact of telomeres in human development, aging, and disease, as telomerase is recognized simultaneously for its potential to cure degenerative disease yet perpetuate the growth and spread of cancer.

While the frontier of telomere research is impacting medically related fields, the story of the ends of our chromosomes can be traced all the way to the

beginning, to our desire to understand the nature of the heritable unit, the gene (Blackburn, 2006). Early cytogeneticists could visualize chromosomes using microscopy, and Thomas Hunt Morgan hypothesized that genes were arranged on chromosomes like "beads on a string" (Morgan, 1911), in a particular order with a beginning and an end. One of Morgan's students, Hermann Muller, would recognize that the "free ends" of linear chromosomes behaved differently than X-ray induced broken ends, and he was the first to call the ends of our chromosomes "telomeres" from the greek words for "end" (*telos*) and "part" (*meros*) (Muller, 1938). Around the same time, Barbara McClintock was learning about the "knobs" of heterochromatin that she could visualize at the ends of individual chromosomes from maize cells. She called these distinct knobs the "natural ends" of the chromosomes (Creighton and McClintock, 1931), and eventually shared Muller's conclusion that these natural ends or telomeres behaved much differently than broken ends induced by X-ray irradiation (McClintock, 1941). The recognition that induced ends were distinctly different from natural ends made notable the observation that, in certain circumstances, an induced end could be altered such that it became a stable free end much like the natural telomere ends (McClintock, 1939). This observation implied that there was some permanent molecular change that occurred at the healed, induced ends, and is consistent with current data regarding the actions of the telomerase reverse transcriptase during chromosome healing.

These early cytogenetic studies paved the way to identifying telomeric DNA as heterochromatin with a unique structure and function in cellular biology, but the molecular characterization of telomeres took several decades to establish. With the elucidation of the structure of DNA as a double stranded helix (Watson and Crick, 1953), it became clear that eukaryotic chromosomes consisted of a single, linear DNA molecule. The concept of the double stranded helix of complementary bases allowed us to understand how genetic material could be copied and transmitted across generations of organisms and across cell division lineages, and the biochemistry of DNA replication was established in the coming years (Lark, 1969; Richardson, 1969). The enzymatic mechanism of DNA replication presented a unique problem when considering the replication of linear chromosomes, which requires a polynucleotide primer with a free 3'-hydroxyl group for initiation of synthesis of the daughter strand. Theoretically, this mechanism precludes the complete replication of linear DNA at the ends, and this proposed "end replication problem" was put forth in the 1970's (Olovnikov, 1973; Watson, 1972) as a challenge to understand the mechanism of DNA replication at the telomeres. With incomplete replication of linear DNA, it was theorized that subsequent cell divisions would lead to an eventual loss of genetic information at the chromosome ends (Watson, 1972). Solving the end replication problem became a central motive in the field that eventually connected telomere length

dynamics to the regulation of cellular senescence, aging, and eventually cancer biology.

As researchers were putting forth models to address the challenges presented by the end replication problem, it became necessary to better understand the molecular aspects of telomeres themselves. The first telomere sequences to be elucidated were from extrachromosomal ribosomal DNA from the ciliated protozoa, *Tetrahymena thermophila* (Blackburn and Gall, 1978). These *Tetrahymena* telomeres consisted of tandem repeats of a G/C-rich hexanucleotide sequence with lengths varying from 20 to 70 repeats (Blackburn and Gall, 1978). In the following years, the sequence and structure of telomeres from a variety of other eukaryotic organisms were identified, all with similar characteristics to that found in *Tetrahymena* (Blackburn, 1990; Shampay et al., 1984). The sequence of human telomeres was established in 1988 (Moyzis et al., 1988) as consisting of tandem 5' TTAGGG 3' repeats, and this same sequence was found to be conserved among more than 90 eukaryotic species (Meyne et al., 1989). Among all telomeres studied, the following characteristics remained conserved: the sequence consisted of tandem repeats of short sequences; the repeat sequences consisted of a G-rich and opposing C-rich strands; the G-rich strand was generally oriented in the 5' to 3' direction; every species had a characteristic telomere sequence; the number of tandem repeats were variable (Blackburn, 2006).

The conserved structure of telomere sequence suggested a conserved function for telomeres across species. The fact that telomeres contained repetitive tracts of specific DNA sequence, coupled with the fact that telomere DNA seemed to be protected from nuclease degradation when compared to non-telomeric DNA (Blackburn and Chiou, 1981), suggested that a unique set of non-histone proteins might be involved in packaging or associating with telomeric DNA. The first telomere binding protein was discovered as a two-subunit protein that recognizes and tightly binds the 3' G-rich overhang of telomeres in the ciliate, *Oxytricha nova* (Gottschling and Zakian, 1986). This protein, TEBP, has since been found to have homologues in the budding yeast (Cdc13p, (Lin and Zakian, 1996; Nugent et al., 1996), and the TEBP homolog, POT1, can be found in species as diverse as fission yeast and humans (Baumann and Cech, 2001). The first protein found to bind the duplex portion of telomere DNA was Rap1p in *S. cerevisiae* (Buchman et al., 1988). Rap1p was originally identified as a transcriptional regulator, and it's *in vivo* association with telomeres was first described in 1990, providing evidence that proteins involved in other cellular functions played an integral role in telomere structure and function (Conrad et al., 1990). Interestingly, Rap1p binding at the telomeres was found to be a negative regulator of telomere length (Conrad et al., 1990; Lustig et al., 1990), and the number of Rap1p molecules bound to the telomere duplex DNA appeared to act as a counting mechanism that regulates telomere length (Krauskopf and

Blackburn, 1996; Marcand et al., 1997). Mammalian double stranded telomeric DNA is bound by TRF1 (Chong et al., 1995), which like Rap1p, is a negative regulator of telomere length (van Steensel and de Lange, 1997); mammalian double stranded DNA is also directly bound by a related protein, TRF2 (Bilaud et al., 1997; Broccoli et al., 1997b), which is involved in telomere length regulation (Smogorzewska et al., 2000) as well as telomere secondary structure formation and end protection (reviewed in (de Lange, 2004). Today, POT1, TRF1 and TRF2 are known to work in concert with three additional proteins to form a six-protein complex called shelterin that is essential for telomeres to function to protect the ends of mammalian chromosomes (de Lange, 2002, 2005, 2009). The structure and function of this telomeric nucleoprotein complex will be discussed in further detail.

Of all the proteins that have been found to interact with telomeres, none has inspired such fascination as that of the holoenzyme complex known as telomerase. Several lines of evidence suggested that there must be a mechanism for generating *de novo* telomere sequence, the first of which was Barbara McClintock's observation that X-ray irradiated broken chromosomes could be "healed" and the once broken ends indefinitely behaved as natural chromosome ends (McClintock, 1939). Barbara McClintock also observed that some maize mutants from her cytogenetic studies lacked the ability to heal their broken chromosomes, suggesting that there was a gene or genes that conferred the

healing property (personal communication between B.M. and E.H.B. discussed in (Blackburn, 2006b). After the discovery of DNA sequence of *Tetrahymena* telomeres, it was discovered that telomere repeat DNA was added to telomere ends in actively dividing yeast cultures (Shampay et al., 1984; Szostak and Blackburn, 1982). In 1985, Carol Greider and Elizabeth Blackburn demonstrated that there was enzymatic activity present in the extract of *Tetrahymena* cells that could generate *de novo* telomere repeats on telomere ends (Greider and Blackburn, 1985). They called this enzymatic activity "terminal transferase," which would later become known as telomerase. The observation that RNase inactivated the terminal transferase activity prompted the characterization of the partially purified active complex, and a low-abundance RNA species copurified with the telomerase activity (Greider and Blackburn, 1987). This was the first evidence that telomerase existed as a ribonucleoprotein complex, and in 1989 the *Tetrahymena* RNA template sequence was identified and confirmed (Greider and Blackburn, 1989; Yu et al., 1990).

Telomerase activity was subsequently found in a variety of species, all of which generated their species' characteristic telomere repeat sequence in an RNA-dependent manner consistent with the results from *Tetrahymena* (Morin, 1989; Shippen-Lentz and Blackburn, 1989; Zahler and Prescott, 1988). The discovery of telomerase activity in human cancer cell extracts proved that the reverse transcriptase activity was widespread, and suggested a mechanism by which

cancer cells could grow indefinitely (Morin, 1989). The first protein component of telomerase to be identified was a yeast mutant with an "ever-shortening telomere" (*est*) phenotype (Lundblad and Szostak, 1989). The mutants exhibited telomere loss over the course of many population doublings, with eventual senescence and cell death. While the presence and nature of the telomerase reverse transcriptase and RNA template subunits were established in the mid- to late 1980's, it would be another decade before they were cloned. The human RNA template was cloned in 1995 (Feng et al., 1995) and was named hTR, (human Telomerase RNA); the human catalytic subunit of telomerase was cloned in 1997 and named hTERT (human telomerase reverse transcriptase) (Harrington et al., 1997a; Nakamura et al., 1997). hTR is ubiquitously expressed in all human cells, and telomerase activity is limited by the expression of hTERT, which is only found in cells with detectable telomerase activity (Ducrest et al., 2002; Takakura et al., 1998).

The interplay between telomerase extension of telomere ends and the end replication problem suggested that telomere length is a tightly controlled regulatory process in cell biology. The first evidence directly linking telomere length to cellular senescence in humans showed that the telomeres of normal human fibroblasts shortened with progressive cell passages until the cells senesced *in vitro* (Harley et al., 1990). Previous data showing that telomeres of the X/Y chromosomes from adult somatic cells were shorter than their

counterparts from germ cells (Cooke and Smith, 1986) suggested that telomerase was active in human germ cells but not in somatic cells such as fibroblasts. Taken together, there was mounting evidence to suggest that shortening telomeres could trigger cells to stop dividing, explaining the long-observed limited replication potential of cells in culture (Hayflick and Moorhead, 1961). A theory relating telomere shortening to aging and cancer was proposed by Woody Wright and Jerry Shay (Figure 1.1) (Wright et al., 1989; Wright and Shay, 1992) in which a two-stage mechanism was responsible for determining a cell population's senescence or immortalization. The two-stage theory suggests that the telomeres of normal diploid cells shorten with every cell division until they reach a critically short length, causing the cells to arrest at cell cycle checkpoints and enter what has been termed Mortality Stage 1 (Wright and Shay, 1992). At this stage, cells cease to divide and undergo replicative senescence. However, cells that have acquired inactivation of common cell cycle checkpoint proteins in the p53 and Rb pathways are able to continue dividing and lose telomeric sequences with each division (Shay et al., 1991). These cells ultimately reach a crisis stage, called Mortality Stage 2, which is marked by genomic instability due to chromosome fusions leading to increased aneuploidy and apoptosis. However, cells which are able to maintain their telomeres escape this crisis stage and continue to proliferate (Counter et al., 1992; Kim et al., 1994; Shay et al., 1993).

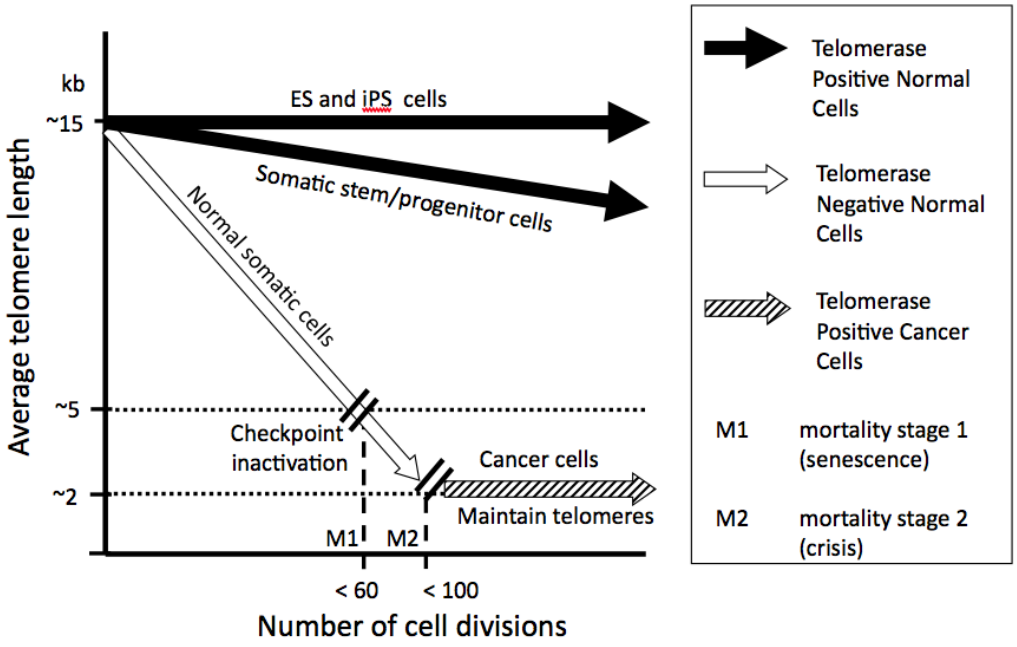

Figure 1.1 Telomere attrition induces senescence (M1) or crisis (M2) in the absence of telomere maintenance. All telomeres of normal diploid somatic cells shorten with each cell division, with telomere attrition rates being much slower in proliferative adult stem-like progenitor cells. When a few telomeres reach a critically short length, DNA damage sensing pathways initiate a growth arrest called replicative senescence, or Mortality Stage 1 (M1). Cells that have acquired mutations which inactivate common DNA damage checkpoints in the p53 and p16/Rb pathways are able to bypass M1 and continue to divide (also called extended lifespan phase). Cells which escape M1 continue to experience telomere shortening until many telomeres become critically short, causing increased chromosomal instability due to telomere fusions and breakage-fusion-bridge cycles, ultimately leading to a state of crisis. The majority of cells that enter crisis, or Mortality Stage 2 (M2), undergo apoptotic cell death. Only rare cells which are able to stabilize telomere length are able to divide past M2/crisis. Activation of telomerase is the most common telomere maintenance mechanism acquired by cells which escape crisis, and more than 85% of human cancers are telomerase positive.

In support of this theory, a pivotal publication showed that approximately 90% of human cancers upregulate telomerase as the mechanism of telomerase maintenance (Kim et al., 1994). The study utilized a novel, PCR-based assay for the detection of telomerase activity in a very small sample of human cells (Telomere Repeat Amplification Protocol, or TRAP). Applying the assay to a large panel of primary normal versus tumor samples, as well as mortal versus immortalized cell lines revealed that telomerase activity is restricted in normal human somatic cells but is activated in cancer and immortalized cells to allow for indefinite replication. The approximately 10% of cancer cells that do not upregulate telomerase have been found to maintain their telomeres through a telomere recombination pathway called ALT (alternative lengthening of telomeres) (Bryan et al., 1997); the ability of cancer cells to replicate indefinitely through telomerase activation or ALT pathway activation has been called one of the hallmarks of cancer (Hanahan and Weinberg, 2000), and emphasizes the importance of telomere length dynamics in the regulation of cell division.

If telomere shortening induced replicative senescence and telomerase upregulation in cancer cells allowed cells to divide indefinitely, it was hypothesized that expression of telomerase in otherwise telomerase-negative cells would allow those cells to divide indefinitely (Levy et al., 1992). Exogenous expression of *in vitro* synthesized hTERT was able to reconstitute normal telomerase activity in normal human diploid cells, suggesting that hTERT is the

limiting component required for telomerase catalytic activity (Weinrich et al., 1997). The introduction of overexpressed hTERT in telomerase negative human cell lines showed telomere elongation and extended cellular lifespans compared to the telomerase negative controls, showing for the first time that cells could be immortalized by expressing telomerase (Bodnar et al., 1998). This study experimentally confirmed the causal relationship between telomere shortening and cellular senescence.

With telomeres firmly established as regulators of cellular senescence and the action of telomerase documented in cancer cells, germ cells and other stem-like cells, new efforts at understanding the medical implications of telomerase activity and thoughts of telomerase manipulation for medical purposes began to gain prominence in the field. Dysfunctional telomere regulation has been implicated in a variety of diseases including dyskeratosis congenita, idiopathic pulmonary fibrosis and aplastic anemia (reviewed in (Calado and Young, 2009). Dyskertaosis congenita is an inherited form of ectodermal dysplasia and is characterized by abnormal skin pigmentation, nail dystrophy and leukoplakia of the tongue (Calado and Young, 2009). The disease was causally linked to telomeres when mutations in dyskerin, a nucleolar protein that associates with the hTR RNA component of telomerase, were identified (Dez et al., 2001; Pogacic et al., 2000). When patients with dyskeratosis congenita were found to have very short telomeres (Vulliamy et al., 2001), additional mutations in telomerase

components or telomere associating proteins were identified as being associated with the disease (reviewed in (Calado and Young, 2009). Dyskeratosis congenita was the first human disease formally linked to telomere maintenance dysfunction. Mutations in telomerase components hTR and hTERT have been found in about 10% of aplastic anemia patients, who also exhibit short telomeres (Yamaguchi et al., 2003; Yamaguchi et al., 2005). Most recently, mutations in telomerase components have been identified in about 15% of idiopathic pulmonary fibrosis patients (Armanios et al., 2007; Mushiroda et al., 2008; Tsakiri et al., 2007), and these patients also exhibit shortened telomeres. Telomere maintenance appears to impact a spectrum of physiological processes that manifest a syndrome of telomere dysfunction disease states.

While much research is directed toward understanding telomere dysfunction in diseases like dyskeratosis congenita and pulmonary fibrosis, telomere regulation and telomerase activity has been most heavily implicated in the field of cancer research. The ideal cancer therapeutic is one that targets cancer cells but has no adverse effects on normal cells. As soon as telomerase was found to be nearly universally expressed in cancer cells, it was proposed that telomerase inhibition therapy might be a valuable tool in fighting cancer (Kim et al., 1994). Telomerase is not expressed in most normal somatic cells, although it is expressed at low levels in the testes, peripheral blood lymphocytes and some adult pluripotent stem cells (Wright et al., 1996). As cancer cells generally have

quite short telomeres and other telomerase-positive cells have much longer telomeres (Wright et al., 1996), targeting telomerase as an anti-cancer therapy theoretically disrupts the cancer cell's essential ability to divide infinitely (Hanahan and Weinberg, 2000), eventually forcing replicative senescence while preserving telomere maintenance of normal cells. Various telomerase inhibition strategies have been developed, including direct telomerase enzymatic inhibitors, small-molecule and oligonucleotide inhibitors, and immunotherapy using primed dendritic cells or direct vaccines against hTERT (reviewed in (Shay and Keith, 2008; Shay and Wright, 2002, 2006); some of these approaches have been advanced to clinical trials.

While the impact of telomerase inhibition as a cancer therapy is still being evaluated, the great advances in the field of telomere biology have certainly brought the connections between cell biology, aging and cancer to a medically relevant and exciting frontier. The 2009 Nobel Prize for Medicine was awarded to Elizabeth Blackburn, Carol Greider and Jack Szostak for their early efforts in elucidating the nature of telomeric DNA and identifying telomerase, the enzyme that is intimately involved in telomere maintenance (Nobelprize.org; Varela and Blasco, 2010). Continued research in the field will include a focus on the molecular mechanisms by which telomeres serve to protect the ends of our chromosomes, the impact of telomere dysfunction in human disease syndromes,

and the regulation and therapeutic potential of telomerase activity in cancer, providing exciting avenues for continued basic and translational research.

II. STRUCTURE AND FUNCTION OF HUMAN TELOMERES

Mammalian telomeres are dynamic and complex structures which consist of repetitive tracts of double-and single-stranded DNA which are bound by telomere-specific proteins and are maintained by the telomerase ribonucleoprotein (Figure 1.2) (reviewed in (de Lange, 2005). The primary function of mammalian telomeres is to cap the ends of linear chromosomes, protecting the genetic material that lays proximal to their end from degradation due to the end replication problem (reviewed in (Levy et al., 1992) as well as from being recognized as a double-strand break in need of repair (reviewed in (de Lange, 2009). The protective properties of telomeres were first described in the earliest cytogenetic studies conducted by Hermann Muller and Barbara McClintock, who observed that the natural ends of chromosomes behaved quite differently than broken chromosome ends that were induced by X-ray irradiation (McClintock, 1941; Muller, 1938). While broken ends were observed to fuse, natural ends remained free and did not fuse (McClintock, 1941). Today, DNA damage-sensing and repair pathways responsible for identifying and repairing broken ends are well-established, and the mechanisms by which telomeres elude these repair pathways are being actively investigated. While much is yet to be learned

regarding the intricate structure of telomeres and their many associating factors, it remains clear that their structure is uniquely tuned to accomplish their protective function.

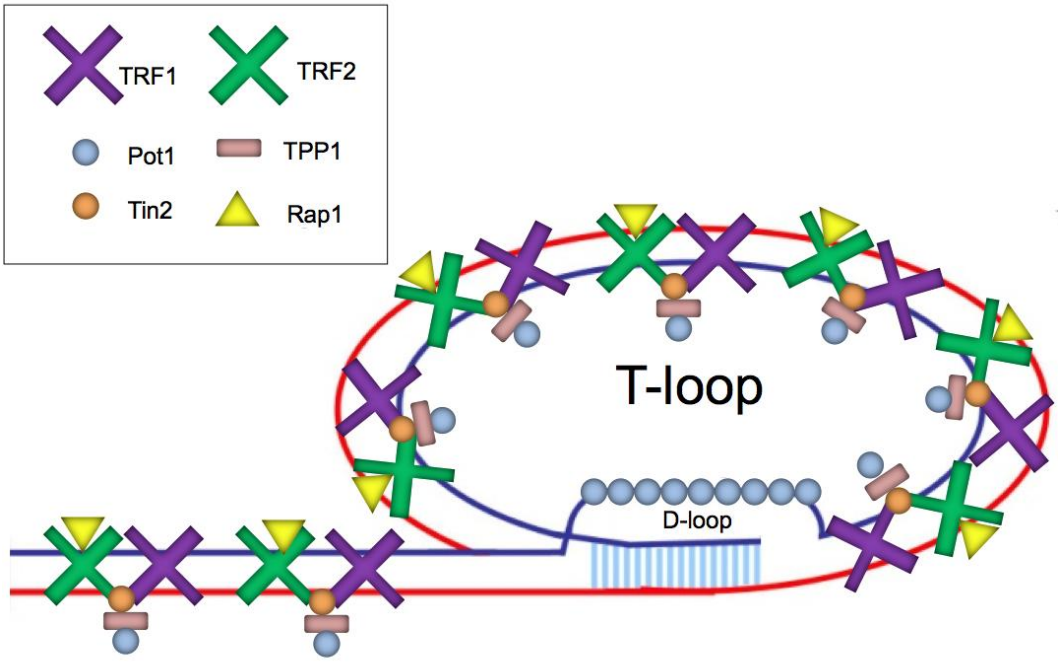

Figure 1.2 The telomere nucleoprotein complex structure. Telomeric DNA ends in a 3' G-rich single stranded overhang, which is obscured by strand invasion of the preceding double stranded DNA, causing a localized displacement loop ("D-loop") at the point of strand invasion, and generating a chromosome cap called a "t-loop." Many proteins interact with the telomere, but a complex of six proteins, known as "shelterin," play an integral role in maintaining telomere structure and function. The six shelterin proteins and their interactions with telomere DNA are depicted above.

Structure of Telomeric DNA

The ends of eukaryotic chromosomes were first observed to contain tandem repeats of short, G-rich sequences in *Tetrahymena* (Blackburn and Gall, 1978), and these tandem repeat sequence were subsequently found to confer end protection properties (Szostak and Blackburn, 1982). All vertebrates have telomeres that are composed of hexameric 5' TTAGGG 3' double stranded tandem repeats (Meyne et al., 1989; Moyzis et al., 1988). The length of the telomere repeat array varies from species to species, with rodents having the longest telomeres of up to 150 kb (Kipling and Cooke, 1990; Makarov et al., 1993; Starling et al., 1990) and humans having telomeres that range in size from 2-30 kb (Cooke and Smith, 1986; de Lange et al., 1990). Telomere length in humans is an inherited trait (Njajou et al., 2007), but the mechanism of inheritance is still unknown (Gilson and Londono-Vallejo, 2007).

Mammalian telomeric DNA ends in a 3' G-rich single-stranded overhang (Makarov et al., 1997) that has been heavily implicated in proper telomere structure and function. Telomerase is not required for overhang generation, suggesting that there must be another mechanism which regulates overhang generation and processing (Hemann and Greider, 1999; Huffman et al., 2000). Overhang generation has been well documented in the model organism *S. cerevisiae*, in which at least two steps are required to produce an overhang of 12-14 nucleotides in a cell cycle dependent, telomerase independent manner

(Larrivee et al., 2004; Wellinger et al., 1993a, b). Determining the length and nature of mammalian telomeres has been challenging due to the technical limitations inherent to the different strategies that have been developed, making it difficult to assess the events leading to overhang production. Electron microscopy of purified telomeres was used to detect long overhangs of approximately 75-300 nucleotides on one telomere end (Huffman et al., 2000; Wright et al., 1997), however this assay requires very large amounts of starting material (making it impractical for routine use); the inability to detect overhangs shorter than 75 nucleotides using electron microscopy could not rule out the presence of shorter overhangs (Wright et al., 1997). Two independent assays based on hybridization to the G-rich overhang were able to detect overhangs as short as 12 nucleotides (non-denaturing hybridization assay, (McElligott and Wellinger, 1997) and 20 nucleotides (hybridization protection assay, (Tahara et al., 2005), however these assays can only measure the relative signal intensity of overhangs with respect to total DNA, and may not be very accurate. Several molecular assays have been developed and used to obtain overhang length measurements that range from 45-300 nucleotides, but each assay has its own inherent challenges, collectively they have had poor resolution to detect short overhangs, and the data has often been contradictory (Chai et al., 2006a; Chai et al., 2005; Cimino-Reale et al., 2001; Makarov et al., 1997).

The most recent and promising overhang assay involves the digestion of all double stranded DNA with a novel protein, duplex-specific nuclease (DSN), which leaves only single stranded telomere overhangs and a characteristic residual 6 double-stranded base pairs intact; the overhangs are then analyzed by gel separation and probed with a labeled C-rich probe to determine the distribution of overhang lengths (Zhao et al., 2008). The DSN method is simple to perform, has been proven to corroborate existing overhang length data, and can accurately detect overhangs as short as 12 nucleotides. Importantly, the DSN method has been used to show that the overhangs of leading and lagging daughter strands have different length distributions, with leading strand overhangs being 2-3 fold shorter than lagging strand overhangs (Zhao et al., 2008). This data suggests a differential mechanism for processing of overhangs on the two strands, which is suggestive of a novel regulatory process that ensures proper telomere function. The determination that the terminal sequence of the C-rich strand is predominately 3'-ATC-5' while the terminal sequence of the G-rich strand has only a modest preference for its terminal sequence suggests yet another regulatory step in the overhang generation pathway (Sfeir et al., 2005). While both Mre11 (Chai et al., 2006b) and Pot1 (Hockemeyer et al., 2005) have been implicated in regulating mammalian overhang length and terminal sequence specificity, no mechanism has been proposed to explain the regulation of overhang end processing. The development of the simple and sensitive DSN overhang assay

should enable progress in elucidating overhang end processing mechanisms in mammalian telomeres.

While mammalian telomere overhang generation and regulation events are still poorly understood, the function of overhangs in the overall telomere end protection role has been widely studied. The G-rich 3' overhang is thought to be crucial to telomere end protection because of its ability to be hidden from DNA damage machinery in a structure called the t-loop (reviewed in (Greider, 1999). T-loops were first identified in human telomeres using electron microscopy to examine telomeric DNA that was psoralen crosslinked as a first step in the DNA extraction process, to retain any secondary structure that may exist *in vivo* (Griffith et al., 1999). The t-loop appears as a lariat-like structure at the end of telomeres in electron micrographs, and is presumed to be formed by strand invasion of the 3' overhang into the preceding double stranded telomeric DNA, and stabilized by bound telomeric proteins (reviewed in (Greider, 1999). Since t-loops were first identified in human telomeres, they have been observed at the ends of telomeres in a number of other organisms, including *Oxytricha nova* (Murti and Prescott, 1999), *Trypanosome brucei* (Munoz-Jordan et al., 2001), *Pisum sativa* (Cesare et al., 2003), *Candida parapsilosis* (Tomaska et al., 2002), *Caenorhabditis elegans* (Raices et al., 2008) and in mouse and chicken (Nikitina and Woodcock, 2004). The size of the loop appears to be related to the length of the telomeric DNA (Griffith et al., 1999), with observed sizes ranging from 1

kilobase in *Trypanosome* (Munoz-Jordan et al., 2001) and up to 50 kilobases in *Pisum sativa* (Cesare et al., 2003).

The t-loop structure is presumed to be an essential component of the end protection properties of telomeres, providing a mechanism for physically obscuring the double strand break at the telomere termini by sequestering the 3' overhang. In vitro modeling experiments have proven that an overhang of at least 6 nucleotides is required for proper t-loop formation (Griffith et al., 1999; Stansel et al., 2001) and that the telomere binding protein, TRF2, stabilizes the structure by binding at the loop junction (Stansel et al., 2001). Structural studies have recently shown that TRF2 might induce t-loop formation by facilitating strand invasion of the overhang (Amiard et al., 2007) and stabilizing the resulting Holliday junction from being resolved by helicase activity (Nora et al., 2010; Poulet et al., 2009). G-quadruplexes may also be involved in stabilizing the t-loop structure, as recent data suggests that G-quadruplexes form preferentially at the 3' termini of telomeres (Tang et al., 2008), and that a dimeric G-quadruplex like that which would theoretically be found in telomeres was able to form a t-loop-like structure in vitro (Xu et al., 2007). However, little is known about the timing or mechanism of t-loop formation *in vivo*. This is due largely to a lack of a facile, sensitive assay that is capable of detecting t-loop presence.

Currently, the only method available to assess the presence and structure of t-loops is electron microscopy (Griffith et al., 1999), which requires extensive

sample preparation and a large amount of starting material. A straightforward, cell biology based assay for t-loops would allow for the routine analysis of t-loop formation and the investigation of t-loop involvement in properties of telomere biology that are pertinent to improving telomerase inhibition therapy in breast cancer. For example, t-loops are obligated to unfold during telomere replication in S phase, but it is not currently known when t-loop repackaging occurs. Because telomeric ends are accessible and uncapped at the S/G2 interface (Verdun et al., 2005), it stands to reason that they are either immediately repackaged into t-loops and then unfolded at S/G2, or that they remain unpackaged throughout all of S phase, in which case a system must exist to hide the telomeric ends from DNA damage sensing machinery during S phase and/or suppress the DNA repair response occurs during S phase. Progress in understanding the regulation and formation of t-loops *in vivo* will improve with the development of a t-loop assay that can be performed routinely; until that time, much of what we know and learn about t-loops will continue to come from *in vitro* modeling and study of telomere binding proteins that are likely to be involved in t-loop packaging.

Structure of the Telomeric Protein Complex

A six-protein complex with remarkable specificity for telomeric DNA has been identified at mammalian telomeres, with orthologs in other eukaryotic species (de Lange, 2005). TRF1 and TRF2 bind to double stranded telomeric DNA, while Pot1 binds to single stranded, G-rich DNA of the 3’ overhang and D-

loop. TIN2 is the central protein of the complex: it binds to both TRF1 and TRF2 causing an increase in their affinity for telomeric DNA, and it also interacts with the fifth protein in the complex, TPP1. TPP1 binds to both TIN2 and Pot1, anchoring the six proteins together and making possible associations between the double- and single-stranded portions of the telomere t-loop superstructure. The final protein in the complex, Rap1, is known to interact with TRF2 and may have other yet-identified protein interactions. This complex has collectively come to be known as "shelterin," and has been implicated in nearly all aspects of telomere biology, from t-loop formation to telomerase recruitment to protection against DNA damage response (reviewed in (de Lange, 2005; Palm and de Lange, 2008; Smogorzewska and de Lange, 2004).

The first shelterin protein to be identified was found in Hela nuclear extracts as specifically binding TTAGGG DNA sequences, and was thus named "TTAGGG Repeat-binding Factor 1," or TRF1 (Zhong et al., 1992). The protein consists of an amino-terminal acidic domain, a dimerization domain, and a carboxyl-terminal Myb DNA binding domain that is specific for duplex telomeric sequence (Bianchi et al., 1997; Chong et al., 1995). The dimerization domain is also known as the TRF homology (TRFH) domain and can be found in mammalian TRF1 and TRF2, TRF in trypanosomes, and the *S. pobme* ortholog, Taz1 (Bianchi et al., 1997; Broccoli et al., 1997a; Broccoli et al., 1997b; Li et al., 2005; Li et al., 2000). The TRFH domain not only serves as a dimerization

domain, but it also has been found to be critical for TRF1 to promote telomere structural stability (Okamoto and Shinkai, 2009) and for recruitment of the shelterin component, TIN2 (Chen et al., 2008). TRF1 forms a homodimer via the TRFH dimerization domain (Griffith et al., 1998), and binds specifically to 5'-YTAGGGTTR-3' sequences (Bianchi et al., 1999); the ability of the TRF1 homodimer to bind two sequences simultaneously increases its DNA binding affinity approximately 10-fold, and can induce bending of telomeric DNA (Bianchi et al., 1997) that may play a role in t-loop formation and stabilization. TRF1 localizes specifically to the telomere at all stages of the cell cycle (Broccoli et al., 1997a; Chong et al., 1995; Scherthan et al., 2000), and levels of TRF1 at the telomere appear to be regulated through competition between TIN2 and a ubiquitin ligase (Zeng et al., 2010). TRF1 is essential in mice, in which knockout models are embryonic lethal, and deletion of p53 partially suppress the lethal phenotype suggesting that the TRF1 is essential for telomere end protection and viability (Iwano et al., 2004; Karlseder et al., 2003). TRF1 is known to be a negative regulator of telomere length in telomerase positive cells (Smogorzewska et al., 2000; van Steensel and de Lange, 1997), and may be essential for efficient replication of telomeric DNA (Sfeir et al., 2009).

The second shelterin component was found based on the similarity of its DNA binding Myb domain to that of TRF1 (Bilaud et al., 1997; Broccoli et al., 1997b). The protein consists of an amino-terminal basic domain, and a TRFH

dimerization and carboxy-terminal Myb domain that are both similar to their respective domains in TRF1 (Broccoli et al., 1997b). TRF2 is also found as a homodimer, and despite the similarity of its TRFH domain to that of TRF1, the two proteins are not found in heterodimers (Broccoli et al., 1997b; Fairall et al., 2001) and have unique protein-protein interactions (Chen et al., 2008; Kim et al., 2009). TRF2 specifically interacts with two other shelterin subunits, TIN2 and Rap1 (Li et al., 2000; Ye et al., 2004a).

TRF1 and TRF2 recognize the same consensus sequence and have similar Myb domains, yet the two proteins interact with telomeric DNA differently. While TRF1 homodimers can induce DNA bending and pairing that appears to be important for t-loop formation (Bianchi et al., 1997; Bianchi et al., 1999), TRF2 binding at the Myb domain does not appear to produce any DNA distortions (Court et al., 2005). TRF2 appears to facilitate t-loop structural organization by binding at telomere double strand/single strand junctions (Khan et al., 2007; Stansel et al., 2001), facilitating strand invasion of the G-rich 3' overhang (Amiard et al., 2007; Fouche et al., 2006), and further stabilizing the t-loop by protecting the Holliday junctions at the loop junction (Nora et al., 2010; Poulet et al., 2009). TRF2 may also play a role in chromatin remodeling at the telomeres, as overexpression of TRF2 in mouse keratinocytes showed aberrant nucleosomal organization at the telomeres (Benetti et al., 2008).

TRF2 is an essential gene, and TRF2 knockout mice have an embryonic lethal phenotype as does TRF1 (Celli and de Lange, 2005; Karlseder et al., 2003). Conditional deletion of TRF2 in mouse embryonic fibroblasts showed a genome-wide DNA damage response and chromosome end-to-end fusions, suggesting that TRF2 is essential for telomere end-protection (Celli and de Lange, 2005). In recent years, a role for TRF2 in DNA damage response outside of the telomeres has been suggested, with some observations of a possible accumulation of TRF2 at non-telomeric DNA double strand breaks (Bradshaw et al., 2005), however DNA double strand breaks alone are not sufficient to recruit TRF2 (Williams et al., 2007). TRF2 has been implicated in the repair of nontelomeric DNA damage sites by facilitating the early stages of homologous recombination (Mao et al., 2007), and may be regulated by ATM (Huda et al., 2009). What is apparent at this point is that TRF2 is implicitly involved in maintaining telomere structure, and the absence of TRF2 causes deprotection of telomeres and a telomeric DNA damage response.

Rap1 was identified as a TRF2-interacting protein and is the highly-diverged mammalian ortholog of the yeast protein (Li et al., 2000). Unlike the yeast protein, mammalian Rap1 does not directly bind DNA with its Myb DNA and interacts with telomeric DNA through its interaction with TRF2. Mammalian Rap1 likely has interactions with other yet-unknown proteins that could associate with its Myb domain (Hanaoka et al., 2001) or its BRCT domain (Li and de

Lange, 2003). While the function of Rap1 is still largely unknown, it has been shown to play a role in telomere length heterogeneity (Li and de Lange, 2003), and to be important for the suppression of telomeric homology-directed recombination (Sfeir et al., 2010) and non-homologous end joining (Sarthy et al., 2009).

TIN2 was identified as a "TRF1-interacting nuclear protein" in a two-hybrid screen (Kim et al., 1999), but is now known to directly interact with TRF2 and TPP1 as well, forming the central hub of the shelterin complex . TIN2 binds TRF1 and TRF2 simultaneously, forming a connection between the two telomere binding proteins and stabilizing their association with telomeric DNA (Houghtaling et al., 2004; Ye et al., 2004a). Overexpression of TIN2 likely leads to telomere shortening in telomerase positive cells, which his likely due to an increase in recruitment of TRF1 and TRF2 (both negative length regulators) to the telomere (Ye and de Lange, 2004). The specific interaction between TIN2, TRF1 and TRF2 likely also explains why TIN2 deficiency in mice leads to an embryonic lethal phenotype such as seen in TRF2 deficient mice (Chiang et al., 2004).

The third protein that interacts directly with TIN2, TPP1, is the most recently identified shelterin subunit (Houghtaling et al., 2004; Liu et al., 2004; Ye et al., 2004b). TPP1 has two domains, a carboxy-terminal TIN2 binding domain and a central domain that binds to POT1. Together, TIN2 and TPP1 serve as the

critical factors in assembling the six subunit shelterin complex at telomeres; TIN2 increases stability of TRF1 and TRF2 at telomeric DNA, while TPP1 stabilizes the TRF1-TIN2-TRF2 complex (O'Connor et al., 2006). TPP1 is also known to be critical for the recruitment of POT1 to telomeres (Hockemeyer et al., 2007; Houghtaling et al., 2004; Ye et al., 2004b), and the TPP1-POT1 interaction is important for the recruitment of telomerase and telomere length regulation (Xin et al., 2007).

POT1 (Protection Of Telomeres 1) was identified as the mammalian single-stranded telomeric DNA binding protein based on its homology to the ciliate telomere binding protein, TEBPα (Baumann and Cech, 2001). POT1 is a critical component of shelterin that is directly involved in telomere length maintenance and end protection (reviewed in (Baumann and Price, 2010). POT1 has two oligosaccharide/oligonucleotide-binding (OB) folds (Lei et al., 2003) that have very high specificity for the single-stranded telomeric nonamer sequence 5'-TAGGGTTAG-3' (Loayza et al., 2004). Because POT1 is localized at telomeres throughout the cell cycle, it likely binds to both free 3' overhangs as well as the displaced G-rich strand (the D-loop) of a t-loop structure (Wei and Price, 2004). When POT1 deletion mutants lacking the DNA binding OB folds are expressed, POT1 still localizes to the telomeres through its association with another shelterin subunit, TPP1 (Liu et al., 2004; Loayza and De Lange, 2003). The POT1-TPP1 heterodimer work to regulate telomere length homeostasis by recruiting

telomerase to the telomere, stabilizing the telomerase primer association, increasing telomerase processivity and increasing the efficiency of telomerase translocation (Latrick and Cech, 2010; Wang et al., 2007). POT1's ability to regulate telomere length is dependent on binding to single-stranded telomeric DNA as well as it's interaction with TRF2 via TPP1 (Kendellen et al., 2009).

Telomere end protection depends on POT1, with partial POT1 knockdowns exhibiting telomeric DNA damage response, shortening of 3' overhangs, altered end processing of the 5' C-rich strand, and telomere fusions (Hockemeyer et al., 2005; Veldman et al., 2004; Yang et al., 2005). While the POT1-TPP1 association is required for telomere end protection (Hockemeyer et al., 2007), it is not necessary for the heterodimer to interact with TRF2 (Barrientos et al., 2008). The POT1-TPP1 complex may inhibit DNA damage signaling by out-competing other DNA damage sensors, such as RPA, at the telomere ends (Barrientos et al., 2008; Denchi and de Lange, 2007). POT1 may also play a role in coupling leading- and lagging strand DNA synthesis during telomere replication (Arnoult et al., 2009).

As a complex, the six proteins of shelterin function to maintain telomere length, structure and to protect the ends of chromosomes from being recognized as DNA damage. TIN2, TPP1 and POT1 have been found in complex in both the nucleus and the cytoplasm, and TPP1 has a nuclear export signal that may control the accumulation of the shelterin proteins in the nucleus (Chen et al., 2007),

suggesting that there is an element of spatial regulation of shelterin that impacts telomere length homeostasis and end protection. Shelterin's ability to fully assemble and function at the telomere may also be regulated by the stoichiometry of the subunits (Takai et al., 2010). Quantitative immunoblotting has revealed that TRF1 and TRF2 are present at levels suitable to coat short telomeres, and that there was enough TIN2 to interact with all TRF1 and TRF2 molecules. POT1 and TPP1 were found to be present at a 1:1 ratio, and the POT1-TPP1 heterodimer is in excess of the amount needed to bind all single stranded telomeric DNA yet is approximately 10-fold lower in abundance than their other shelterin binding partner, TIN2. This suggests that some regulatory mechanism is in place that relies on POT1-TPP1 being the limiting factor in assembling the complete shelterin complex (Takai et al., 2010).

Telomere Function: End Protection

An evolutionary model has been proposed (de Lange, 2004) which suggests that early eukaryotic species first acquired heterochromatin at the ends of their linear chromosomes to protect against genetic degradation due to the end replication problem; the evolution of telomerase not only strengthened the protection against DNA attrition, but also established the repetitive nature of the telomere sequence. When all chromosomes had a uniform and repetitive telomere sequence, binding proteins that recognized this sequence evolved to further distinguish the natural ends of chromosomes from DNA damage sites. Without

these telomere binding proteins, telomeres could easily be mistaken for damage-induced double strand breaks by the DNA damage sensing machinery. The shelterin complex is uniquely suited to protect telomere ends, as the complex only binds telomeric DNA sequence, and telomeric DNA is not added to double stranded breaks that are not bound by shelterin. This feedback loop between shelterin and telomerase ensures that telomeric DNA sequence and the shelterin complex only accumulate at natural chromosome ends (de Lange, 2009).

The evidence that shelterin normally functions to suppress a DNA damage response at telomeres is well documented (reviewed in (de Lange, 2005). Overexpression of a dominant negative TRF2 which lacks both the basic and Myb domains leads to a dissociation of the shelterin complex (Celli and de Lange, 2005; Loayza and De Lange, 2003; van Steensel et al., 1998), and formation of telomere-dysfunction focis (TIFs) characterized by localization of damage response proteins such as gamma-H2AX, 53BP1, Rad17 and p-ATM (Fagagna et al., 2003; Silverman et al., 2004; Takai et al., 2003). Conditional deletion of TRF2 leads to the accumulation of TIFs on all telomere ends (Celli and de Lange, 2005). TIF formation is also observed with the loss of normal endogenous TIN2 and POT1 activity (Hockemeyer et al., 2005; Kim et al., 2004). Damage signaling at telomeres is transduced largely through the ATM and ATR pathways (Denchi and de Lange, 2007; Herbig et al., 2004; Silverman et al., 2004; Takai et

al., 2003), both of which respond to DNA double strand breaks, and functional telomeres must evade both pathways.

TRF2 is the main shelterin component that represses ATM signaling at functional telomeres; loss of functional TRF2 leads to ATM activation (Celli and de Lange, 2005; Karlseder et al., 1999) and subsequently DNA damage response factors are recruited to the resulting TIFs (Fagagna et al., 2003; Takai et al., 2003). ATM activation in TRF2-deficient cells is dependent on the Mre11/Rad50/Nbs1 (MRN) complex, a DNA double-strand break sensor that interacts with DNA ends (Attwooll et al., 2009; Deng et al., 2009; Dimitrova and de Lange, 2009). ATM activation and TIF formation lead to p53-mediated apoptosis or cellular senescence, depending on the cell type (Chin et al., 1999; Fagagna et al., 2003; Karlseder et al., 1999; Takai et al., 2003; van Steensel et al., 1998). The ability of TRF2 to repress ATM signaling might be due to its role in promoting t-loop formation (Griffith et al., 1999; Poulet et al., 2009; Stansel et al., 2001). The t-loop conformation may create a physical barrier that prevents the MRN complex from accessing telomere ends, which would inhibit ATM activation. There is also evidence that TRF directly represses ATM activation at the telomere by interfering with the autophosphorylation of the ATM S1981 site (Karlseder et al., 2004).

The ATR pathway is independently controlled at telomeres by POT1 (Denchi and de Lange, 2007). POT1 partial knockdowns result in TIF formation,

shortening of 3' overhangs, altered end processing of the 5' C-rich strand, and telomere fusions (Hockemeyer et al., 2005; Veldman et al., 2004; Yang et al., 2005). In mice, deletion of both POT1 genes causes the phosphorylation of Chk1, a downstream ATR target (Guo et al., 2007; Hockemeyer et al., 2006), suggesting that POT1 works to repress ATR signaling at functional telomeres. The ATR pathway is known to be activated by interaction with the single-stranded binding protein, Replication Protein A (RPA) (Shechter et al., 2004). POT1 is known to bind to the single-stranded telomeric overhang, and is thought to bind to the single-stranded D-loop of the t-loop end structure. Thus, POT1 likely works to repress ATR signaling at functional telomeres by outcompeting RPA for binding to telomeric single-stranded DNA (Barrientos et al., 2008; Denchi and de Lange, 2007). RPA is not normally found at telomere ends, but accumulates quickly in the absence of functional POT1 (Barrientos et al., 2008). POT1 is present in cells in excess of the amount needed to coat telomeric single-stranded DNA (Takai et al., 2010), and accumulates at telomeres as a component of the shelterin complex. POT1 repression of ATR signaling is dependent on POT1 interaction with the rest of the shelterin core via TPP1 (Guo et al., 2007; Hockemeyer et al., 2007), suggesting that POT1's association with shelterin allows it to accumulate at the telomere and competitively inhibit RPA activation of the ATR kinase pathway (Barrientos et al., 2008; Denchi and de Lange, 2007).

POT1 and TRF2 have been shown to independently regulate ATR and ATM signaling, respectively (Denchi and de Lange, 2007). These two proteins are also involved in protecting telomeres from two major DNA repair pathways, Non-Homologous End Joining (NHEJ) and Homologous Recombination (HR) (de Lange, 2009). NHEJ at the telomere leads telomere fusions that result in dicentric chromosomes and genomic instability, a hallmark of telomere dysfunction (Bertuch, 2002). HR at the telomere can lead to telomere sister chromatin exchanges (T-SCE) and rapid telomere deletion (Bailey et al., 2004a; Bechter et al., 2004; Sonoda et al., 1999). Functional telomeres must inhibit both of these pathways in order to protect telomere ends from being "repaired" as if they were damage-induced ends (de Lange, 2009).

TRF2 plays an important role in repressing both NHEJ and HR. Loss of TRF2 leads to chromosome end-fusions (Celli and de Lange, 2005; van Steensel et al., 1998) that are dependent on NHEJ factors such as DNA Ligase IV and Ku70 (Celli and de Lange, 2005; Smogorzewska et al., 2002) and DNA the DNA damage factor 53BP1 (Dimitrova et al., 2008). TRF2 protection against NHEJ appears to be cell-cycle dependent, with protection conferred during G1 and G2 of the cell cycle ((Celli and de Lange, 2005; Konishi and de Lange, 2008; Smogorzewska et al., 2002). Association of Rap1 with TRF2 may play a role in the protection against NHEJ (Bae and Baumann, 2007; Sarthy et al., 2009). TRF2 also plays a role in repressing HR at telomeres, likely through an interaction with

the Ku70/80 complex (Celli et al., 2006; Wang et al., 2004b). In the absence of normal TRF2 function, t-loop sized telomeric circles are found, suggesting a rapid telomere deletion event is occurring through HR at telomeric t-loop junctions (Wang et al., 2004b). The fact that TRF2 protection against HR is dependent on Ku70/80 represents a fascinating dichotomous role for this heterodimer in telomere end protection: Ku70/80 is directly involved in promoting NHEJ at DNA ends (Lieber et al., 2003), but is required for suppression of HR at telomeres (Celli et al., 2006). Ku70/80 normally functions in the NHEJ pathway to bind DNA ends, and TRF2 likely protects against NHEJ by arranging telomeric DNA in a t-loop formation that hides the telomere end from recognition by Ku70/80. The fact that Ku70/80 is found at telomeres and is required for suppression of HR suggests (Hsu et al., 2000) that Ku70/80 interacts in some unique way with the telomere nucleoprotein complex which confers end protection without activating NHEJ (Hsu et al., 2000; Palm and de Lange, 2008). POT1 is also directly involved in suppressing both NHEJ and HR. While TRF2 suppresses NHEJ in both G1 and G2, POT1 protection is found only in G2 (Wu et al., 2006). Loss of POT1 causes aberrant HR at telomeres in an MRN complex-dependent context (Palm et al., 2009; Wu et al., 2006).

Telomeres have been recognized as being functionally distinct since the first cytogenetic studies of X-ray irradiated chromosomes (McClintock, 1941; Muller, 1938). Today, we know that functional mammalian telomeres achieve

this distinction by mechanistically suppressing two major DNA damage-sensing pathways, ATM and ATR, as well as two major DNA repair pathways, NHEJ and HR. TRF1 and POT1, in coordination with other shelterin proteins, cause the telomeric DNA to be arranged in a t-loop conformation and thus structurally obscure telomeric ends from being recognized by DNA damage sensors (MRN) and DNA repair effectors (Ku70/80). While this conceptual model is elegant, there is still much to be learned regarding the many protein interactions that occur at the telomere. For example, many DNA damage proteins such as Ku70/80 and DNA-dependent protein kinase (DNA-PKc) are actively recruited to telomeres and are necessary for normal telomere function (Espejel et al., 2002; Espejel et al., 2004; Hsu et al., 2000). *In vitro* studies have shown that p53 can bind telomeric DNA and promote t-loop formation, suggesting that p53 may play a role in normal telomere function (Stansel et al., 2002). The mechanism by which these proteins can contribute to telomere function without targeting telomeres as DNA damage remains unclear. The observation that there is a localized DNA damage response at telomeres following telomere replication (Verdun et al., 2005) suggests that a transient, localized DNA damage signals may be required for normal telomere maintenance and assembly. Additional data on the regulation of t-loop formation, telomere end processing and telomere length dynamics during replicative senescence will provide additional insights on this complex end protection mechanism.

III. HUMAN TELOMERE LENGTH DYNAMICS

Today it is widely accepted that most normal human somatic cells have a finite lifespan in culture, and the role of telomeres as the molecular replication counter, or "replicometer," has been well documented (reviewed in (Collado et al., 2007).. In summary, telomeres shorten with each cell division due to an inability to fully replicate linear DNA molecules as well as more rapid telomere deletions due to oxidative or other DNA damage. As telomeres become critically short, their ability to suppress DNA damage and repair pathways becomes weakened, likely due to a decreased ability to bind the shelterin complex and form a functional t-loop (reviewed in (de Lange, 2005; Martinez and Blasco, 2010). The outcome of the deprotection of critically short telomeres is chromosomal instability, activation of cell cycle arrest or apoptosis. This phenomenon has been called "replicative senescence," as cells naturally reach a point at which they can no longer divide as a function of the number of prior cell divisions (for review, (Wright and Shay, 2005). Cells that can infinitely divide must employ a mechanism to maintain their telomere length and preserve functional telomere end protection. The telomerase ribonucleoprotein complex is known to facilitate this telomere maintenance function in many "immortal" organisms such as ciliates and yeast, as well as the majority of human cancer cells (reviewed in (Blackburn, 2005). For these immortal cells, maintaining telomere length involves regulating

the dynamic between telomere shortening and telomere elongation. The role of telomeres and telomerase in the replicative potential of human cells has implications for cancer diagnosis and treatment, regenerative medicine and tissue engineering. However, there are still many aspects of this dynamic regulatory process that are unknown. Presented here is a historical perspective on replicative senescence and an overview of what is currently known about the regulation of telomere length dynamics.

Telomere Attrition: Replicative Senescence

The study of replicative potential is currently being conducted at the molecular level, but began with the advent of tissue culture in 1907, when human nerve tissue explants were grown on a hanging-drop coverslip for the first time (Harrison et al., 1907). The first data regarding the replicative potential of cells in culture came from a Nobel-prize winning vascular surgeon, Alexis Carrel, who demonstrated that fibroblasts from chicken heart tissue could grow in culture for more than 30 years (Carrel and Ebeling, 1921). This data was largely accepted and led to the general conclusion that cells were able to divide indefinitely in culture, and Peyton Rous called the finding the "largest fact to have come from tissue culture in the last fifty years…. (discussed in (Shay and Wright, 2000)."

A challenge to this idea of cellular immortality did not come until 1961, when Leonard Hayflick and Paul Moorehead published data that supported the alternative hypothesis that human fibroblasts had a limited lifespan in culture

(Hayflick and Moorhead, 1961). In these early experiments, equal numbers of "old" male fibroblasts were mixed with "young" female fibroblasts, and grown alongside unmixed control cultures. The young female control culture was still growing when the old male control stopped dividing, and examination of the mixed cultures revealed that the only cells remaining were female. This carefully planned experiment showed that cells were not immortal in culture, and that they had an inherent mechanism for remembering how old they were (Hayflick and Moorhead, 1961). The finite doubling time of normal diploid cells was distinct from that of cultured cancer cells, which could divide infinitely (Hayflick, 1965) and would eventually come to be called "the Hayflick limit (Burnett, 1974)."

Around the same time that Hayflick was challenging paradigms of cell biology, advances in genetics and molecular biology were challenging scientists to understand how eukaryotic organisms maintained and replicated their DNA. In 1971, a Russian theoretical biologist proposed his "theory of marginotomy," in which he describes the consequences of successive rounds of DNA replication where the ends are not fully replicated due to the nature of the replication machinery (Olovnikov, 1971, 1973). During semi-conservative DNA replication, the double helix is unwound by a protein complex to form a replication fork, and replication of the two DNA strands begins simultaneously in the 5' to 3' direction. The leading daughter strand is synthesized in the direction of the replication fork, with the potential to replicate to the end of the linear chromosome template. The

lagging daughter strand is synthesized in the opposite direction of fork progression, and involves the discontinuous synthesis of Okazaki fragments which are individually primed, extended, and ligated together to create a continuous DNA strand. While leading strand synthesis can copy the entire length of the linear template, lagging strand synthesis can only copy up to the location of the primer closest to the chromosome terminus. If the terminal primer is placed at the very end of the chromosome, the length of the uncopied region would equal the length of the primer (approximately 10-14 nucleotides). If the terminal primer is placed randomly with respect to the chromosome end, the length of the uncopied region would correspond to the position of the last primer. Both primer placement scenarios predict the gradual shortening of chromosomes over time, as each round of lagging strand synthesis is unable to fully replicate the template strand. Olovnikov was aware of Hayflick's findings that cells had a limited replication potential in culture, and he recognized that his theory of progressive chromosome shortening might provide the molecular explanation for the Hayflick limit (Olovnikov, 1971, 1973). The concept of progressive shortening of chromosomes was independently published in 1972 by James Watson, and called the "end-replication problem (Watson, 1972)." Finding the solution to the problem of how linear chromosomes could fully replicate became a main focus in the new field of molecular genetics, but Olovnikov's hypothesis

that the end replication problem was the cause of cellular lifespan did not gain popular support for almost 20 years (Olovnikov, 1996) .

Hayflick continued to explore the finite lifespan of cultured cells, and he was convinced that cells had an inherent counting mechanism, or "replicometer (Hayflick, 1998)." In his first published study, the mixed old and young cells remembered that they were old or young, despite being grown under the same culture conditions and in the presence of cells with a different replicative potential (Hayflick and Moorhead, 1961). Cells could even remember how many times they had divided after they had been frozen and thawed (Hayflick, 1998). There were two prevailing hypotheses of what constituted the replicometer: either some element of genetic control emanating from the nucleus, or the progressive accumulation of damage to organelles and molecules in the cytoplasm. In order to examine these two possibilities, a series of experiments were performed in which anucleate cells ("cytoplasts") were fused with whole cells of a different replicative potential. The results indicated that there was no reason to believe that the replicometer was located in the cytoplasm, and that replicative potential emanated from the nucleus (Wright and Hayflick, 1975). A recent experiment reiterated these results using modern-day techniques, showing that replicative potential is conserved after nuclear transfer (Clark et al., 2003).

While the mechanism of the cellular replicometer was known to come from the nucleus, it was still unclear if it was some programmed genetic

regulatory process, or if it was Olovnikov's theory of marginotomy and progressive chromosome shortening that was counting cell divisions. The nature and function of telomeres started to become more clear when repetitive DNA were discovered at the ends of ciliate chromosomes (Blackburn and Gall, 1978). Human telomeres were also found to have thousands of repeats of a hexameric sequence, TTAGGG, which is conserved among many vertebrates (Meyne et al., 1989; Moyzis et al., 1988). Furthermore, telomere length was found to be variable among cells from different tissues (Cooke and Smith, 1986). The first direct evidence of the connection between shortening telomeres and Hayflick's limit on replicative potential came in 1990, when it was demonstrated that the telomeres of normal human fibroblasts progressively shorten in culture (Harley et al., 1990). A series of subsequent studies supported the relationship between telomere attrition and cellular lifespan (Allsopp et al., 1995a; Allsopp and Harley, 1995; Allsopp et al., 1992; de Lange et al., 1990; Hastie et al., 1990; Lindsey et al., 1991; Vaziri et al., 1994).

Today, the association between telomere shortening and replicative senescence is widely studied and accepted. Telomere attrition was first attributed to the end replication problem (Olovnikov, 1971, 1973; Watson, 1972), this alone is not likely to account for the rate of telomere shortening observed in cultures. Other factors contributing to telomere attrition are either mechanistic, such as nuclease resection (Makarov et al., 1997; Wellinger et al., 1996), or stochastic

events such as oxidative damage (Serra et al., 2000; von Zglinicki, 2000, 2002; von Zglinicki et al., 2000) and rapid telomere deletion events (Baird et al., 2006; Baird and Kipling, 2004; Baird et al., 2003; Wang et al., 2004b). Computational modeling of telomere shortening from both mechanistic and stochastic events can explain replicative senescence by relating mitotic events to telomere attrition (Portugal et al., 2008).

Telomere attrition likely leads to cellular senescence because of a disruption of their ability to protect chromosome ends from DNA damage and repair mechanisms. Short telomeres are known to trigger a localized DNA damage response and TIF formation (Fagagna et al., 2003; Zou et al., 2004b), which leads to p53-mediated cell cycle arrest (Chin et al., 1999; Fagagna et al., 2003; Karlseder et al., 1999; Takai et al., 2003; van Steensel et al., 1998). It is possible that telomeres reach a critically short length that is no longer competent to assemble into the t-loop structure, and that even a few "uncapped" telomeres in a cell is enough to initiate replicative senescence (Zou et al., 2004b). A recent computational model looking at data from human diploid fibroblasts and human cancer cell lines determined that t-loop formation as a function of telomere length was a reasonable explanation for the initiation of replicative senescence (Rodriguez-Brenes and Peskin, 2010).

Telomere Elongation: The Telomerase Holoenzyme

Since shortening telomeres lead to a finite cellular lifespan, there must be a mechanism for maintaining telomere length in cells and organisms that can replicate indefinitely. Such a mechanism was first identified in the ciliate protozoan, *Tetrahymena*, when an enzyme was discovered that generated *de novo* telomeric repeats at the ends of chromosomes (Blackburn, 2005; Greider and Blackburn, 1985, 1987, 1989). Telomerase activity was found in a variety of species (Morin, 1989; Shippen-Lentz and Blackburn, 1989; Zahler and Prescott, 1988), including human cancer cell lines and primary tumors (Kim et al., 1994; Morin, 1989). The introduction of exogenous telomerase in telomerase negative human cell lines showed telomere elongation and extended cellular lifespan compared to controls, showing for the first time that cells could be immortalized by expressing telomerase (Bodnar et al., 1998). This study experimentally confirmed the causal relationship between telomere shortening and cellular senescence.

The human telomerase holoenzyme core components are a catalytic reverse transcriptase called hTERT (human telomerase reverse transcriptase) (Harrington et al., 1997a; Nakamura et al., 1997), and an associated template RNA called hTR (human Telomerase RNA) (Feng et al., 1995) which add TTAGGG repeats onto the 3' end of chromosomes. hTR is ubiquitously expressed in all human cells, and telomerase activity is limited by the expression of hTERT,

which is only found in cells with detectable telomerase activity (Ducrest et al., 2002; Takakura et al., 1998). Telomerase activity is found in human testes, peripheral blood lymphocytes, and some adult pluripotent stem cells, but is not found in most normal somatic cells (Wright et al., 1996). Telomerase activity is nearly universal in human cancer cell lines, and in about 90% of primary tumors (Kim et al., 1994).

The telomerase RNA (TR) component is found in a large number of species, from ciliated protozoa to yeast to vertebrates (Chen and Greider, 2004). While there is a significant divergence in the sequence and size of the TRs, there are common structural elements that have been conserved. The template region is always single-stranded, and is approximately two times longer than the telomere repeat motif. The template region is also always flanked by a 3' pseudoknot domain and a 5' boundary element domain (Chen and Greider, 2004). The single stranded template region is long enough to base pair with the telomeric 3' overhang, and serves as the template for the synthesis of one telomere repeat (Greider and Blackburn, 1985, 1989). The 5' boundary element domain serves to limit reverse transcription past the end of the template, and hTR uses the P1b helical structure to define the 5' template boundary (Chen and Greider, 2003). The role of the pseudoknot domain in hTR is still poorly understood (Ly et al., 2003), but its presence in hTR been confirmed by various structural methods

(Gavory et al., 2006; Kim et al., 2008; Theimer and Feigon, 2006; Yeoman et al., 2010).

The hTERT catalytic component of the telomerase holoenzyme has reverse transcriptase motifs that are universally conserved (Lingner et al., 1997), and is thought to be one of the earliest eukaryotic reverse transcriptases to evolve (Eickbush, 1997; Nakamura and Cech, 1998). Another conserved motif among TERT proteins is an RNA binding domain that allows for the stable association with the TR when the template region is moving through the TERT catalytic site (Bryan et al., 2000). Aside from these conserved protein motifs, TERT family members also have domains which are involved in recruitment to telomeres, dimerization and nuclear localization (Arai et al., 2002; Cech et al., 1997; Harrington et al., 1997b; Nakamura et al., 1997). In addition to the two core components of the telomerase holoenzyme complex are many confirmed and putative telomerase-associating proteins. The size of the human telomerase holoenzyme has been measured at approximately 1.5 megaDa, which is significantly larger than the expected mass of a single hTR and hTERT (approximately 280 kD) (Schnapp et al., 1998). A recent purification strategy was designed to isolate only catalytically active telomerase, revealing that only one additional component, dyskerin, was required for *in vitro* telomerase activity (Cohen et al., 2007). This study concluded that catalytically active human telomerase is composed of a homodimer of a complex consisting of a single hTR,

hTERT and dyskerin (Cohen et al., 2007). While other telomerase-associated proteins may not be necessary for catalytic activity, they may play a role in holoenzyme stability, recruitment or regulation.

Telomerase extends telomeres by binding to the 3' single stranded overhang at the telomere end, catalyzing the addition of a single telomere repeat, and translocating to the new terminus; this cycle continues until the holoenzyme dissociates from the telomere (Figure 1.3) (Cong et al., 2002; Kelleher et al., 2002). Telomerase levels must be limiting for cells to maintain normal telomere length homeostasis, demonstrated by the continued elongation of telomeres when both hTERT and hTR were overexpressed in human primary and cancer cell lines (Cristofari and Lingner, 2006). Telomerase levels are regulated at every level of protein and RNA processing, as well as at the level of complex assembly and subcellular localization (Cong et al., 2002; Kelleher et al., 2002). Telomerase activity at the telomere is also regulated at the level of telomerase recruitment to the telomere. While the exact mechanism of telomerase recruitment is still not fully known, it is likely part of a negative feedback loop created by shelterin proteins bound at the telomere that serve as negative regulators of telomerase extension of telomeres (reviewed in (De Boeck et al., 2009; Smogorzewska and de Lange, 2004).

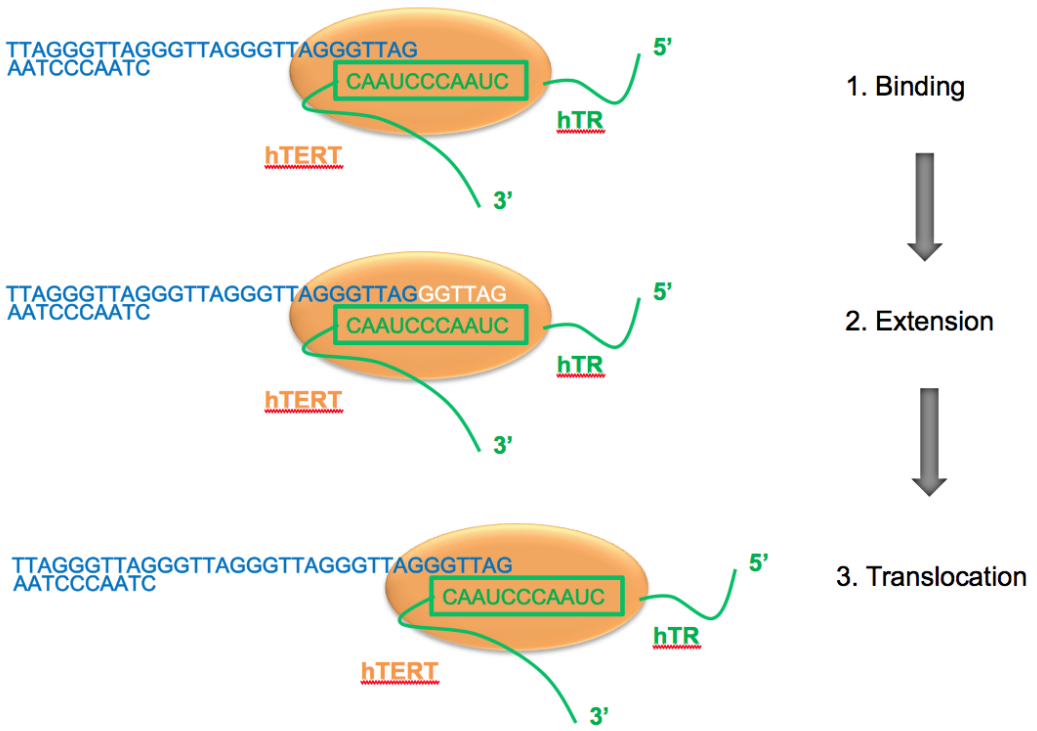

Figure 1.3 Telomerase extension of the G-rich telomere. Telomerase binds to the 3' G-rich overhang through complementarity of the template region of hTR. hTERT catalyzes the addition of one telomere repeat, and then the entire holoenzyme translocates. Multiple rounds of extension and translocation are performed in each cell cycle.

The prevailing model of shelterin-mediated telomere length regulation is that the longer the telomere, the more shelterin is recruited to the telomere, which in turn limits future telomerase elongation. This negative feedback loop is thought to be responsible for the stable telomere length found in cancer cells, and is likely also responsible for maintaining telomere length homeostasis in germ cells and other stem-like cells in which telomerase is active (Smogorzewska and

de Lange, 2004). TRF1 was the first shelterin component to be implicated as a negative regulator of telomere length, as overexpression of TRF1 causes gradual telomere shortening and inhibition of TRF1 caused telomere elongation (van Steensel and de Lange, 1997). The effects of TRF1 on telomere length did not affect levels of telomerase expression or activity, suggesting that TRF1 somehow limits telomerase from working on the telomere (Smogorzewska et al., 2000; van Steensel and de Lange, 1997). Because the amount of TRF1 bound to the telomere increases with increasing telomere length, it has been proposed that TRF1 constitutes a protein counting model of telomere length control such as that found in yeast (Marcand et al., 1997; Smogorzewska et al., 2000). TRF1 must be bound to the telomere in order to confer telomere length regulation (Ancelin et al., 2002), and TRF1 binding to the telomere can be modulated by its interactions with TIN2 and Tankyrase. Tankyrase catalyzes a conformational change on TRF1 which leads to dissociation from the telomere and subsequent elongation by telomerase (Smith and de Lange, 2000); however, when TRF1 is bound to its shelterin partner TIN2, tankyrase activity is mitigated and TRF1 is stabilized at the telomere (Ye and de Lange, 2004; Ye et al., 2004a). TRF1 levels at the telomere are further controlled by selective ubiquitination and proteolysis of the unbound TRF1, mediated by an SCF E3 ubiquitin ligase (Sarraf and Harper, 2010; Zeng et al., 2010). TRF2 (Smogorzewska et al., 2000) and Rap1 (Li and de Lange, 2003) have also been identified as a negative regulators of telomere

length, indicating that shelterin binding to double stranded telomeric DNA is imperative for regulating telomere elongation by telomerase.

Because telomerase must work on the 3' overhang of the telomere terminus, shelterin is thought to confer negative length regulation by telomerase access to the overhang. While TRF1 and TRF2 binding of the double stranded telomeric DNA promotes t-loop formation and sequestration of the overhang, POT1 is considered to be the crucial shelterin component in regulating telomere length. POT1 is the only shelterin component to bind single stranded DNA, and mutants which lack the DNA-binding OB folds cause extensive telomere elongation independent of the binding of other shelterin components at the telomere (Loayza and De Lange, 2003). *In vitro* studies have shown that POT1 binding to the overhang can block telomerase from accessing the overhang (Kelleher et al., 2005), and that the absence of POT1 binding at the overhang leads to enhanced telomerase activity (Lei et al., 2003; Lei et al., 2004; Lei et al., 2005). Data also suggests that POT1 must interact with TRF2 through TPP1 in order to confer negative telomere length regulation, which suggests that the entire shelterin-induced t-loop conformation is imperative for limiting telomerase access to the telomere (Kendellen et al., 2009). While POT1 is critical for negative telomere length regulation, it can also work to facilitate telomerase action at the telomere (Colgin et al., 2003; Lei et al., 2005). The POT1-TPP1 complex directly interacts with telomerase, and may be involved in recruiting the holoenzyme (Xin

et al., 2007; Zaug et al., 2010). The interaction between POT1-TPP1 and telomerase also increases telomerase processivity (Cristofari et al., 2007; Latrick and Cech, 2010; Wang et al., 2007).

Despite the large body of data regarding shelterin-mediated telomere length regulation, many key questions remain regarding the mechanism of telomerase maintenance of telomere length. For instance, telomere length in telomerase positive cells is known to be maintained within a narrow range, yet mechanism for determining the length set-point is not well understood. There is also little data on the timing of telomerase activity in mammalian cells, and how changes in the telomere structure throughout S-phase may affect telomerase inhibition or recruitment. It is unclear if telomerase acts in a processive manner, being recruited to a telomere and adding long tracts of telomere sequence, or if it functions more distributively, with telomerase adding short stretches of telomere repeats before dissociating and moving onto another telomere. Finally, there is no direct evidence indicating whether short telomeres are preferentially elongated by telomerase under conditions when telomere length is being maintained. Answers to these questions will require sophisticated techniques for measuring telomere length, and will provide insight into the regulatory processes that ensure the continued replication of telomerase-positive cells.

CHAPTER TWO

UNIVERSAL STELA: A NOVEL ASSAY FOR MEASURING TELOMERE LENGTH

INTRODUCTION

Telomere length heterogeneity

The length of telomeres is known to be influenced by a variety of factors, and must be studied at different levels of control in order to get a clear understanding of telomere length regulation. At the level of comparative biology, different species have characteristic average telomere lengths. An iconic example is the difference between the average telomere length of human cells (approximately 10 kb) and that of mice (20-50 kb). Further investigation of telomere length and telomerase activity throughout the phylogenetic tree has led to the development of hypotheses regarding the evolutionary history of the use of telomere length to control replicative aging (Austad, 2010; Seluanov et al., 2007; Shay and Wright, 2007). Human studies have suggested that telomere length is a characteristic that is determined in part by inheritance, suggesting that telomere length is regulated across generations within a given species (Graakjaer et al., 2003; Graakjaer et al., 2006; Graakjaer et al., 2004b; Slagboom et al., 1994; Wu et al., 2003). Telomere length within an individual has been shown to vary with tissue type and disease state (Calado and Young, 2009; Rando, 2006; Shay and

Wright, 2007). Telomere length is even heterogeneous within a single human cell (Lansdorp et al., 1996a; Londono-Vallejo, 2004; Martens et al., 1998). There have been many reports of a chromosome-specific pattern of telomere length distribution (Graakjaer et al., 2003; Graakjaer et al., 2004a), as well as evidence that telomere length is positively associated with chromosomal length (Martens et al., 1998), however there is also evidence that the telomeres of homologous chromosomes may also have different lengths, suggesting that chromosome specific telomere length may be determined by a combination of inherited and regulatory factors that are independent of telomere length itself (Londono-Vallejo et al., 2001). Indeed, a study of the length distribution of individual telomere molecules in normal human fibroblasts revealed a bimodal length distribution that was attributed to stochastic allelic variation (Baird et al., 2003). Over the course of many cell doublings, the length of an individual telomere is determined by the balance of telomere elongation by telomerase and events which cause the telomere to shorten, such as incomplete replication of the lagging strand (the "end replication problem"), oxidative damage, and telomere processing events that are yet to be fully understood (Harley, 1991; Shore and Bianchi, 2009; von Zglinicki, 2002). Studies of telomere length thus have practical and theoretical implications in a wide variety of fields, from evolutionary biology to medicine and epidemiology to molecular and cellular biology.

Methods of telomere length measurement

Many methods of telomere length assessment have been developed that utilize a variety of molecular techniques, including southern blotting, PCR, FISH and flow cytometry (Canela et al., 2007; Lin and Yan, 2005). These methods are summarized in Table 2.1, and are briefly described including shortcomings and advantages below.

Southern Blot/Telomere Restriction Fragment (TRF) Analysis

TRF analysis is the most commonly used method of telomere length measurement, and consists of a Southern blot (Southern, 1975) for telomere-containing genomic DNA (Oexle, 1998). In a TRF southern blot, genomic DNA is extracted and digested with a combination of frequent cutter restriction enzymes which digest the DNA to the last available restriction site before the beginning of the telomere. This DNA is resolved by gel electrophoresis and probed with a telomere-specific radioactively labeled probe. The resulting Southern blot will display a signal distribution that represents the distribution of terminal restriction fragments which contain telomeric sequences as well as any undigested adjacent subtelomeric DNA. Densitometry analysis of the blot will result in a measurement of the average detectable telomere length (Harley et al., 1990; Oexle, 1998). There are two chief drawbacks to TRF measurements which stem from both the assay design and limitations to its interpretation.

First of all, the nature of restriction digestion results in measured TRF lengths that include a variable and unknown tract of subtelomeric DNA (Steinert et al., 2004); the use of many frequent-cutting restriction enzymes may minimize the contribution of subtelomeric DNA to the final length measurement, but it is difficult to predict how much of the measured length is due to telomeric sequences. Secondly, TRF blots yield a distribution of telomere lengths which have a strong bias against shorter telomeres: smaller telomere molecules have fewer telomere repeats, and thus bind less labeled probe, making them relatively less observed than longer telomeres that produce a much stronger signal. Loading increasing amounts of genomic DNA can improve the sensitivity to lower molecular weight signal, but limits the assay to experimental conditions in which large amounts of DNA are obtainable.

Hybridization protection assay (HPA)

HPA was developed as a faster and easier alternative to TRF, and can also be performed on comparatively lesser amounts of DNA. The assay involves incubating a small amount of genomic DNA with an acridinium ester labeled probe specific to either telomere repeats or *AluI* recognition sequence; chemiluminescence readings allows for the calculation of the ratio of telomere:*AluI* sequence, and this is ratio (TA ratio) is normalized to telomere length as measured by TRF (Nakamura et

al., 1999). HPA conveys an advantage over TRF in that it requires less starting material and less time to completion, however it is an indirect measurement of telomere length. The assay is most useful in a clinical setting in which small numbers of cells are obtained from swabs or biopsies (Nakamura et al., 1999).

Quantitative Flourescent In Situ Hybridization (Q-FISH)

FISH allows for the direct labeling of telomere sequences at the level of an individual cell. Flourescent probes are designed to hybridize to telomeric DNA using peptide nucleic acid (PNA), phosphoamidate or traditional oligonucleotide backbones. Cells are generally collected and prepared in a metaphase spread, incubated with telomere probe and a counterstain (usually DAPI or PI), visualized using fluorescent microscopy and the images are analyzed to quantify the fluorescent signal to determine telomere length (Lansdorp et al., 1996a; Slijepcevic, 2001). Q-FISH has many advantages as a telomere length assessment tool. Telomere-specific probes are small in size, allowing for excellent penetration through cells. When PNA probes are used, a more stable duplex structure is formed and yields a more intense signal at the telomere and increases sensitivity. Many modifications of the Q-FISH strategy have been developed which confer different advantages to telomere length measurements. Notable among these modified strategies are "TELI-

FISH," which combines immunostaining and FISH in fixed, embedded archival tissues (Meeker et al., 2002), and "Flow-FISH," which combines flow cytometry with FISH (Baerlocher et al., 2002; Hultdin et al., 1998; Ishikawa, 1998; Lauzon et al., 2000; Rufer et al., 1998; Schmid et al., 2002). Flow-FISH allows for the simultaneous sorting of cells into different subpopulations, as well as allowing for the measurement of telomere length in cells which are actively cycling instead of only those that are arrested in metaphase.

Primed *in situ* (PRINS)

PRINS is a method that allows for the detection of long repetitive DNA tracts, making it suitable for telomere analysis. A synthetic primer(s) that is complementary to one or both telomeric strands is annealed to metaphase spread chromosomes, incubated with a DNA polymerase and fluorescently labeled nucleotides, and the primers are extended to include the full length of the telomere tract. The fluorescent signal is then detected to give a quantitative analysis of telomere content (Lavoie et al., 2003; Therkelsen et al., 1995). The efficacy of the PRINS method depends on the ability to produce a detectable, specific telomere signal. Short telomeres and poor primer annealing can lead to decreased signal, while non-specific priming can reduce the specificity of the signal.

Quantitative Polymerase Chain Reaction (Q-PCR)

There are many challenges inherent to PCR amplification of telomeric DNA, which is repetitive and stretches for many kilobases. The first challenge to overcome is that of the design of the forward and reverse primers: the sequences 5' TTAGGG 3' and 5'CCCTAA 3' are self-complementary and can easily form primer dimmers. The Q-PCR method for telomere length assessment uses primers that are variants of telomeric sequence such that there are mismatches which are sufficient to prevent primer dimer products (Cawthon, 2002; Gil and Coetzer, 2004). This Q-PCR method results in a relative measure of average telomere length by reporting the ratio of telomere (T) signal to that of a single copy gene (S). The meausrement of a constant single copy gene likely makes the T/S ratio more accurate than the relative ratio calculated by the HPA assay, which reports telomere signal relative to that of AluI sequence, which is highly variable between samples (Cawthon, 2002; Gil and Coetzer, 2004). However, the method still reports telomere length in a relative, rather than absolute, manner. The method is simple and straightforward, and can thus be used for medical and epidemiological studies.

Single Telomere Length Analysis (STELA)

While the Q-PCR method reports a relative amount of telomere DNA as compared to that of a single-copy gene, STELA is a PCR-based

assay that amplifies individual telomere molecules for direct length assessment (Baird et al., 2003). STELA produces telomere amplification products that represent the full spectrum of telomere lengths found on a specific chromosome (Figure 2.1). The first critical component of the STELA method is to ligate an oligonucleotide that contains a unique sequence "tag" to the end of the otherwise repetitive C-rich strand of the telomere; this serves as the site for the reverse primer in the PCR reaction. The chromosome specificity of STELA relies on the design of a forward primer that is both unique to a specific chromosome arm and relatively close to the beginning of true telomeric repeats. Genomic DNA that has been incubated with the reverse telomere tag ("telorette") is diluted to the point that there are very few amplifiable molecules in each PCR reaction. The resulting PCR products are resolved by electrophoresis and analyzed by southern blot to yield a distribution of bands that represent the full distribution of telomere lengths found on that chromosome in that cell population. A major advantage of STELA in comparison to the TRF southern blot method is that short telomeres are readily detected. The major drawback to using the STELA method to study short telomeres is that it can only be applied to a relatively small number of chromosomes which have suitable forward primer sites (Britt-Compton and Baird, 2006).

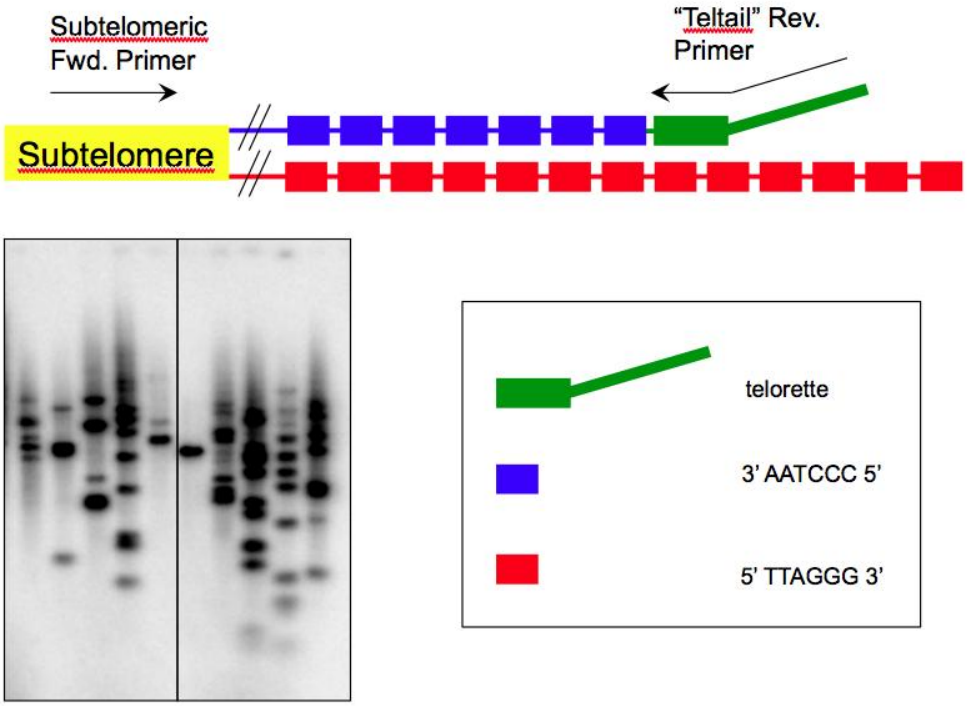

Figure 2.1: Single Telomere Length Analysis (STELA)
The first step of STELA ligates a tag to the end of the C-rich telomere strand with a "telorette" oligo, which has a short tract of nucleotides complementary to the G-rich overhang, and ends with a unique DNA sequence. During PCR amplification of tagged telomeres, the reverse primer utilizes the unique telorette tag, while the forward primer is subtelomere specific. Each product represents an individual telomere molecule. When the input DNA is diluted such that only a few amplifiable molecules are present in each reaction, the telomere amplification products can be resolved by electrophoresis and analyzed for molecular weight by telomere-specific Southern blot.

Telomere Length Measurement Assay	Advantages	Disadvantages	Reference
Telomere Restriction Fragment (TRF)	Easy for routine use	Provides only average length; includes subtelomeric region of unknown length; bias against detection of shorter telomeres	(Harley et al., 1990; Oexle, 1998; Southern, 1975)
Hybridization protection assay (HPA)	Quick and easy; requires less starting material than TRF	Indirect measure of telomere length	(Nakamura et al., 1999)
Quantitative Flourescent In Situ Hybridization (Q-FISH)	Flow-FISH allows for analysis of cycling cells	Q-FISH of metaphase spreads is restricted to arrested/non-cycling cells	(Lansdorp et al., 1996a; Slijepcevic, 2001)
Primed *in situ* (PRINS)	Alternative to Q-FISH for quantitative *in situ* telomere length analysis	Metaphase spreads require cells to be arrested; Weak signal due to poor annealing; non-specific signal due to poor primer specificity	(Lavoie et al., 2003; Therkelsen et al., 1995).
Quantitative Polymerase Chain Reaction (Q-PCR)	Simple and suitable for high-throughput clinical and epidemiological studies	Indirect telomere length measurement, although more accurate than HPA indirect measurement	(Cawthon, 2002; Gil and Coetzer, 2004).
Single Telomere Length Analysis (STELA)	Detects full range of telomere lengths; is telomere specific	Can only be applied to telomeres with an available unique forward primer site	(Baird et al., 2003).

Table 2.1 Comparison of available telomere length measurement methods

Critically Short Telomeres and Senescence: The Rationale behind Universal STELA

Years of telomere length studies using these many methods of telomere length assessment have produced the data needed to link telomere length with cellular senescence. Telomeres were first shown to shorten with each cell division using the TRF method (Harley et al., 1990), and much of what we know regarding telomere length dynamics in dividing and senescent cells is based on mean telomere length. Mean telomere length correlates with both the cell age and the replicative potential of a cell (Allsopp et al., 1995b; Allsopp et al., 1992), and preventing telomere shortening by the expression of telomerase circumvents senescence altogether, providing the experimental evidence that short telomeres have a causal role in the induction of senescence (Bodnar et al., 1998). Progressive telomere shortening has been attributed to the end replication problem (Olovnikov, 1973), oxidative damage (von Zglinicki, 2000; von Zglinicki et al., 2000) and processing with nucleases (Sfeir et al., 2005; Shore and Bianchi, 2009). There is considerable evidence, however, that senescence is induced by a single (or small group of) short telomeres rather than the consistent progressive shortening of all telomeres in a cell (Abdallah et al., 2009; Hemann et al., 2001b; Zou et al., 2004b). These short telomeres are sometimes found in cells that have otherwise long mean telomere length, appearing as a signal-free end when using FISH methods (Martens et al., 2000) or as a very short telomere amplification

products using STELA (Baird et al., 2003; Xu and Blackburn, 2007). One possible explanation for the presence of these ultra-short telomeres is that chromosomes which are known to have shorter telomeres, such as 17p, are the first to become critically short due to progressive and gradual telomere shortening, and are thus "programmed" to trigger senescence (Martens et al., 1998). This possibility suggests that ultra short telomeres would often be found on the same group of chromosomes. Another possible explanation for the existence of ultra short telomeres is that large tracts of telomeric DNA can be suddenly lost from telomeres of any chromosome due to a variety of mechanisms such as oxidative damage (Passos et al., 2007; Richter and Zglinicki, 2007; von Zglinicki et al., 1995), replication slippage (Baird et al., 1995), unequal sister chromatid exhachange (Baird, 2008) and circular telomere recombination deletion events (Ferenac et al., 2005; Rubelj et al., 2002; Rubelj and Vondracek, 1999; Wang et al., 2004b). These events would target telomeres stochastically, making it impossible to predict which chromosomes in a replicating cell will eventually harbor a critically short telomere that triggers senescence.

As a cell population ages, a combination of progressive telomere erosion and stochastic, sudden telomere loss is predicted to generate the critically short telomeres that are thought to ultimately trigger the induction of replicative senescence through cell cycle arrest (d'Adda di Fagagna et al., 2003). Obtaining

direct experimental evidence to link critically short telomeres to senescence has been a challenge, however, due to the fact that currently available methods of telomere length assessment do not allow for the routine analysis of single rare telomeres. Because TRF and Q-FISH methods are based on quantifying signal from hybridization to telomeric DNA, they are biased against the routine detection of short telomeres. Even a detailed analysis of TRF length distributions (Kimura et al., 2008) is not able to identify a single, rare short telomere. While Q-FISH of telomeres on metaphase spreads often reveals signal-free ends indicative of critically short telomeres, this method requires cells to be actively dividing and thus eliminates the possibility of a direct comparison between dividing versus senescent cells (Graakjaer et al., 2003; Lansdorp et al., 1996a). Flow-FISH easily allows for the determination of the percentage of cells that have a short mean telomere length, but does not allow for the detection of a single short telomere within a cell (Rufer et al., 1998). STELA allows for the detection of a single short telomere among the distribution of telomere lengths on a given chromosome. This gives us more information regarding the presence of short telomeres than any other method, but still has limitations. In order to accept the distribution of short telomeres identified by STELA as indicative of the distribution of short telomeres in the cell population, one must make the assumption that sudden catastrophic telomere loss occurs with equal frequency and magnitude on all chromosomes. Since STELA only amplifies and measures

telomeres of a specific chromosome (determined by the design of the forward primer), and STELA primers are only available for a small number of chromosomes, it is impossible to validate that assumption.

A variation of STELA which retained the ability to detect individual telomere molecules but which was not constrained to telomeres of a single chromosome would allow for the creation of a universal distribution of all telomere lengths in a cell population. This method would be superior to TRF in that it would not have a bias against short telomeres, and would be superior to the original STELA when studying short telomeres because it would require no assumptions about the relative frequency of short telomeres among all chromosomes. Thus, the objective of this work was to develop a variant of STELA, named Universal STELA, which would yield an accurate distribution of telomere lengths on all chromosomes and allow for the study of the shortest telomeres in experimental settings.

METHOD DEVELOPMENT AND RESULTS

Summary of approach

Telomere specific STELA involves the ligation of a terminal "telorette" tag to the end of either the C- or G-rich strand, and multiple rounds of PCR amplification use a reverse primer specific to the ligated tag and a forward primer that is specific to a unique, telomere-specific sequence located in the subtelomere. In order to use a similar approach but exchange telomere specificity for the universal amplification of all telomeres, genomic DNA is digested with chosen restriction enzymes which leave a characteristic overhang near the beginning of the telomere. Subsequently, a proximal "panhandle" linker is ligated to the subtelomeric restriction overhang, and this proximal linker serves as the universal proximal tag for all telomeres. In this way, all telomeres are similarly tagged with a proximal "panhandle" linker and a terminal "telorette" linker, and have an equal probability of being amplified during PCR (Figure 2.2).

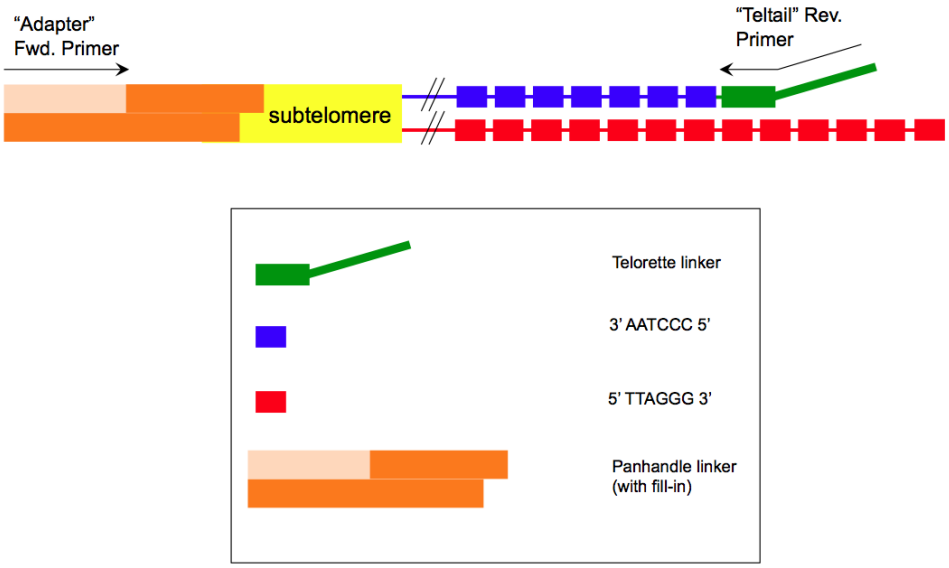

Figure 2.2 Universal STELA General Strategy. Genomic DNA is digested with a chosen enzyme(s) to create a characteristic overhang in the subtelomeric DNA near the beginning of the telomere. A proximal "panhandle" linker is ligated to this subtelomeric overhang and a terminal "telorette" linker is ligated to the end of the C-rich telomere strand. During PCR amplification, the reverse primer is specific to the terminal linker while the forward primer is specific to the proximal linker. All telomeres are tagged with both linkers, so all telomeres have an equal probability of being amplified during PCR.

1. CHOICE OF RESTRICTION ENZYME AND PROXIMAL LINKER DESIGN

Choosing a restriction enzyme for digestion of genomic DNA. Because this general strategy is essentially measuring the length of a telomere restriction fragment, the choice of restriction enzyme is very important. First of all, the restriction enzyme (or group of enzymes) must generate an overhang that can serve as an annealing site during ligation of the proximal linker. Longer overhangs, such as the 4 nt overhang produced by the enzyme NlaIII, provide a

good target for annealing and ligation. A group of 4 enzymes (MseI, NdeI, CviQI and BfaI) all produce the same 2 nt –TA overhang. After considering the overhang generation, it is important to consider how frequently the enzymes will digest the genomic DNA, and how close to the telomere they will cut. Of the above enzymes, all but NdeI are 4 base cutters, so they cut relatively frequently in the genome. It is difficult to determine exactly how close to the telomere the enzymes will cut, due to the unknown length of the "X-region" (a portion of the subtelomere that is resistant to restriction digestion) (Steinert et al., 2004). Additionally, not all subtelomere sequences are known, making it difficult to directly map a restriction site as one would do in molecular cloning. A TRF showing genomic DNA from Hela cells digested with either NlaIII or the combination of four –TA overhang producing enzymes show that the –TA enzymes produce shorter telomere restriction fragments as compared to NlaIII (Figure 2.3), suggesting that one or all four of these enzymes cut closer to the telomere than NlaIII.

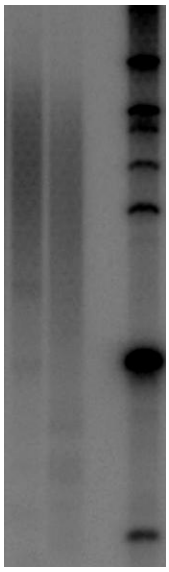

Figure 2.3 TRF of Hela DNA digested with NlaIII (left) or –TA overhang enzymes MseI, NdeI, BfaI, CviQI (right). Digestion with the –TA overhang enzymes produces shorter telomere restriction fragments as compared to digestion with NlaIII, suggesting that one or more of the –TA overhang enzymes cuts closer to the telomere.

Designing the proximal "panhandle" linker to amplify tagged telomeres while limiting amplification of tagged genomic fragments. Because all genomic DNA restriction fragments will also have the restriction overhang on both ends, whatever proximal linker that is designed for use in Universal STELA will also be ligated to both ends of genomic fragments. In subsequent PCR reactions, these tagged genomic fragments could outcompete tagged telomeres for amplification since they will likely be shorter (and thus more easily amplified) as well as orders of magnitude more abundant. The "panhandle" design of the proximal linker is designed to suppress PCR amplification of these genomic fragments by promoting formation of a hairpin loop structure during PCR when a

fragment is tagged with the linker on both ends. While this suppression PCR method is generally useful for low molecular weight products, it is not certain that it will be completely successful in suppressing amplification of genomic fragments that are potentially large. The design is theoretically solid, however, and is adaptable to any restriction enzyme that produces an overhang. We designed panhandle linkers for both –TA overhangs as well as the 4 nt NlaIII overhang. A schematic and description of the –TA overhang design which details the suppression PCR of genomic fragments as well as amplification of the telomere fragments is shown in Figure 2.4. A listing the sequences of the oligonucleotides used to make the proximal panhandle linker is found in Table 2.2.

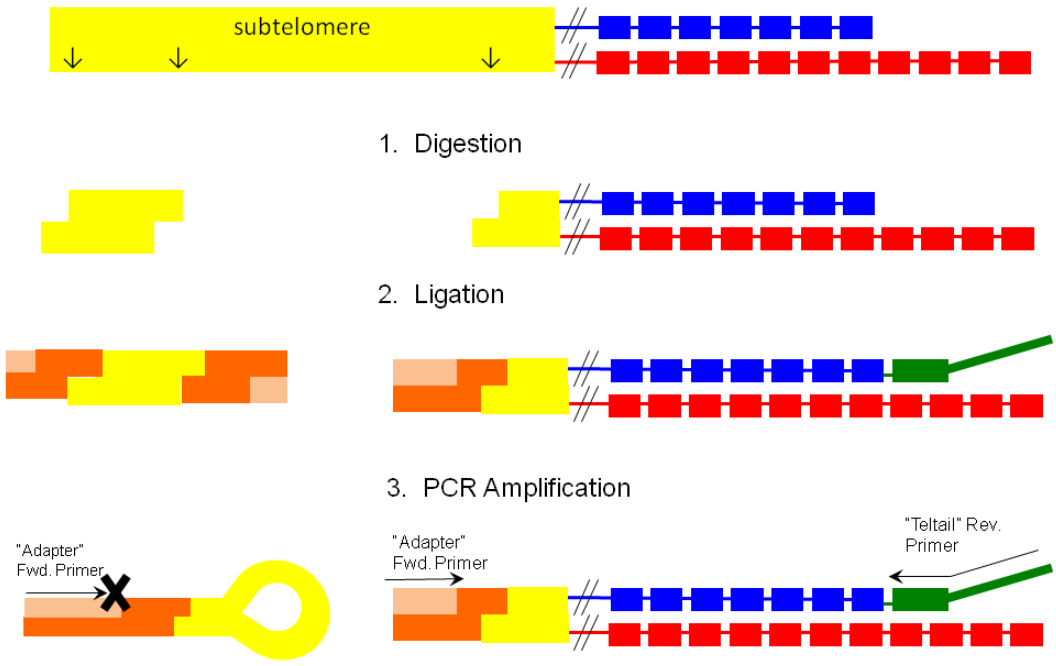

Figure 2.4 Schematic of Universal STELA using the –TA overhang strategy
Genomic DNA is digested with four enzymes which all produce a –TA overhang. Digestion yields a multitude of genomic restriction fragments (left), which have the –TA overhang on both ends, as well as telomere restriction fragments (right) which have the –TA overhang on the proximal fragment end. On telomere fragments, a terminal telorette linker (green) is complementary to the 3' G-rich overhang and is ligated to the end of the C-rich telomere strand, while the pre-annealed, proximal "panhandle" linker (orange) is annealed to the –TA overhang. During the ligation reaction, all genomic fragments will have the panhandle linker ligated to both ends. A fill-in step (light orange) copies the primer binding site onto the C-rich strand in telomere fragments, while generating self-complementary ends on genomic fragments. During the PCR melt/annealing steps, tagged genomic fragment ends will self-anneal and form a hairpin that cannot be amplified, while telomere fragments will be amplified by the forward and reverse primers.

Table 2.2 Sequences of oligonucleotides for NlaIII and –TA panhandle designs

NlaIII:

Long panhandle:
5’TGTAGCGTGAAGACGACAGAAAGGGCGTGGTGCGGACGCGGGCATG3’
Short panhandle:
5’CCCGCGTCCGC 3’
Forward Primer:
5’TGTAGCGTGAAGACGACAGAA 3’

-TA overhang:

Long panhandle:
5’TGTAGCGTGAAGACGACAGAAAGGGCGTGGTGCGGACGCGGG 3’
Short panhandle:
5’TACCCGCGTCCGC 3’
Forward Primer:
5’TGTAGCGTGAAGACGACAGAA 3’

2. LIGATION OF PROXIMAL "PANHANDLE" AND TERMINAL "TELORETTE" LINKERS

A single ligation step performed at 17° C for 15 hours tags both the proximal and terminal ends of telomere restriction fragments. Any STELA-based method requires the ligation of a unique tag, called a "telorette," at the end of the telomere strand (either C- or G-rich) that is to be amplified during PCR. The telorette serves as a unique DNA sequence at the end of the otherwise repetitive telomeric DNA which can be utilized as the reverse primer site in PCR. While the original STELA method utilizes a subtelomeric forward primer site that is telomere specific, Universal STELA requires ligating a proximal linker to the subtelomere. This proximal "panhandle" linker provides a unique primer site that allows for the amplification of all telomeres. The major consideration when designing the ligation step of Universal STELA was whether the two linkers needed to be ligated individually in separate ligation reactions, or if ligation conditions could be determined which would allow for a single ligation step in which both proximal and terminal linkers were ligated to their respective telomere locations. The original STELA method (Baird et al., 2003) performed ligation of the terminal telorette linker using T4 DNA ligase at 35° C for 12+ hours. This high ligation temperature theoretically increases the specificity of the ligation products. This high ligation temperature is critical in scenarios where it is critical that the linker be perfectly aligned and ajoined to the last base of the telomere

(Sfeir et al., 2005), however the telorettes are designed with ~7 nt of complementarity to the 3' overhang, and can thus stably anneal at the telomere end at a lower ligation temperature; we currently use a 17° C ligation temperature for 15+ hours for C- and G-STELA for routine telomere length measurements (Zhao et al., 2009). The proximal linkers designed for use with either NlaIII digestion or MseI/"-TA" digestion have a 4 or 2 nt overhang for ligation, respectively, which requires a lower ligation temperature for annealing to be able to occur. A single ligation step which allowed for the ligation of the proximal and terminal linkers is highly preferable to individual ligations because it streamlines the assay and eliminates approximately one day of passive time from the protocol. To test the efficiency of a one-step ligation, ligation reactions of both NlaIII and -TA overhang digested genomic DNA were set up to include both proximal and terminal linkers with T4 DNA ligase, and incubated at 17° C, RT and 35° C for 15+ hours/overnight. Ligation at 17 C consistently produced bands for both the NlaIII and –TA linker Universal STELA strategies, and was adopted as the temperature for a single ligation step.

Ratio of proximal:terminal linkers in a single-step ligation reaction. Since we chose to ligate both the proximal and terminal linkers in a single reaction, it was important to consider the ratio of the linkers added to the ligation reaction. The original STELA protocol (Baird et al., 2003) used a final concentration of 0.9 μM of telorettes, while subsequent assay developments

showed that telorette concentration could be reduced many orders of magnitude, increasing ligation specificity without reducing yield of tagged telomeres available for PCR amplification (Sfeir et al., 2005). We chose to use a final concentration of 10^{-2} μM of a mixture of all six C-telorette oligos (0.16×10^{-2} μM each), which should increase specificity while maintaining high sensitivity and having plenty of amplifiable, tagged telomeres. Because the proximal linker in theory will be ligated to both ends of all genomic restriction fragments in addition to the proximal restriction site on telomere restriction fragments, it was important to include enough of the oligo in the ligation reaction to ensure that all telomeres could be tagged. The panhandle linker was created by incubating the 100 μM "long" and 100 μM"short" oligos for each respective restriction site in a 1:2 ratio at 95°C for 5 minutes in order to eliminate any secondary structure that may have formed in the "long" oligo. The panhandle mixture was then cooled to RT for one hour in presence of 50 mM NaCl to promote annealing. We chose to use a final concentration of 10 μM of the annealed panhandle linker in the single-step ligation reaction.

Ligation Specificity: ligation of both proximal and terminal linkers is required for amplification of telomeres. Universal STELA is designed to measure the length of individual telomere molecules which have a proximal linker ligated at a restriction site close to the beginning of the telomere and a terminal linker ligated to the end of the telomere. In Universal STELA reactions,

restriction fragments that are tagged on both ends by the panhandle linker will be in great excess compared to true telomere fragments, and if any of these were to be amplified and contain any telomere sequence (such as interstitial telomere repeat sequences), this would produce a band that would be mistaken for a true telomere. Additionally, non-specific ligation of either linker could result in bands that are not representative of true telomere molecules. In order to test the specificity of our ligation conditions, multiple ligation controls were conducted in which no linkers were added to the reaction, or only one (proximal panhandle OR terminal telorette) linkers were added to the reaction (Figure 2.5). These ligation controls indicate that ligation is very specific and only produces tagged telomeres capable of being amplified when both the proximal panhandle and the terminal telorette linkers are included in the single-step ligation reaction. The presence of a very small number of nearly undetectable bands in the control that includes only the proximal panhandle linker could be due to amplification of a genomic fragment that includes a small amount of interstitial telomeric DNA sequences that caused a small amount of probe to hybridize. These bands are largely negligible, and the results indicate that the established ligation conditions are specific and lead to robust amplification of telomeres. This single-step ligation of both linkers is an improvement on a previously described two-step ligation (Bendix et al., 2010).

Established Ligation Conditions: An restriction site-specific panhandle linker (either –TA overhang or NlaIII overhang) was designed and created by incubating two oligonucleotides ("long" and "short") in a 1:2 ratio at 95°C for 5 minutes and cooling to room temperature over one hour in 50 mM NaCl100 ng of digested genomic DNA was incubated in a10 μl ligation reaction containing 1x ligase buffer, 50 U T4 DNA ligase (NEB), 10^{-2} μM of a mixture of all six C-telorettes (0.16×10^{-2} μM each) and 10 μM NlaIII-specific panhandle for 15 hours at 17°C.

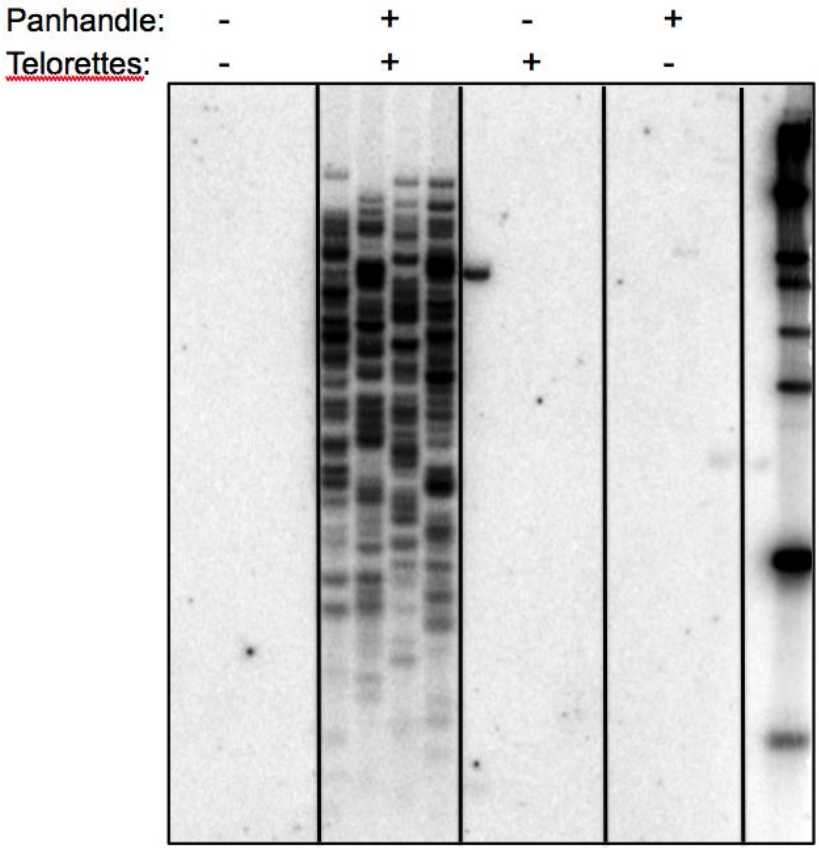

Figure 2.5 Ligation of both proximal panhandle and terminal telorette linkers is required for telomere amplification. Multiple ligation control reactions were performed in which no linkers were provided, or only one linker was provided. These controls indicate that both linkers are necessary in order to amplify telomere molecules, and exclude the possibility that Universal STELA produces large numbers of artefact bands which are not representative of true telomere molecule lengths. These controls indicate that the single-step ligation of both linkers is specific and only produces amplification of molecules that are tagged by both proximal and terminal linkers.

3. PCR AMPLIFICATION OF TAGGED TELOMERE MOLECULES

The use of the PCR additive DMSO increases specificity of telomere amplification and reduces background amplification of genomic DNA. STELA PCR is complicated due to the nature of telomeres: they are long and repetitive. Universal STELA adds another degree of complexity to the PCR process, because there are vast excesses of non-target molecules (genomic restriction fragments) which could theoretically be amplified by the single forward primer because they are tagged on each end with the primer recognition sequence. The panhandle design of the assay is one step to limit this "background" amplification of genomic restriction fragments, and is designed to suppress amplification of molecules that can self-anneal and form a hairpin during the melt/anneal stages of PCR. However, this suppression PCR strategy is most effective for low molecular weight molecules and examination of the Ethidium Bromide stained Universal STELA agarose gels reveals a background DNA smear that is always present to some degree. While this smear does not affect the analysis of Universal STELA data in any way (bands are only detected on the Southern blot if they contain telomere DNA), it is a theoretical and practical challenge because amplification of the multitude of genomic fragments in effect competes with the amplification of the less frequent tagged telomeres. In an attempt to further increase the specificity of amplification of telomere molecules only, and to reduce the background amplification of genomic fragments, the

addition of the PCR additives DMSO and Betaine were tested. In PCR reactions, DMSO facilitates DNA strand separation in GC-rich sequences as well as secondary structures by disrupting base pairing; Betaine is an isostabilizing agent that reduces secondary structure formation in GC-rich regions and also equalizes the contribution of A/T and G/C base pairs to the stability of double stranded DNA (Frackman et al., 1998).

PCR controls were established where a 1:10,000 dilution of a previously amplified Universal STELA sample were incubated in new PCR reactions containing either 1M Betaine, 5% DMSO, or a combination of both 1M Betaine and 5% DMSO (Figure 2.6). The Ethidium Bromide-stained gel is shown next to the Southern blot of the same gel. While the reamplification samples that included no PCR additives showed an intense background smear in the higher molecular weight range, the Southern blot of those samples showed poor amplification of telomere bands, with bands in the higher molecular weight not being amplified at all. The addition of both 5% DMSO and 1M Betaine decreased the background amplification on the EtBr gel, with the samples including both 5% DMSO and 1M Betaine showing virtually no background amplification. The use of both additives appeared to reduce the efficiency of amplification of telomere molecules as well, with telomere bands appearing less crisp and less intense. Because 5% DMSO reduced the background amplification significantly and also led to robust amplification of the full range of telomere

molecules, we chose to supplement Universal STELA PCR reactions with 5% DMSO.

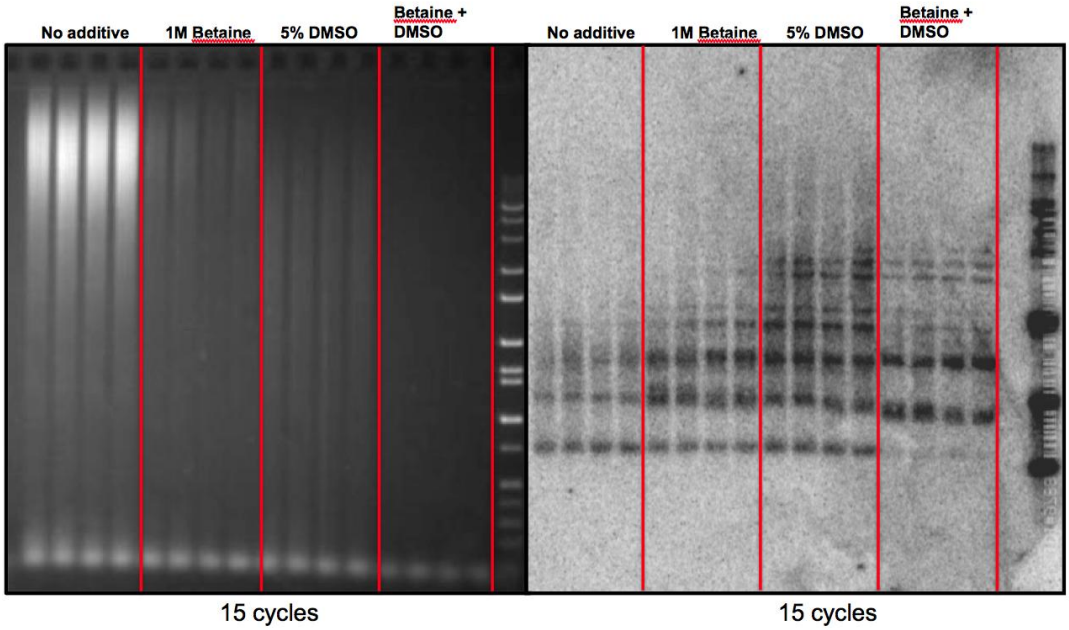

Figure 2.6 The use of the PCR additive DMSO increases specificity of telomere amplification and reduces background amplification of genomic DNA. A Universal STELA PCR amplification product with a known band pattern was diluted 1:10,000 and reamplified for 15 cycles in the presence of either 1M Betaine, 5% DMSO, or both 1M Betaine + 5% DMSO. The resulting products were resolved on a 0.7% agarose gel, stained with EtBr, and proved with a telomere-specific C-rich probe. 5% DMSO added to the PCR reaction reduced the background amplification seen on the EtBr image of the gel while improving the robustness and range of molecular weights of telomere products detected by in-gel hybridization.

Reducing the duration of the initial melting step of PCR increases the range of lengths of amplified telomere molecules. Universal STELA has the potential for a bias against amplifying long telomeres, because shorter telomeres

have an increased probability of being fully extended in earlier cycles, precluding longer telomere molecules from becoming fully extended and exponentially amplified in later cycles. One of the primary goals of optimizing the PCR reaction was to ensure that the full range of telomere lengths could be amplified. A previous study and work in our lab (unpublished) indicated that telomere DNA could potential degrade into smaller molecular weight fragments during even short (5-10 minute) incubations at 95° C. The duration of the initial melt stage of STELA PCR is generally 3-5 minutes at 94-95° C (Zhao et al., 2009), which could theoretically cause a degree of degradation of longer telomeres. We decided to test whether we could observe such degradation in Universal STELA telomere amplification, and if shorter initial melting stages would be capable of producing bands and if those bands would include higher molecular weights. Universal STELA PCR reactions were assembled and the initial melt stage of 94° C was timed at 15 min, 10 min, 5 min, 3 min, 1 min, 30 sec and 15 sec (Figure 2.7). The longest initial melt stages (10 and 15 min) showed a marked decrease in total number of bands; these are longer than the duration one would choose for an initial melt in STELA PCR, but were meant only to test whether prolonged incubation at 94° C would decrease the quantity or quality of the amplified products. Incubations of 5 and 3 minutes are representative of standard STELA protocols, and showed more bands than the longer melting incubations. Surprisingly, very short melting incubations of 1 min, 30 sec and even 15 sec not

only produced the greatest number of bands but also produced higher molecular weight bands. It is possible that longer incubations at 94° C cause enough damage to the integrity of telomere DNA that the number of amplifiable molecules is decreased. The shorter melting durations allow for longer telomeres to be amplified, which improves the overall length distribution that can be assayed using this method. We chose to use an initial melt stage of 30 seconds, which is also the duration of all subsequent melt stages in the PCR program for Universal STELA.

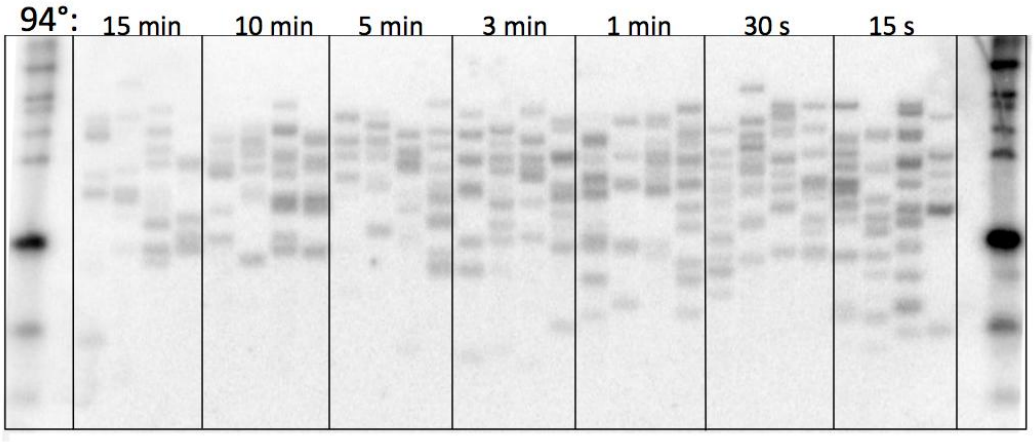

Figure 2.7 Shorter duration of initial melting stage of PCR produces more amplified telomeres across a wider length distribution. The initial melting stage of the Universal STELA PCR program was scaled from 15 minutes to 15 seconds at 94° C. The quantity and range of bands produced with longer 94° C incubations was decreased compared to incubations of 1 min, 30 sec and 15 sec.

Annealing temperature gradient suggests that two-step PCR is efficient and increases specificity for amplification of telomere molecules. A

Universal STELA PCR amplification product with a known band pattern was diluted 1:10,000 and reamplified with an annealing temperature gradient that ranged from 62° C (the annealing temperature used for C- and G-STELA) to 68° C (the extension temperature). The gradient was performed both with and without the addition of 5% DMSO. Ethidium bromide images of the gel and Southern blots probed with telomere-specific C-rich probe are shown (Figure 2.8). As expected, the reactions that contained 5% DMSO had reduced background amplification on the EtBr image of the gel as compared to the samples that contained no PCR additive. In the reactions that did not contain DMSO, the lower annealing temperatures had increased intensity of the background amplification, especially at higher molecular weights, suggesting that increasing the annealing temperature increased the specificity for amplification of telomere molecules. There was little detectable difference in the quantity or quality of the telomere products on the Southern blot, indicating that using higher annealing temperatures still produced efficient amplification. Based on this evidence, a two-step PCR program was adopted in which the annealing step was eliminated, and each PCR cycle consisted of only a 30 second melt at 94°, followed by a 12 minute extension step at 68° C.

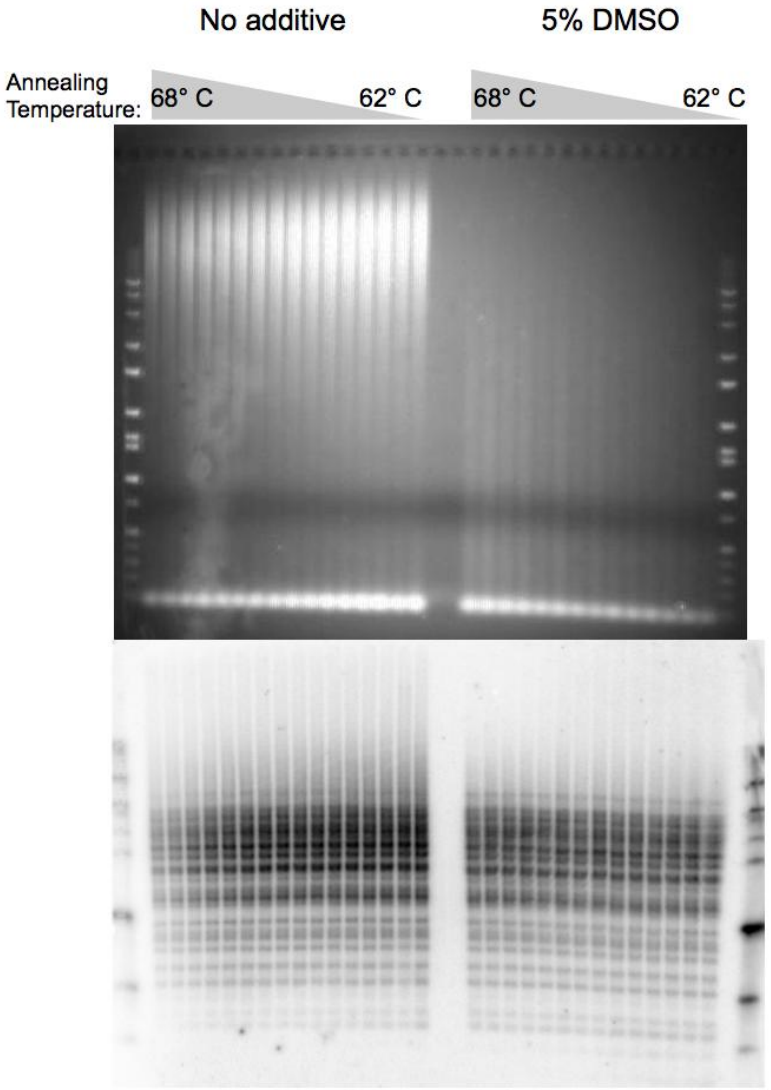

Figure 2.8 Annealing temperature gradient suggests that two-step PCR is efficient and increases specificity for amplification of telomere molecules. A Universal STELA PCR amplification product with a known band pattern was diluted 1:10,000 and reamplified with an annealing temperature gradient that ranged from 62° C to 68° C. Ethidium bromide image of gel (top) and Southern blot (bottom) indicate that primers can anneal at 68° C – the temperature used for extension – and thus a two-step PCR program in which the annealing step with a lower annealing temperature could be eliminated to retain efficiency and improve specificity of telomere amplification.

Primer controls indicate that two-step PCR specifically amplifies telomere molecules. To demonstrate the specificity of the Universal STELA PCR reaction, primer controls were established in which PCR was carried out with no primers, or only the forward/reverse primers (Figure 2.9). When an annealing temperature of 62° C was used, amplification products were detected when only the forward primer was included in the reaction. However, when a two-step PCR program that did not allow primers to anneal at a lower annealing temperature was used, amplification products were very specific to the samples which included both the forward and reverse primers. This reinforces the use of the two-step PCR protocol, and demonstrates that Universal STELA products detected by Southern blot must contain both the proximal panhandle linker (targeted by the forward primer) and the terminal telorette linker (targeted by the reverse primer). This indicates that bands which are analyzed for molecular weight likely represent full-length, true telomere molecules. It is unclear why bands were present in the forward primer only samples amplified with a three-step protocol (Ta = 62), but not in the two-step PCR protocol. This difference suggests that the products are a result of non-specific annealing of the primer. Because the molecular dynamics of amplifying repetitive telomere tracts of many kilobases are complex and not completely understood, there is always the possibility for molecular artifact. Primer controls like the ones performed here are the best way to ensure that artifact is kept to a minimum.

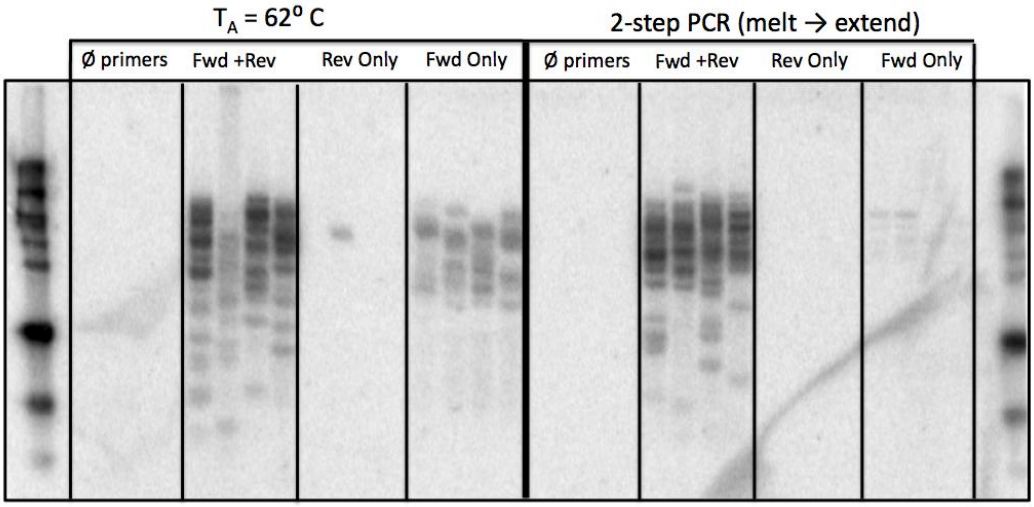

Figure 2.9 Primer controls indicate that two-step PCR protocol specifically amplifies telomere molecules. Primer controls were established in which PCR was carried out with no primers, or only the forward/reverse primers. Primer controls were performed with a traditional three-step PCR protocol with an annealing temperature of 62° C, as well as a two-step PCR protocol which has only a melt and extend step for each cycle.

Established PCR conditions: Multiple PCR reactions were performed (Initial fill-in step of 68°C for 20 min; Initial melt of 94°C for 30 s followed by 22 cycles of 94°C for 15 s + 68°C for 12 min) using Extensor Hi-Fidelity PCR Master Mix 1 (ABGene, Thermo Scientific) in 25 µl reaction containing 100 pg ligated DNA, 0.5 µM primers (Adapter forward primer and C-Teltail reverse primer) and supplemented with 5% DMSO.

4. RESOLUTION OF TELOMERE BANDS AND IN-GEL HYBRIDIZATION WITH TELOMERE-SPECIFIC PROBE

Telomere amplification products were resolved on a 0.7% agarose gel, and subject to in-gel hybridization using a ^{32}P-labeled telomere-specific

[$(TTAGGG)_4$] oligonucleotide probe in a hybridization oven at 42 ^{o}C for at least four hours. The gel was then washed once with low-stringency buffer (2x SSC) and twice with high stringency wash (0.1x SSC, 0.1% SDS) for 15 minutes each at 42° C. The gel was then exposed to a PhosphorImager screen and scanned on a Typhoon biomolecular imager (GE Healthcare Life Science). This represents a departure from the C- and G-STELA protocols in that traditional STELA generally utilizes capillary transfer of the products to a charged nylon membrane and probing with a subtelomere-specific probe generated by random priming. While a subtelomere probe provides great specificity in traditional STELA, it is impossible in Universal STELA when all telomeres have an equal probability of being amplified and represented on the gel. The use of a long, random-primed subtelomere probe precludes the use of in-gel hybridization because the probe is too large to efficiently penetrate the gel matrix. Because the telomere-specific probe used for Universal STELA is a small molecule, it can easily enter the gel for in-gel hybridization. This is faster than capillary transfer, which is another advantage of Universal STELA.

5. UNIVERSAL STELA LENGTH MEASUREMENTS IN HELA AND T24 CANCER CELL LINES

In order to test Universal STELA, two cancer cell lines were chosen which are known to have different telomere lengths. T24 bladder cancer cells are known to have a short average telomere length, while Hela cervical cancer cells have

average to long telomeres. The cells were expanded in culture and genomic DNA was isolated. The gels shown below are from the Universal STELA performed on genomic DNA digested with –TA overhang producing enzymes and ligated with the –TA overhang proximal panhandle and a mix of six C-telorettes. All ligation and hybridization procedures were performed as described above. Many PCR amplification reactions were performed for each cell type, and a total of approximately 550 telomere amplification products were analyzed for molecular weight using AlphaEaseFC (AlphaInnotech) software and all statistical analyses was carried out using Microsoft Excel and GraphPad Prism. Representative gels and summary statistics of all analyzed bands are shown in Figure 2.10.

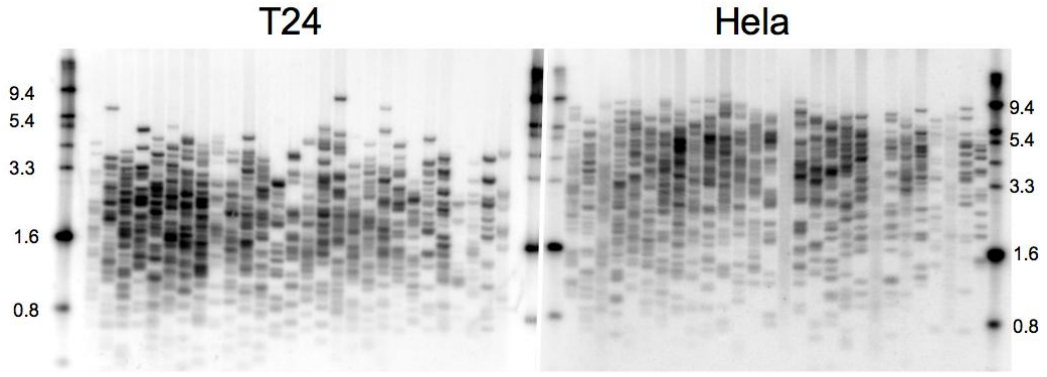

Mean (kb)	2.16
Standard Error	0.05
n =	540
Range (kb)	7.47
Minimum (kb)	0.39
Maximum (kb)	7.86

Mean (kb)	3.80
Standard Error	0.08
n =	561
Range (kb)	8.27
Minimum (kb)	0.63
Maximum (kb)	8.90

Figure 2.10 Representative Universal STELA gels and summary statistics of telomere length analysis in T24 and Hela cancer cell lines.

Visual examination of the distribution of the telomere amplification products allowed for the immediate detection of a difference between the two cell lines. While both cell lines had very short telomeres (< 800 bp) and some long telomeres (> 7 kb), the T24 telomeres had a tighter distribution at lower molecular weights while the Hela telomeres had a wider distribution that spanned the full range of detected telomere products. The first analysis performed was to calculate basic summary statistics such as the mean telomere length, the range of the length distribution, and the median. The calculated mean length in T24 was 2.16 kb, while the calculated mean length in Hela was 3.80 kb. Both of these mean length measurements are slightly lower than the normally attributed mean telomere length of the two cell lines (as usually measured using TRF analysis). This is likely due to the fact that Universal STELA is better able to measure short telomeres, and is also a function of the enzymes used to digest the genomic DNA for both Universal STELA and TRF. Both assays are essentially measuring the length of a telomere restriction fragment, so the variable amount of subtelomeric DNA that remains attached to the telomere has great influence on the final length measurement. In Universal STELA using the –TA overhang method, one enzyme in particular (MseI) cuts very close to the beginning of the telomere, which would make the resulting length measurements shorter than when other enzymes which cut further away are used.

In order to visualize the telomere length distribution, fine-resolution histograms with bin size of 100 bp were created, and cumulative percentage was superimposed (Figure 2.11A). A box plot in which the whiskers represent the maximum and minimum measured telomere lengths, and the box respresents the middle 50% of telomeres, was created to directly compare the telomere length distributions of the two cell lines (Figure 2.11B). These visual representations of telomere length distribution in the two cell lines provide much more information than a simple mean telomere length. In T24, the shortest 75% of telomeres were less than 3 kb, and yet the longest 25% of telomeres was widely distributed to a maximum length of nearly 8 kb. It would be interesting to isolate clones of T24 and measure telomere length of the clones using Universal STELA; analysis of the skewed T24 length distribution suggests the possibility that rare T24 cells have much longer telomeres than the mean T24 telomere length. The distribution in Hela is much more evenly distributed than in T24, however there was a high frequency of shorter than average telomeres that produces a large spike in the distribution curve at approximately 1.5 kb. This similarly suggests that analysis of telomere lengths in Hela clones may reveal that some clones have shorter telomeres than the average telomere length. This cluster of short telomeres could also be attributed to oxidative damage or other culture-related stresses.

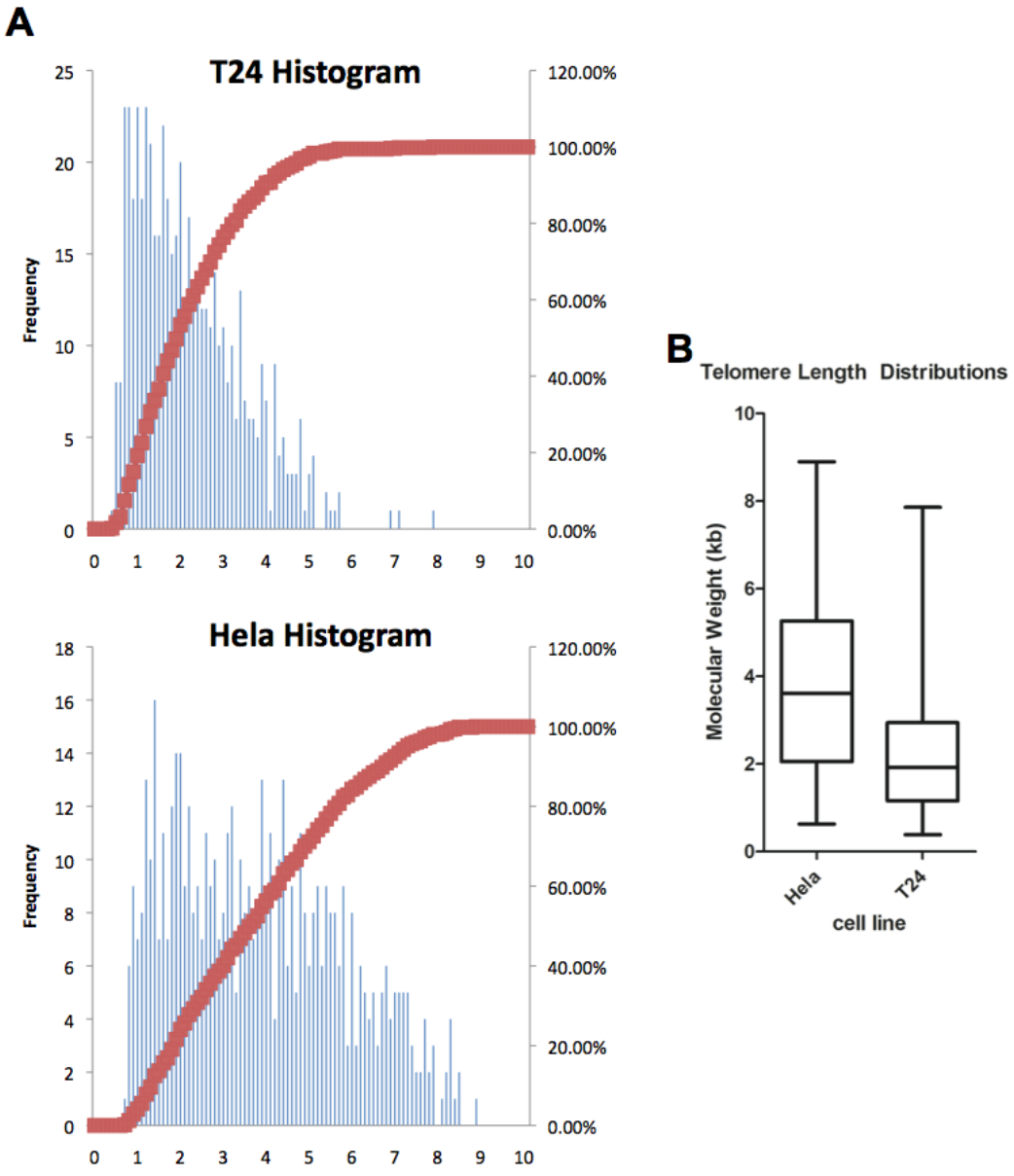

Figure 2.11 Telomere length distribution in T24 and Hela cancer cell lines. A) Distribution curve with superimposed cumulative frequency. **B)** box-and-whisker plot of quartile analysis. Whiskers represent maximum and minimum telomere lengths, while box outlines middle 50% of telomeres.

DISCUSSION

Universal STELA amplifies individual telomere molecules, similarly to the original STELA design, however it is capable of assaying all telomeres in the cell at the same time. This means that Universal STELA retains all of the advantages of the original method design (such as being able to measure lengths of short telomeres and being able to measure telomere length with a very small amount of DNA starting material), yet it also has the added advantage of obtaining a global look at telomere length instead of being limited to studying a single telomere. The role of short telomeres in telomere biology is crucial, as it is the shortest telomeres which induce cells to undergo replicative senescence (Abdallah et al., 2009; Hemann et al., 2001b; Zou et al., 2004b). Thus, examining short telomeres is of critical importance to both aging biology and cancer, as one field seeks to discover how replicative senescence causes aging-related disease and the other seeks to induce replicative senescence in otherwise immortal cancer cells.

The original STELA method has been used to examine short telomeres in the past (Baird et al., 2006; Baird et al., 2003), however these studies are confined by their chromosome specificity. Universal STELA will allow for the study of all short telomeres in the cell, without being limited to assaying just one telomere, or being limited to the handful of telomeres for which telomere-specific STELA is limited to due to subtelomere primer availability. This is especially important

considering it is thought that any telomere can become critically short and thus cause senescence. While telomeres are thought to maintain a relative length over time (Graakjaer et al., 2003; Graakjaer et al., 2004a), suggesting that some telomeres are inherently longer than average and some are inherently shorter than average, any telomere can potentially be targeted by oxidative damage or some other rapid telomere deletion event which would cause it to become critically short.

Because Universal STELA is essentially measuring the length of telomere restriction fragments, the choice of restriction enzyme is critical to the final length measurements. Unlike in molecular cloning experimental designs, it is impossible to determine exactly where restriction enzymes will cut subtelomeric DNA. First of all, not all subtelomeres have been sequenced, and those that have been often contain highly repetitive tracts which make it difficult to pinpoint actual restriction sites. Additionally, there is ample data which suggests that a variable and unknown portion of the subtelomere is resistant to digestion by restriction endonucleases (Steinert et al., 2004). This region of the subtelomere, called the "X-region," is not well understood and is difficult to characterize, but is sure to influence the digestion of genomic DNA with any chosen restriction enzyme, and thus the final length measurement obtained by Universal STELA. While the unknown influence of the X-region likely causes a variable amount of undigested subtelomere to remain attached to telomere fragments, one of the –TA overhang

enzymes (MseI) produces TRF smears so much shorter than when DNA is cut with a mixture of 6 frequent cutting enzymes that it is possible that this enzyme actually cuts telomere variant sequences within the actual telomere. This would cause the –TA overhang Universal STELA to produce variably shorter telomere amplification products than would be measured using other restriction enzymes. The restriction site of MseI is 5' TTAA 3', which is both a telomere variant sequence as well as contains only thymidine and adenine bases. It is unclear why this enzyme is able to cut so close to – or within – the telomere, while other restriction enzymes are not able to cut in the "X-region" of the subtelomere. One proposed explanation for the mechanism behind the X-region protection against restriction digestion is that the DNA may be composed of nucleotides with altered bases, such as "Base J" found in the telomeric DNA of trypanosomes (Ulbert et al., 2004). Since the restriction site of MseI contains only T and A, additional enzymes which cut sites containing only T and A were tested in a TRF to see if they also showed extensive subtelomeric digestion and short TRF smears (data not shown). None of the enzymes tested produced a similar digestion pattern to that exhibited by MseI, ruling out base modification of T/A as the cause for the enhanced subtelomeric digestion. Another possibility is that MseI cuts telomere variant sequence. Additional enzymes that cut potential telomere variants could likewise be tested in a TRF to try to determine why MseI cuts so close to the telomere. Regardless of the reason that MseI produces shorter telomere

restriction fragments than other restriction enzymes, it is important to take into account the effect that enzyme choice plays on interpreting Universal STELA data. Mean length measurements and length distributions of a single sample are likely to be different depending on whether the –TA overhang or NlaIII Universal STELA (or any other subsequently designed strategy utilizing a different restriction enzyme) is used.

In summary, Universal STELA is the only available method of telomere length measurement which can assay all telomeres in the cell and detect critically short telomeres, producing a complete telomere length distribution. While some have suggested that such an analysis is not suitable for measuring mean telomere length (Bendix et al., 2010), the ligation and PCR optimization steps outlined in this chapter have ensured that for most cancer cells, the range of telomere lengths which can be amplified by Universal STELA is sufficient to determine a mean telomere length. The true power of the assay is not in its ability to calculate a mean, but to view the shape of the distribution of telomere lengths in a cell population. In studies where telomere length is shortening (such as in aging cell lines or in aging biology experiments) or elongating (such as during telomerase extension), the change of the length distribution over time could be evaluated. This assay can also be used to compare the fraction of short telomeres in different samples. This could potentially have clinical and epidemiological ramifications, since short telomeres have been associated with a number of human aging related

diseases as well as pre-cancerous lesions. Universal STELA provides another valuable tool to telomere and telomerase biologists that are interested in conducting telomere length studies, especially ones which concern short telomeres.

CHAPTER THREE

TELOMERE LENGTH IN CANCER STEM CELLS AS AN INDICATOR OF SUSCEPTIBILITY TO TELOMERASE INHIBITION THERAPY

SUMMARY

The ideal cancer treatment would specifically target cancer cells yet have minimal or no adverse effects on normal somatic cells. Telomerase is expressed in more than 85% of cancer cells, making it a nearly universal cancer marker, while the majority of normal somatic cells are telomerase negative. Telomerase activity confers limitless replicative potential to cancer cells, a hallmark of cancer which must be attained for the continued growth that characterizes almost all advanced neoplasms (Hanahan and Weinberg, 2000). Taken together, telomerase is both specific to cancer and essential for cancer progression, making it an ideal target for cancer therapeutics (Ouellette et al., 2011; Shay and Wright, 2002). Telomerase inhibition therapy causes telomeres of cancer cells to gradually shorten, imposing a biological limit on the ability of a tumor to grow, and the telomerase inhibitor Imetelstat (GRN163L) is currently being tested in several phase II clinical trials. Telomerase inhibition therapy has the potential to prevent recurrent disease by limiting the replicative potential of residual and metastatic cancer cells. Cancer stem cells (CSC) are rare, slow-dividing, drug-resistant

cancer cells that are proposed to be responsible for cancer recurrence and metastasis. To further evaluate the potential of telomerase inhibition therapy to prevent recurrence and metastasis, it is critical to characterize cancer stem cells in terms of their telomere length and their response to telomerase inhibition therapy. A recent study indicated that telomerase inhibition using Imetelstat caused depletion in the cancer stem cell population, suggesting that the CSC populations were particularly susceptible to telomerase treatment. In this study, we use Universal STELA to measure the distribution of telomere lengths in three cancer cell lines and their matched, sorted cancer stem cell populations, to evaluate the hypothesis that the sorted CSCs have a larger fraction of short telomeres than the unsorted, parent cancer cell population.

INTRODUCTION

Telomerase Inhibition as a targeted cancer therapeutic

A fundamental quality of cancer cells is their capacity to replicate without limits, which is achieved by telomerase-mediated telomere maintenance in the majority of advanced tumors (Ouellette and Choi, 2007; Shay and Wright, 1996). Thus, telomerase inhibitors have the potential to be used as a selective anti-cancer therapy which disrupts the replicative capacity of telomerase-positive cancer cells (Ouellette et al., 2011). Normal somatic cells which do not utilize telomerase

activity to maintain telomere length would be largely unaffected, and normal telomerase positive cells (such as germ cells and stem-like cells) almost always have longer telomeres compared to telomerase-positive cancer cells (Wright et al., 1996), limiting their susceptibility to telomerase inhibition. This may provide a therapeutic window where tumor cells could be driven to apoptosis before normal telomerase positive cells are adversely affected. The region of the telomerase RNA (hTR) that serves as the template for reverse transcription offers an accessible substrate for direct enzymatic inhibition using oligonucleotide-based small molecule inhibitors (Akiyama et al., 2003; Dikmen et al., 2005; Dikmen et al., 2008; Djojosubroto et al., 2005; Gellert et al., 2006; Gomez-Millan et al., 2007; Gryaznov et al., 2007; Hamilton et al., 1997; Herbert et al., 2005; Hochreiter et al., 2006; Jackson et al., 2007; Norton et al., 1996; Ozawa et al., 2004; Shay and Wright, 2005; Wang et al., 2004a; White et al., 2001). While much still needs to be learned regarding the conformation, composition and recruitment of the catalytically active telomerase holoenzyme, it is certain that the template region of hTR must be exposed and accessible in order to synthesize *de novo* telomere repeats. Thus, oligonucleotides that can hybridize to the 11-base hTR template region act as competitive telomerase inhibitors (not antisense targeting messenger RNA). One such compound that has been developed is GRN163L, currently known as Imetelstat. This small molecule is a lipidated N3'-P5' thio-phosphoramidate 13-mer. The thio-phosphoramidate backbone causes

the oligonucleotide to be water soluble, acid stable, nuclease resistant and to form stable RNA duplexes (Asai et al., 2003; Dikmen et al., 2005; Gellert et al., 2006; Gryaznov et al., 2001; Herbert et al., 2002). The 5' palmitoyl moiety of GRN163L causes the compound to be lipid soluble, allowing for cellular uptake without the use of lipophilic carriers and improving telomerase inhibition (Djojosubroto et al., 2005; Gellert et al., 2006; Herbert et al., 2005). The sequence of GRN163L (5'-palmitate-TAGGGTTAGACAA-NH_2-3') targets a 13 nucleotide region of hTR, preventing it from forming an active complex with hTERT.

The effects of GRN163L have been investigated in a number of cancer cell lines and mouse xenograft models. Chronic exposure to GRN163L has been shown to inhibit telomerase and cause telomere shortening in cancer cell lines derived from diverse origins, including tumors of the brain, breast, bladder, liver, lung, prostate and stomach (Dikmen et al., 2005; Dikmen et al., 2008; Djojosubroto et al., 2005; Hochreiter et al., 2006; Marian et al., 2010a; Marian et al., 2010b; Shammas et al., 2008a; Shammas et al., 2008b). GRN163L-induced telomere shortening initiates cellular crisis caused by chromosomal fusions, anaphase bridges and subsequent apoptosis (Dikmen et al., 2005). In mice with human tumor xenografts, GRN163L was well-tolerated and induced telomerase inhibition in doses ranging from 5 mg/kg to 1000 mg/kg (Dikmen et al., 2005).

Xenograft models showed that GRN163L works to inhibit tumor growth, prevent growth of metastases, and sensitizes tumors to conventional chemotherapy agents (Dikmen et al., 2005; Djojosubroto et al., 2005). GRN163L is also able to cross the blood-brain barrier to target glioblastoma xenograft tumors, supporting the further study of using telomerase inhibition alone or in combination with conventional therapies in glioblastoma patients (Marian et al., 2010a). GRN163L has already completed several Phase I trials in patients with chronic lymphocytic leukemia and solid tumors such as breast cancer and non small cell lung cancer (Molckovsky and Siu, 2008). These Phase I trials showed that intravenously infused GRN163L has excellent bioavailability, pharmacokinetics and tolerability, and Phase II trials of GRN163L are now being conducted for patients with NSCLC, advanced breast cancer, chronic leukemia, essential thrombocythemia and multiple myeloma.

Because telomerase inhibitors may require a period of treatment to produce telomeres short enough to trigger cancer cell death, telomerase inhibition therapy may be most effective when used in conjunction with conventional chemotherapies, radiation or other targeted therapeutics such as angiogenic inhibitors. The long lag phase between initiating telomerase inhibition and induction of cancer cell death may allow for increasing the tumor mass, and is likely to be inefficient at reducing tumor bulk as an individual treatment. In

contrast, conventional chemotherapy approaches result in immediate tumor mass reduction without effecting telomere length causing tumors to often develop treatment resistance and eventually there is recurrence of disease (Figure 3.1). Using a telomerase inhibitor such as GRN163L in combination with conventional cancer therapies should cause progressive telomere shortening in cancer cells that are not initially susceptible to combination treatment, theoretically leading to a more durable response and decreased disease recurrence (Figure 3.1). Telomerase inhibitor therapy may also be used as a maintenance therapy following conventional chemotherapy, radiation or surgery to extend survival with reduced side effects of long-term treatment (Figure 3.1). Yet another potential use for telomerase inhibitors is as chemotherapy and/or a radiation sensitizing agent, enabling the efficient use of lower doses of chemotherapy drugs and radiation.

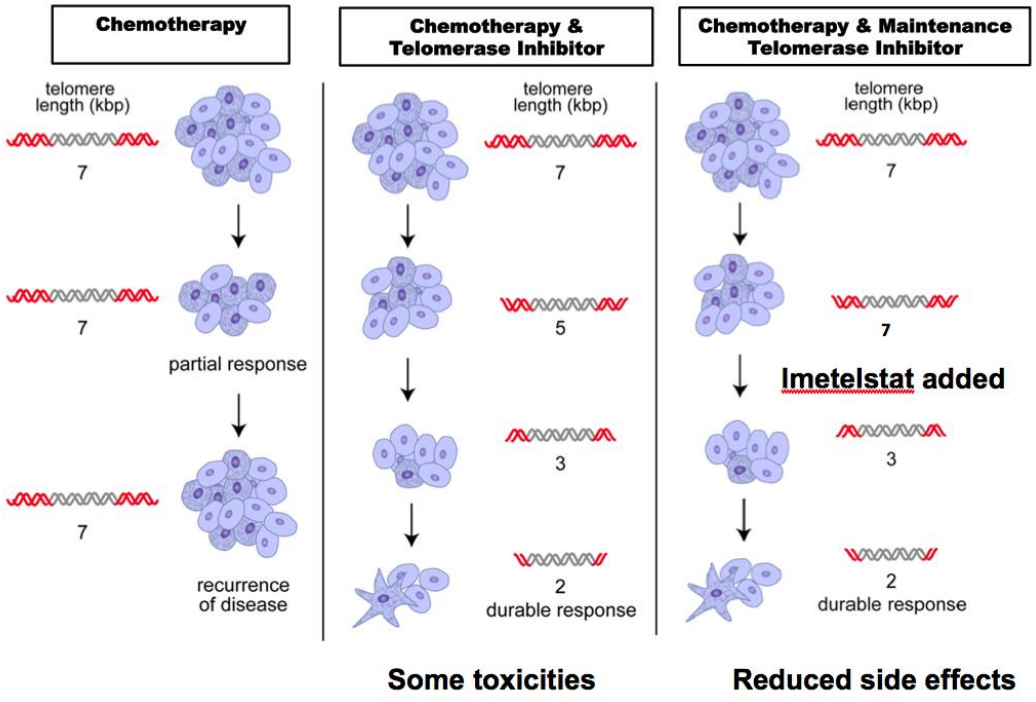

Figure 3.1 Telomerase inhibitors used as combination or maintenance cancer therapies. Traditional de-bulking cancer therapies invoke an initial tumor burden reduction that elicits a partial response, potentially leaving residual cancer cells with intact telomeres and continued replicative potential which lead to disease recurrence. The use of telomerase inhibitors in combination with traditional chemotherapies or radiation induces progressive telomere shortening in any residual cancer cells, limiting the proliferative capacity of these tumor cells and creating a more durable response to therapy. Alternatively, telomerase inhibitors can be administered as a maintenance therapy following traditional de-bulking therapies. It is predicted that residual cancer cells (including cancer stem cells) will lose their infinite proliferative capacity, while minimizing any side effects of long-term telomerase inhibition.

Cancer Stem Cells and Telomerase Inhibition Therapy

An important factor in whether telomerase inhibitors such as GRN163L are able to limit cancer recurrence and relapse is whether the drug is able to target

residual stem-like cancer cells. Tumors are collections of different cell populations that have different biological properties and these cells have a hierarchical organization (Bonnet and Dick, 1997; Dick, 2009). At the top of this hierarchy is the cancer stem cell (CSC), which can be defined as a cell that can self-renew, initiate tumor formation and regenerate all of the cell types found in a tumor (Clarke et al., 2006). CSCs are thought to exhibit a transient quiescence, with lower rates of cell division than the more differentiated cells that compose the bulk of the tumor, and these rare cell divisions are thought to be asymmetrical, resulting in one daughter cell that preserves CSC properties and one daughter cell that can proliferate rapidly and add to the bulk tumor (Clarke et al., 2006) (Figure 3.2 A). Since many standard chemotherapy agents target rapidly dividing cells, the more quiescent CSCs are frequently resistant to drugs that are effective at reducing the bulk tumor population (Dean et al., 2005; Donnenberg and Donnenberg, 2005). There is increasing evidence that rare cancer stem cell populations which are refractory to conventional treatments are responsible for initiation and recurrence in a variety of hematologic and solid tumors (Allan et al., 2006; Farnie and Clarke, 2006; Hermann et al., 2007). Thus, therapies which can target CSCs are needed in order to prevent disease recurrence and create a durable response to treatment (Figure 3.2 B) (Al-Hajj and Clarke, 2004).

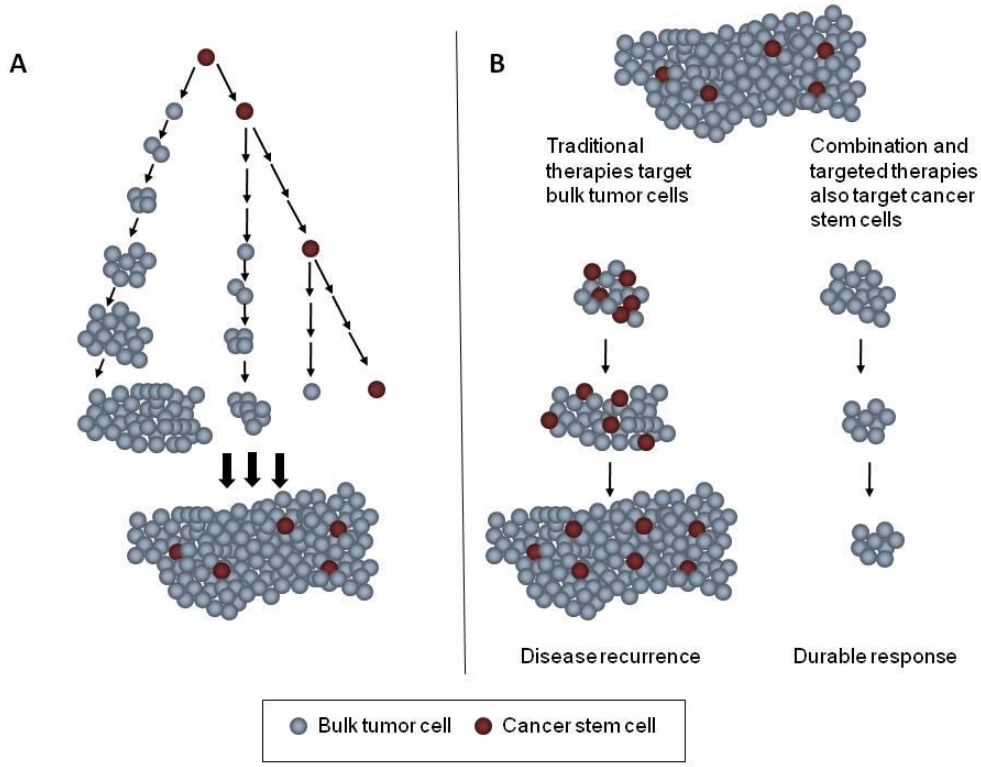

Figure 3.2 Cancer stem cells divide infrequently and asymmetrically, and are resistant to standard cancer therapies. A. Cancer stem cells are more quiescent than more differentiated tumor cells, and divide infrequently. When they divide, they divide asymmetrically to produce one daughter cell which divides rapidly and contributes to the tumor bulk, as well as one daughter cell that retains stem-like properties. **B.** Traditional cancer therapies generally target rapidly dividing cells, and are successful at reducing the size of the tumor bulk. Quiescent CSC are thought to be largely unaffected by de-bulking therapies, and their continued asymmetrical proliferation leads to disease recurrence. Combination and targeted therapies which limit CSC proliferation are thought to produce a more durable disease response.

Although CSCs do not divide as rapidly as bulk tumor cells, both express telomerase suggesting that CSCs may be sensitive to telomerase inhibition (Ju and Rudolph, 2006). While conventional therapies do not target these cancer stem

cells, progressive telomere shortening induced by combination or maintenance treatment with telomerase inhibitors would impair their self-renewal properties. Recent studies have shown that telomerase inhibitors target cancer stem cell populations in multiple myeloma, prostate, brain, breast and pancreatic cancer (Brennan et al., 2010; Castelo-Branco et al., 2011; Joseph et al., 2010; Marian et al., 2010a; Marian et al., 2010b). Cancer stem cell populations were reduced in size (Castelo-Branco et al., 2011; Joseph et al., 2010; Marian et al., 2010b), had reduced proliferation (Brennan et al., 2010), shortened telomeres (Castelo-Branco et al., 2011; Marian et al., 2010b), and impaired ability to form characteristic free-floating spherical colonies (Joseph et al., 2010; Marian et al., 2010a) after treatment with the GRN163L telomerase inhibitor. In this study, we use Universal STELA to investigate whether telomere length can explain CSC susceptibility to telomerase inhibition by measuring the full distributions of telomere lengths in sorted cancer stem cell populations versus their unsorted, parent cell populations of three different cancer cell lines.

RESULTS

Experimental Design Summary

Three cancer cell lines (PANC1 pancreatic cancer cells, MDA-MB-231 breast cancer cells and RPMI8226 multiple myeloma cells) were previously

determined to have imetelstat-susceptible CSC populations (Joseph et al., 2010). Imetelstat treatment of the MDA-MB231 and PANC1 cells was previously found to reduce the size of the CSC population among the total cell population, and this depletion of CSCs was subsequently proven to reduce the tumorigenic potential in xenograft models (Joseph et al., 2010). The rate of depletion of CSCs upon telomerase inhibition in this study led to the hypothesis that these CSCs generally have a larger fraction of short telomeres than the rest of the cell population. To test this hypothesis, Universal STELA was performed on genomic DNA isolated from both CSC and non-CSC populations of PANC1, MDA-MB231 and RPMI8226 cell lines. Statistical analyses were performed to determine the distribution of telomere lengths and to determine whether there was a difference in the mean telomere length.

Mean telomere length in sorted CSC versus non-CSC sorted populations

Universal STELA was used to analyze isolated genomic DNA from sorted CSC and non-CSC sorted populations from three different cancer cell lines. The first statistical parameter examined was the mean telomere length. Universal STELA is capable of providing a good measure of mean telomere length in cancer cells that generally have relatively short telomeres. Calculating a mean telomere length for the sorted CSC and unsorted populations for each cell type allowed for direct comparisons of the means using a two-sample t test. The results were

difficult to interpret, and are detailed in Figure 3.3. PANC1 CSCs had a longer calculated mean (4.887 kb) than the unsorted cell population (4.596 kb); the two-sample t test gave a p value of 0.0492, which indicates that this difference is significant at the 0.05 significance level (although the p value is very close to 0.05). In the RPMI 8226 cells, the CSCs also had a longer calculated mean (1.814 kb) than the unsorted population (1.594 kb), with a p value of $p<0.0001$, suggesting that this relationship is statistically significant. In contrast, the MDA-MB231 CSCs had a shorter calculated mean telomere length (3.243 kb) than the unsorted population (3.463 kb), however the p value ($p<0.0657$) indicates that there is not a statistically significant difference between the two means. This analysis did not reveal a clear pattern for a difference in mean telomere length between CSC sorted and unsorted populations. The fact that PANC1 and RPMI8226 CSCs had longer mean telomere lengths than their respective unsorted cell populations was contrary to the hypothesis that the enhanced susceptibility to growth restriction observed by imetelstat-treated CSCs could be due to shorter telomeres. Only MDA-MB231 CSCs showed a shorter mean telomere length than their unsorted cells, but this relationship was weak and statistically insignificant at the 0.05 significance level. In order to further investigate the potential role of short telomeres in CSC imetelstat susceptibility, detailed telomere length histograms were constructed.

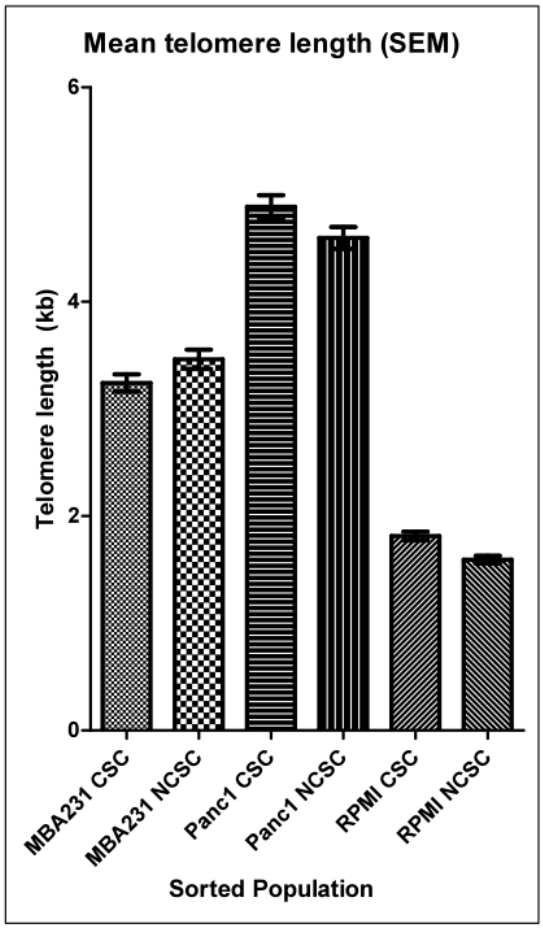

	CSC	Non-CSC	p-value
Panc1	4.887	4.596	**0.0492**
MDA-MB231	3.243	3.463	0.0657
RPMI	1.814	1.594	**<0.0001**

Figure 3.3 Mean telomere lengths of CSC vs. non-CSC sorted populations. Mean telomere lengths were calculated by analyzing hundreds of Universal STELA telomere amplification products for each sample, and means were compared using a two-sample t test.

Telomere length distributions in PANC1 CSC and Non-CSC

Telomere amplification products from Universal STELA were analyzed for telomere length and descriptive statistics were generated (Figure 3.4A). A total of 535 PANC1 CSC bands and 634 PANC1 non-CSC bands were analyzed. Visual examination of the Universal STELA Southern blots (Figure 3.4A) displayed a larger fraction of short telomere amplification products in the non-CSC sorted population when compared to the CSC sorted population. Statistical analysis confirmed this visual assessment. A detailed histogram of telomere amplification products was constructed with a bin size of 100 bp; cumulative frequency of bands was superimposed on the histogram (Figure 3.4B). Quartile analysis was performed and a box plot was constructed to compare the quartile distribution of the PANC1 CSC and non-CSC samples (Figure 3.4B). Finally, the fraction of short telomeres (as represented by the frequency of telomere amplification products that were less than the mean at intervals of < 1 kb, < 2kb, < 3k and < 4kb) was calculated and compared between the CSC and non-CSC populations (Figure 3.4 C). The non-CSC sorted PANC1 population consistently showed a trend of shorter telomeres than the PANC1 CSC population. The PANC1 non-CSC had a shorter mean telomere length ($p<0.0492$), a shorter minimum telomere length, shorter median telomere length, histogram that was more skewed to the left for a preponderance of shorter bands, and displayed a

greater fraction of short telomeres than the sorted PANC1 CSC. The initial hypothesis was that the CSC would have shorter telomeres than the unsorted, non-CSC population, given the rapid decline of the PANC1 CSC population upon telomerase inhibition using imetelstat (Joseph et al., 2010). All of the data collected comparing telomere length distribution in the PANC1 CSC and non-CSC cannot confirm this hypothesis. The comparison of the two mean telomere lengths shows that the PANC1 non-CSC has a shorter mean than the PANC1 sorted CSC population at the 0.05 significance level; however, the 95% confidence intervals of these two means slightly overlap (Figure 3.4A). The conservative interpretation of this data is that there is no detectable difference in the mean telomere length of the PANC1 CSC and non-CSC sorted populations. A more convincing argument for shorter telomeres in the PANC1 non-CSC population is the larger fraction of shorter telomeres (Figure 3.4C) the shape of the distribution, as demonstrated in three independent analyses: histogram, cumulative percentage and quartile analysis (Figure 3.4B).

Figure 3.4A PANC1 CSC and Non-CSC Southern blot and descriptive statistics

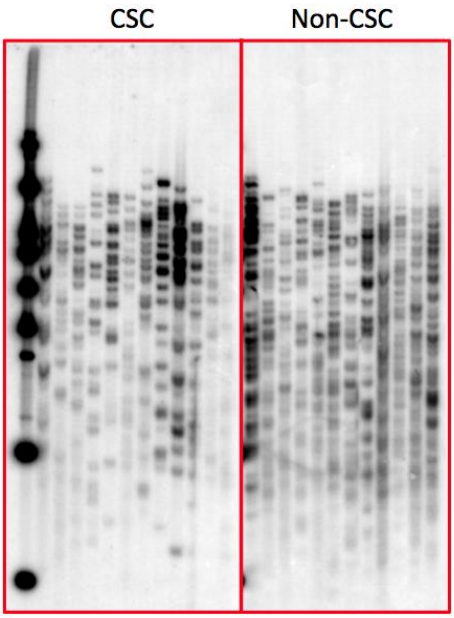

	Panc1 CSC	Panc1 Non-CSC
Number values (n)	535	634
Minimum	0.8	0.64
25% Percentile	2.78	2.308
Median	4.74	4.195
75% Percentile	6.88	6.8
Maximum	10.93	10.52
Mean	4.887	4.596
Std. Deviation	2.496	2.539
Std. Error	0.1079	0.1008
95% CI	(4.675, 5.099)	(4.398, 4.794)

Figure 3.4B PANC1 CSC and non-CSC telomere length distribution

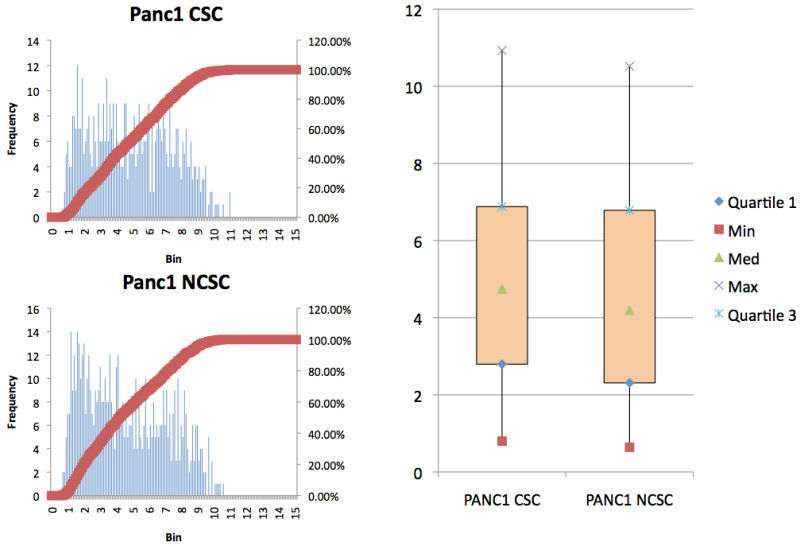

Figure 3.4C PANC1 CSC and non-CSC fraction of short telomeres

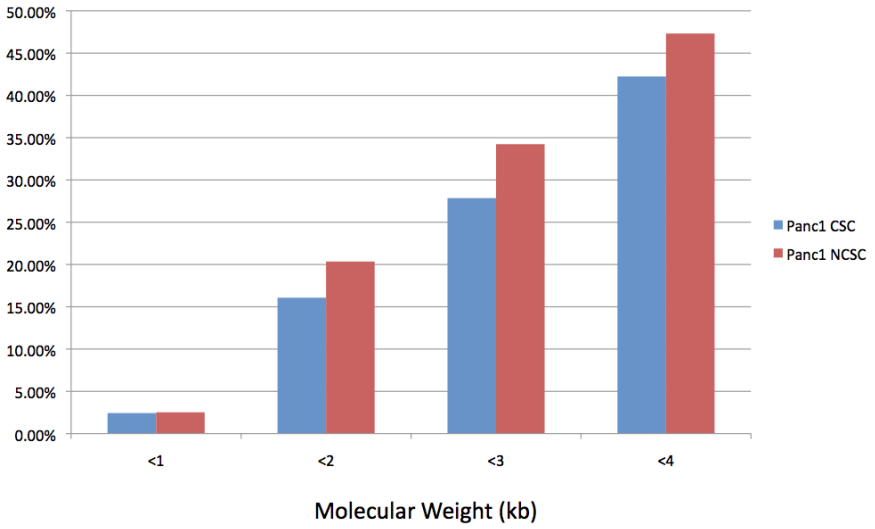

Figure 3.4 Comparison telomere lengths in PANC1 CSC and non-CSC sorted populations. A: Representative Universal STELA Southern blot and descriptive statistics. **B:** histogram and cumulative percentage of telomere lengths binned in 100bp intervals; box plot representing quartile analysis of telomere lengths. **C:** fraction of short telomeres shown by comparing the percentage of all telomere lengths that are < 1kb, < 2kb, < 3kb, and < 4kb. Taken together, these data indicate that the PANC1 non-CSC sorted population has a larger fraction of short telomeres and a lower mean telomere length than the PANC1 sorted CSC population.

Telomere length distributions in MDA-MB231 CSC and Non-CSC

Telomere amplification products from Universal STELA were analyzed for telomere length and descriptive statistics were generated (Figure 3.5A). A total of 359 MDA-MB231 CSC bands and 311 MDA-MB231 non-CSC bands were analyzed. Visual examination of the Universal STELA Southern blots (Figure 3.5A) did not indicate an obvious relationship between the telomere lengths of the sorted CSC and unsorted, non-CSC populations. A detailed histogram of telomere amplification products was constructed with a bin size of 100 bp; cumulative frequency of bands was superimposed on the histogram (Figure 3.5B). Quartile analysis was performed and a box plot was constructed to compare the quartile distribution of the MDA-MB231 CSC and non-CSC samples (Figure 3.5B). Finally, the fraction of short telomeres (as represented by the frequency of telomere amplification products that were less than the mean at intervals of < 1 kb, < 2kb, < 3k and < 4kb) was calculated and compared between the CSC and non-CSC populations (Figure 3.5 C). Analysis of the descriptive statistics indicates that there is not a statistically significant difference between the two mean telomere lengths, with the two-sample t test giving a p value of $p<0.0657$ and the 95% confidence intervals for the two samples showing significant overlap. However, the relationship between the two calculated mean telomere lengths was consistent with the analysis of the distribution of the

telomere lengths in the two samples. In MDA-MB231, the sorted CSC population had a shorter mean telomere length as well as a distribution that was more skewed to the left (shorter telomeres) (Figure 3.5B). Quartile analysis indicated that the MDA-MB231 CSCs had a shorter median telomere length, and that the middle 50% of telomeres were shorter and more tightly distributed than the MDA-MB231 unsorted non-CSCs (Figure 3.5B). Additionally, the MDA-MB231 CSCs had a greater fraction of short telomeres < 4kb as compared to the unsorted, non-CSC population (Figure 3.5C). Taken together, these data suggest that while there is not a statistically significant difference between the mean telomere lengths of these two populations, there may be a larger fraction of shorter telomeres in the MDA-MB231 CSC population.

Figure 3.5A MDA-MB231 CSC and Non-CSC Southern blot and descriptive statistics

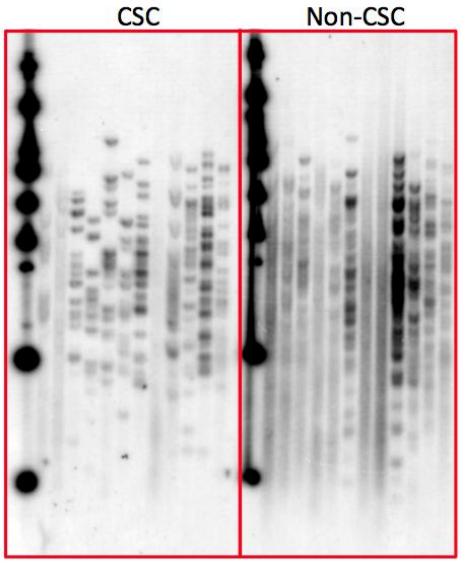

	MDA-MB231 CSC	MDA-MB231 Non-CSC
Number of values	359	311
Minimum	0.67	0.76
25% Percentile	2.11	2.07
Median	3.01	3.28
75% Percentile	4.24	4.71
Maximum	7.6	7.99
Mean	3.243	3.463
Std. Deviation	1.498	1.59
Std. Error	0.07906	0.09014
95% CI	(3.088, 3.399)	(3.286, 3.641)

Figure 3.5B MDA-MB231 CSC and non-CSC telomere length distribution

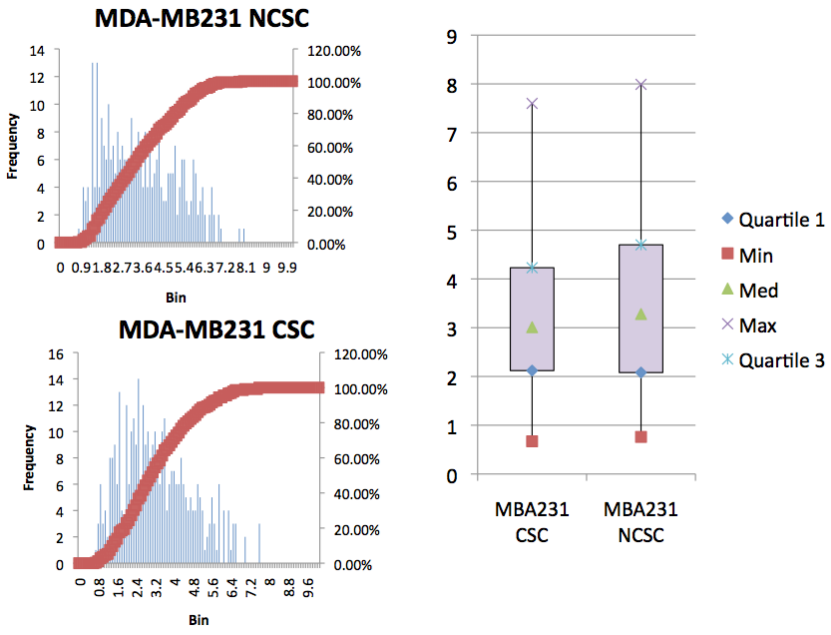

Figure 3.5C MDA-MB231 CSC and non-CSC fraction of short telomeres

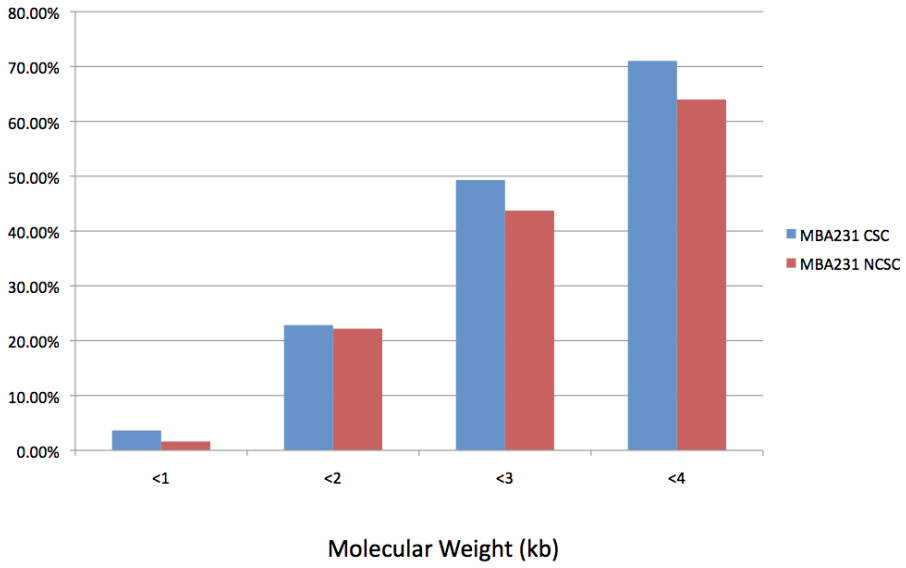

Figure 3.5 Comparison telomere lengths in MDA-MB231 CSC and non-CSC sorted populations. A: Representative Universal STELA Southern blot and descriptive statistics. **B:** histogram and cumulative percentage of telomere lengths binned in 100bp intervals; box plot representing quartile analysis of telomere lengths. **C:** fraction of short telomeres shown by comparing the percentage of all telomere lengths that are < 1kb, < 2kb, < 3kb, and < 4kb. Taken together, these data indicate that the MDA-MB231 sorted CSC population has a larger fraction of short telomeres and a lower mean telomere length than the MDA-MB231 unsorted, non-CSC population, however there is not a statistically significant difference in the means.

Telomere length distributions in RPMI8826 Multiple Myeloma CSC and Non-CSC

Telomere amplification products from Universal STELA were analyzed for telomere length and descriptive statistics were generated (Figure 3.6

A). A total of 356 RPMI8226 CSC bands and 374 RPMI8226 non-CSC bands were analyzed. Visual examination of the Universal STELA Southern blots (Figure 3.6A) suggested that there was a larger fraction of short telomere amplification products in the non-CSC sorted population when compared to the CSC sorted population. The RPMI8226 non-CSC consistently showed a trend of shorter telomeres than the sorted CSCs upon analysis of a detailed histogram and quartile analysis (Figure 3.6B) and analysis of the fraction of short telomeres (Figure 3.6C). The RPMI8226 non-CSC had a statistically significant shorter mean telomere length ($p<0.0001$), a shorter minimum telomere length, shorter median telomere length, histogram that was more skewed to the left for a preponderance of shorter bands, and displayed a greater fraction of short telomeres than the sorted RPMI8226 CSCs. The telomere length distribution data of RPMI8226 CSCs and non-CSCs show that, like the PANC1 cell line, the non-CSCs have a greater fraction of shorter telomeres than the CSC population; however, the difference in the mean telomere length for RPMI8226 was more robust.

Figure 3.6A RPMI8226 CSC and Non-CSC Southern blot and descriptive statistics

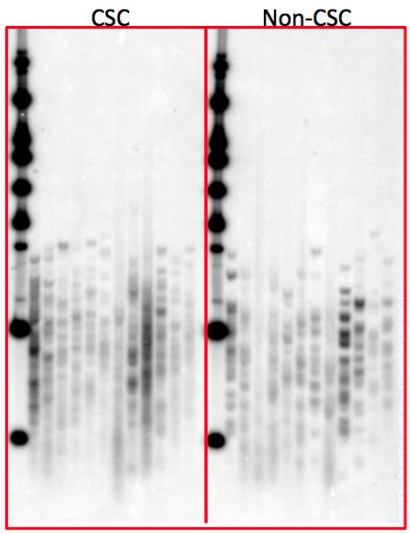

	RPMI CSC	RPMI Non-CSC
Number of values	356	374
Minimum	0.59	0.57
25% Percentile	1.233	1.08
Median	1.705	1.475
75% Percentile	2.31	1.983
Maximum	4.66	4.78
Mean	1.814	1.594
Std. Deviation	0.7467	0.679
Std. Error	0.03958	0.03511
95% CI	(1.736, 1.892)	(1.525, 1.663)

Figure 3.6B RPMI8226 CSC and non-CSC telomere length distribution

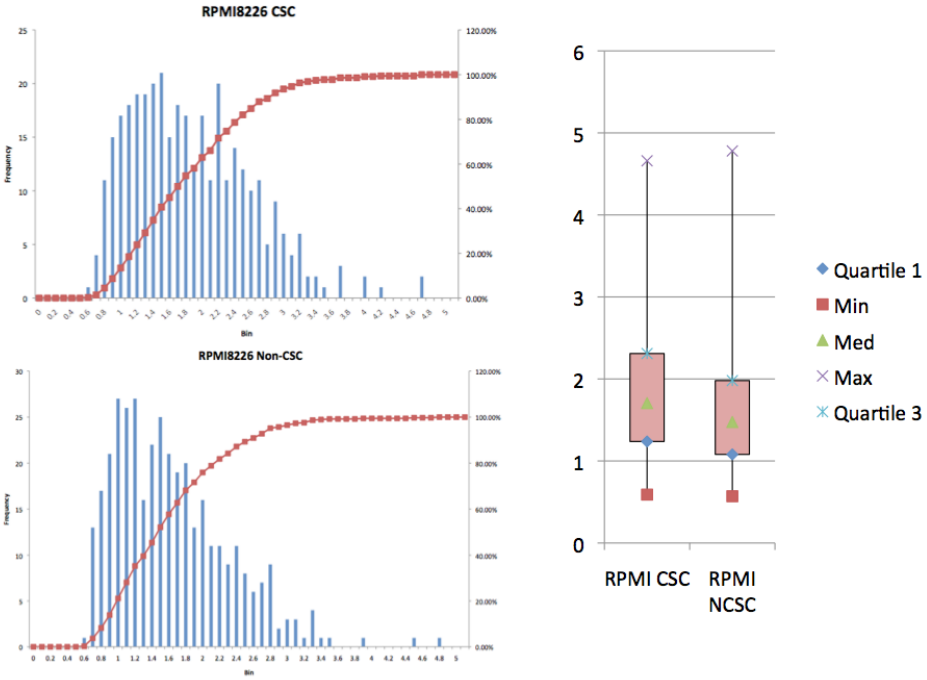

Figure 3.6C RPMI8226 CSC and non-CSC fraction of short telomeres

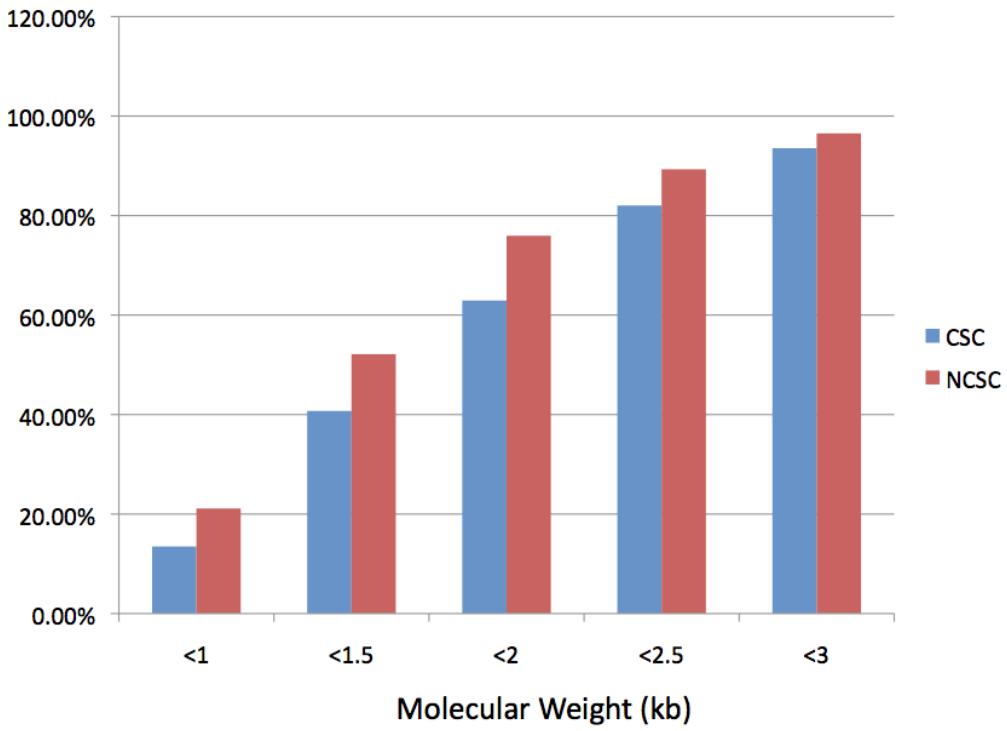

Figure 3.6 Comparison telomere lengths in RPMI8226 CSC and non-CSC sorted populations. **A:** Representative Universal STELA Southern blot and descriptive statistics. **B:** histogram and cumulative percentage of telomere lengths binned in 100bp intervals; box plot representing quartile analysis of telomere lengths. **C:** fraction of short telomeres shown by comparing the percentage of all telomere lengths that are < 1kb, < 1.5kb, < 2kb, and < 3kb. Taken together, these data indicate that the RPMI8226 non-CSC sorted population has a larger fraction of short telomeres and a lower mean telomere length than the RPMI8226 sorted CSC population.

Absence of pattern in difference of telomere length between CSCs and bulk tumor cells

Results from the universal STELA assays showed that there was no consistent pattern of differences in telomere lengths between sorted CSCs and non-CSCs in PANC1, MDA-MB231, and RPMI8226 cell lines (summarized in Figure 3.7). The only cell line that showed a significant difference in mean telomere length was RPMI8226. CSCs showed a trend for shorter telomeres in one cell line, MDA-MB231, while the bulk tumor non-CSC population showed trends for shorter telomeres in PANC1 and RPMI8226. Because no consistent trend was observed between the three cell lines, the increased sensitivity of CSCs to imetelstat could not be explained by telomere length differences between CSC and bulk tumor cells.

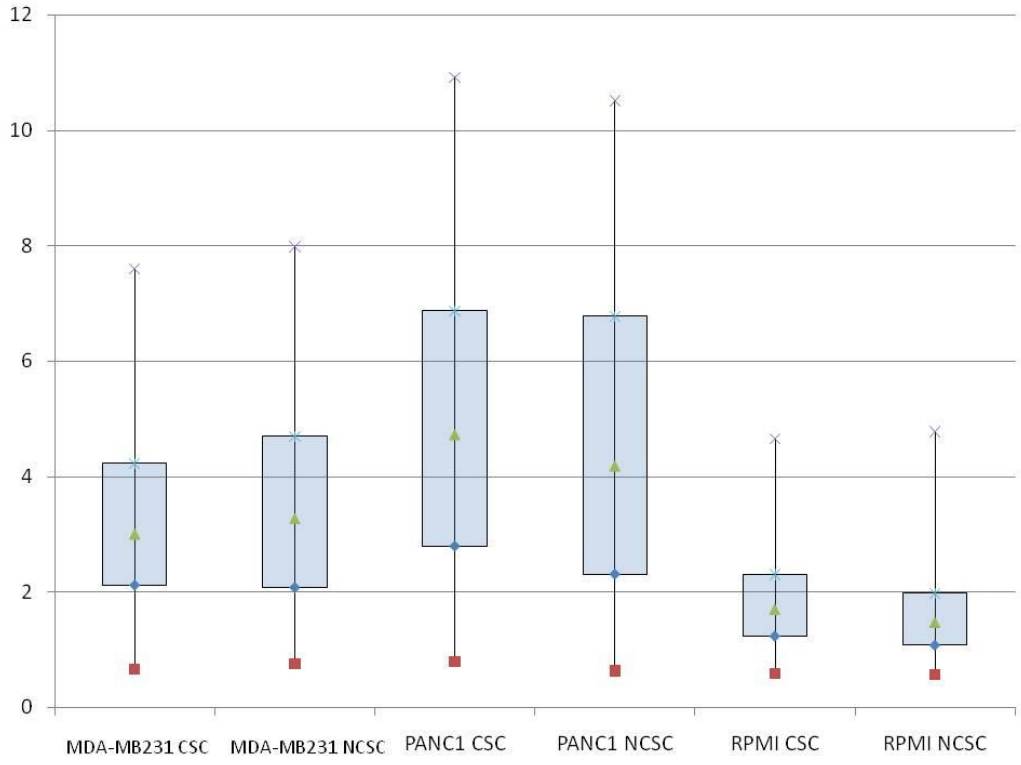

Figure 3.7 Absence pattern in difference of telomere length between CSCs and bulk tumor cells. There was no consistent difference in the mean or distribution of telomere lengths between CSC and bulk tumor cells in three cancer cell lines. These data make it impossible to make a correlation between telomere length and CSC susceptibility to telomerase inhibition with imetelstat.

DISCUSSION

In cancer cells, telomerase extension of telomere ends functions to maintain functional telomeres by counteracting normal telomere attrition due to the end replication problem, oxidative damage, and other end processing events. Telomerase inhibition disrupts telomere maintenance, eliminating the capability

of cancer cells to divide without limitation. However, there is inevitably a time lag between the beginning of telomerase inhibition therapy and the induction of replicative senescence. This time lag represents the amount of time it takes for the treated cancer cells to undergo as many cell divisions that are necessary to cause their telomeres to reach a critically short length in the absence of telomerase maintenance. The hypothesis that the sorted CSCs from PANC1, MDA-MB231 and RPMI8226 had shorter telomeres than the non-CSCs from each respective cell line was based on the experimental observation that these sorted CSCs had an enhanced susceptibility to telomerase inhibition using imetelstat as compared to the non-CSCs (Joseph et al., 2010). CSC susceptibility to imetelstat is based on the fact that the fraction of CSCs sorted from the treated cell populations decreased significantly after a period of imetelstat treatment that is shorter than the expected time lag between treatment initiation and the onset of cell senescence. This observed CSC depletion was accompanied by a decrease in observed CSC function, as demonstrated by a decrease in the tumorigenicity of PANC1 and MDA-MB231 in mouse xenograft models (Joseph et al., 2010). A plausible explanation for the rapid depletion of CSCs upon telomerase inhibition is that either the baseline mean length of CSC telomeres is shorter than that of the non-CSCs, of that the CSCs have a greater fraction of short telomeres (which would rapidly become critically short) than non-CSCs. Universal STELA is the ideal assay to test these hypotheses, because it allows for the detection of very

short telomeres on all chromosomes and the construction of a detailed distribution analysis of telomere lengths in the cells.

The Universal STELA data on mean telomere length and telomere length distribution did not show a consistent pattern of differences between the CSC and non-CSC populations among the three cell lines analyzed. Only one cell line, RPMI8226, showed a robustly significant difference ($p<0.0001$) upon comparison of the mean telomere lengths of the CSCs and non-CSCs. In RPMI8226, the non-CSC population had a shorter mean telomere length (1.594 kb) than the sorted CSCs (1.814). This difference in mean telomere length was accompanied by a greater fraction of short telomeres in the non-CSCs, and a tighter length distribution of the middle 50% of telomeres as compared to the CSCs. The non-CSCs of PANC1 likewise showed a trend of having shorter telomeres than the sorted CSCs, however the difference in mean telomere length ($p<0.0492$) was not as strong and the 95% confidence intervals of the two means slightly overlapped. The relationship between CSC and non-CSC telomere length in these two cell types do not support the hypothesis that CSCs have shorter telomeres than non-CSCs. The alternative hypothesis – that CSCs have longer telomeres than non-CSCs (as suggested by the Universal STELA data for PANC1 and RPMI8226) – is plausible in the context of the notion that CSCs may share properties and lineages with other stem-like cells. Normal telomerase positive cells, such as

hematopoietic stem cells and germ cells, generally have longer telomeres than non-CSCs from surrounding tissues (Allen and Baird, 2009; Wright et al., 1996), and several studies have suggested that telomere dysfunction in normal stem cells can lead to cancer (Blasco, 2007). Some have theorized that cancer stem cells may arise as transformed stem-like cells (Bjerkvig et al., 2005; Croker and Allan, 2008). However, the possibility that CSCs truly have a longer baseline telomere length than non-CSCs does not explain the observed susceptibility to imetelstat treatment from the current study. The telomere length distribution obtained by Universal STELA for MDA-MB231 CSCs and non-CSCs suggested that in this cell type, there was a greater fraction of short telomeres in the CSCs as compared to the non-CSCs, however there was not a significant difference in the mean telomere length ($p<0.0657$). A previous study showed that sorted CSCs from gliomas had shorter telomeres (as measured by TRF) than the cells from the tumor bulk (Marian et al., 2010a); the CSCs in this study were also susceptible to imetelstat treatment.

The Universal STELA data on telomere length differences between CSC and non-CSC presented here do not follow a pattern and therefore do not support a model in which CSC telomeres are always either longer or shorter than the telomeres of non-CSCs. This lack of a pattern in telomere length is consistent with other independent studies, some of which show that CSCs have markedly

shorter telomeres as compared to bulk tumor cells (Marian et al., 2010a) and others where there is no detectable difference in telomere length between CSCs and non-CSCs (Marian et al., 2010b). Similarly, there is no consistent pattern of differences in telomerase activity observed in CSCs versus non-CSCs (Brennan et al., 2010; Joseph et al., 2010; Marian et al., 2010b; Shervington et al., 2009). It is possible that telomerase inhibition therapy using imetelstat targets CSCs in a telomere length independent manner. Several studies have indicated that the catalytic reverse transcriptase component of telomerase, TERT, has biological functions independent of the RNA template component of telomerase. In mouse hair follicles, mTERT promoted stem cell proliferation independently of mTERC (the mouse telomerase RNA template) (Sarin et al., 2005). TERT from human, mouse and xenopus was found to be an active component of the canonical WNT signaling pathway independent of hTR, suggesting that this activity is independent of telomere length maintenance activities (Park et al., 2009). Overexpression of mTERT promoted epidermal stem cell proliferation without accompanying telomere elongation (Flores et al., 2005). The absence of a clear connection between baseline telomere length in CSCs and their susceptibility to imetelstat-mediated telomerase inhibition suggests that telomere length independent factors may be responsible. With the continued study of non-canonical roles of telomerase components in cancer and stem cell biology, we

should gain additional insight into telomerase regulation (Bollmann, 2008; Parkinson et al., 2008).

This study exemplifies the major strengths of Universal STELA as a tool for telomere length assessment. While many methods of telomere length measurement give only a mean telomere length, Universal STELA is able to generate a complete distribution of all telomere lengths in the cell population. This allows for the detection of very short telomeres, which are often undetected or underrepresented in other telomere length assays. The presence of a few very short telomeres is significant when asking questions about the induction of replicative senescence, since it has been shown that a few critically short telomeres can trigger senescence independently of mean telomere length (Zou et al., 2004b). The sensitivity of the Universal STELA data in this study can clearly rule out the possibility that CSCs are sensitive to imetelstat treatment because they have a unique subset of telomeres that are significantly shorter than other telomeres, given that the detailed length distributions show that the minimum telomere length is approximately similar across all samples. In summary, Universal STELA has a broad applicability to questions regarding replicative potential and cellular aging, and will be a valuable tool in examining the role of short telomeres in the induction of senescence.

MATERIALS AND METHODS

Cell culture and sorting

Purified genomic DNA from PANC1, MDA-MB231 and RPMI8226 CSCs and non-CSCs was obtained from Geron Corp. for analysis by Universal STELA. The experimental conditions used to generate these genomic DNA samples are detailed in (Joseph et al., 2010) and briefly summarized below: Cells were maintained in DMEM/F12 media supplemented with 20% FBS. CSCs were sorted using a FACSAria (BD Biosciences) according to previously published CSC markers: MDA-MB231 (CD44+/CD24 low) (Fillmore and Kuperwasser, 2008); RPMI8226 (CD138-); PANC1 (CD44+/CD24+/ESA+) (Huang et al., 2008; Li et al., 2007).

Universal STELA

Universal STELA was performed using a strategy modified from that previously described (Bendix et al.). 500 ng purified DNA was digested for 1 hour at 37°C with the restriction enzyme NlaIII (New England Biolabs). An NlaIII restriction site-specific panhandle linker was designed and created by incubating two oligonucleotides ("long" and "short") in a 1:2 ratio at 95°C for 5 minutes and cooling to room temperature over one hour in 50 mM NaCl. 100 ng of digested genomic DNA was incubated in a10 μl ligation reaction containing 1x ligase buffer, 50 U T4 DNA ligase (NEB), 10^{-2} μM of a mixture of all six C-telorettes (0.16×10^{-2} μM each) and 10 μM NlaIII-specific panhandle for 15 hours

at 17°C. Multiple PCR reactions were performed (Initial melt of 94°C for 30 s followed by 22 cycles of 94°C for 15 s + 68°C for 12 min) using Extensor Hi-Fidelity PCR Master Mix 1 (ABGene, Thermo Scientific) in 25 µl reaction containing 100 pg ligated DNA, 0.5 µM primers (Adapter forward primer and C-Teltail reverse primer) and supplemented with 5% DMSO. Telomere amplification products were resolved on a 0.7% agarose gel, and subject to in-gel hybridization using a ^{32}P-labeled telomere-specific [$(TTAGGG)_4$] oligonucleotide probe in a hybridization oven at 42 ^{o}C for at least four hours. The gel was then washed once with low-stringency buffer (2x SSC) and twice with high stringency wash (0.1x SSC, 0.1% SDS) for 15 minutes each at 42° C. The gel was then exposed to a PhosphorImager screen and scanned on a Typhoon biomolecular imager (GE Healthcare Life Science). Universal STELA telomere amplification products were analyzed for molecular weight using AlphaEaseFC (AlphaInnotech) software and all statistical analyses was carried out using Microsoft Excel and GraphPad Prism. A listing of all primers used for Universal STELA and their sequences is found in Table 3.1.

Table 3.1 Primers used in Universal STELA

Name	Function	Sequence
Adapter	Forward Primer	5′- TGT AGC GTG AAG ACG ACA GAA - 3′
Long	Panhandle linker	5’TGTAGCGTGAAGACGACAGAAAGGGCGTGGTGCGGACGCGGGCATG 3’
Short	Panhandle linker	5’ CCCGCGTCCGC 3’
C-telorette 1	C-telomere tag	5' TGCTCCGTGCATCTGGCATCCCCTAAC-3'
C-telorette 2	C-telomere tag	5'-TGCTCCGTGCATCTGGCATCTAACCCT-3'
C-telorette 3	C-telomere tag	5'-TGCTCCGTGCATCTGGCATCCCTAACC-3'
C-telorette 4	C-telomere tag	5'-TGCTCCGTGCATCTGGCATCCTAACCC-3'
C-telorette 5	C-telomere tag	5'-TGCTCCGTGCATCTGGCATCAACCCTA-3'
C-telorette 6	C-telomere tag	5'-TGCTCCGTGCATCTGGCATCACCCTAA-3
C-teltail	Reverse Primer	5'-TGCTCCGTGCATCTGGCATC-3'

CHAPTER FOUR

TELOMERE LENGTH STUDIES FACILITATE THE EXAMINATION OF TELOMERASE ACTION IN HUMAN CANCER CELLS

SUMMARY

Despite great advances in understanding the mechanism and regulation of telomerase, many questions remain. Among these central questions in telomere biology is how telomerase recruitment is regulated in order to maintain telomere length. Neither the mechanism of telomerase recruitment, nor the dynamics that guide the timing and choice of substrate of telomerase is well understood. Many of these questions are very challenging to study in human telomeres, which are long and heterogeneous in length. We chose to utilize STELA and Universal STELA to conduct high resolution telomere length measurements in order to ask the following questions: when does telomerase extend the G-rich strand of the telomere? When is the C-rich strand of the telomere extended? Is telomerase activity coupled to telomere replication, or is it guided by cell-cycle related events? Does telomerase extend short telomeres at a faster rate than longer telomeres? Our findings indicate that telomerase extends the G-rich strand quickly following telomere replication, while C-strand fill-in is delayed until late S phase. We are also able to use Universal STELA to gain insight into the rate of elongation of telomeres under conditions where telomeres are growing faster than

their equilibrium length following long-term telomerase inhibition. These results highlight the usefulness of STELA and Universal STELA in studying details of telomere biology, and provide insight into telomere maintenance regulation which may provide additional targets for anti-telomerase cancer therapeutics.

INTRODUCTION

One key question that remains unanswered in telomere biology is how different regulatory processes act concertedly to maintain telomere length. Mammalian telomeres are heterogeneous in length when comparing telomeres of different chromosomes (Lansdorp et al., 1996b; Londono-Vallejo et al., 2001; Martens et al., 1998), however each chromosome appears to have a characteristic maintenance length (Graakjaer et al., 2003; Graakjaer et al., 2004b). In telomerase positive cells, telomere length is a result of the balance of actions which shorten telomeres, such as replicative aging, oxidative damage and end processing, and telomerase extension (Cong et al., 2002; Olovnikov, 1973; Sfeir et al., 2005; Shore and Bianchi, 2009; von Zglinicki et al., 2000). Telomerase levels must be limiting in the cell in order to maintain telomere length homeostasis (Cristofari and Lingner, 2006). Cellular levels of active telomerase are known to be regulated on multiple levels, including protein processing, complex assembly and subcellular localization (Cong et al., 2002; Kelleher et al., 2002). Telomere length maintenance is also dependent on the regulation of

telomerase recruitment to the G-rich strand of the telomere. The telomerase recruitment regulatory pathway is not fully understood, but it is currently thought that members of the shelterin complex of telomere binding proteins act together in a negative feedback loop which limits telomerase extension of telomeres (Bianchi and Shore, 2008; De Boeck et al., 2009; Palm and de Lange, 2008; Smogorzewska and de Lange, 2004).

Every cell cycle, telomeres of telomerase positive cells must undergo semiconservative DNA replication as well as be elongated by telomerase. Telomerase elongation of the G-rich telomere strand must also be accompanied by the subsequent fill-in and processing of the C-rich telomere strand in order to produce fully replicated and extended double stranded telomeres with functional 3' overhangs (Figure 4.1). Many studies have examined the timing and mechanism of telomerase recruitment in yeast. In *S. cerevisae*, telomerase activity is highly regulated and restricted to late S phase (Chandra et al., 2001; Fisher et al., 2004; Marcand et al., 2000; Taggart et al., 2002), coinciding with the timing of telomere replication (McCarroll and Fangman, 1988). The yeast telomerase components Cdc13, Est1 and Ku are only found at telomeres during S phase (Chandra et al., 2001; Fisher et al., 2004; Marcand et al., 2000; Taggart et al., 2002). Telomerase extension of the G-rich telomere strand in yeast is blocked when the C-rich lagging strand DNA replication components Pol α, Pol δ and

DNA primase are absent (Diede and Gottschling, 1999). Taken together, these studies suggest that in yeast, telomerase activity is coupled to semiconservative telomere replication. However, it is difficult to distinguish whether the timing of telomerase recruitment is regulated to late S phase due to cell cycle control processes or if telomerase recruitment and telomere replication are directly coupled. In contrast to yeast telomeres, human telomeres have been shown to replicate throughout S phase (Ten Hagen et al., 1990; Wright et al., 1999). Some *in situ* studies indicate that both hTERT and hTR are dynamically recruited to small subsets of telomeres throughout S phase (Jady et al., 2006; Tomlinson et al., 2006), which is consistent with the model of telomerase recruitment being coupled to telomere replication, however there is no direct evidence regarding the temporal regulation of telomerase activity in mammalian cells. Such evidence would allow us to distinguish whether mammalian telomerase activity is regulated by to occur at a particular point in the cell cycle, or if it is directly coupled to the semiconservative replication of telomeres.

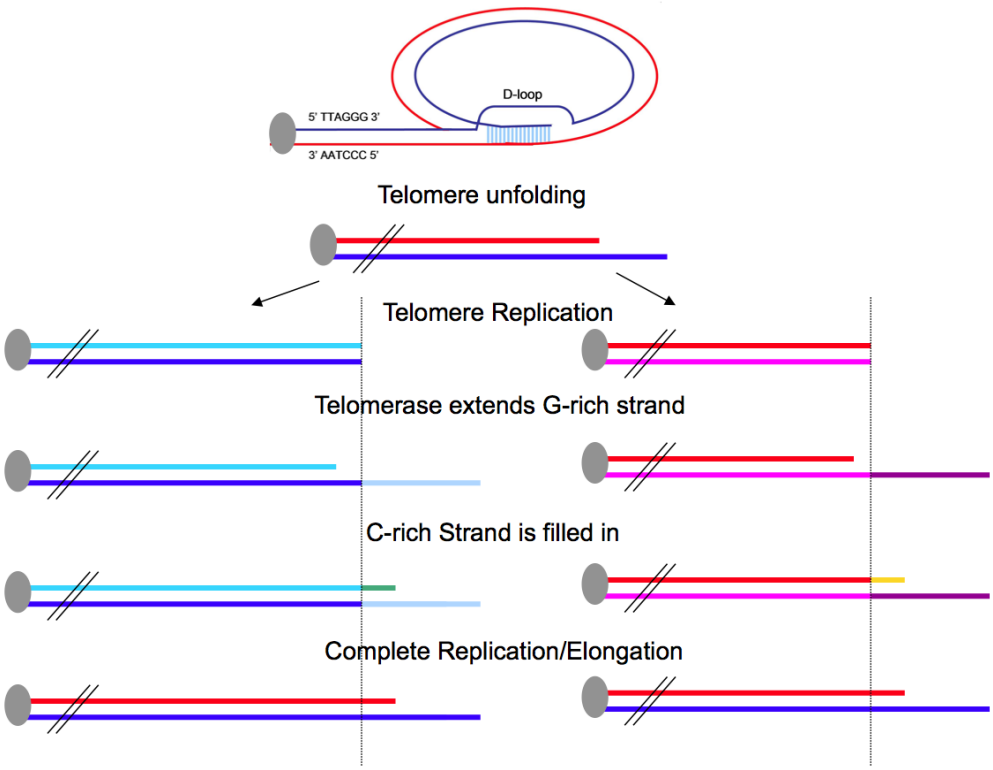

Figure 4.1: Telomere Replication and Telomerase Extension Events Telomeres normally form a complex structure called a "t-loop" in which the 3' single stranded overhang invades the proximal telomeric duplex DNA, obscuring the telomere end from being recognized as a double stranded break by the DNA damage sensing machinery. During each cell division, the t-loop must unfold to allow access of the replication machinery. Following each round of semiconservative DNA replication, telomerase extends the G-rich strand of each daughter telomere and then the C-rich strand must be filled in and processed to achieve consistent overhang length and terminal nucleotide specificity.

Another aspect of telomerase recruitment that remains unclear is how telomerase prevents telomeres from becoming critically short. There are different components to this question that must be addressed. Firstly, it is important to

understand whether telomerase extends all telomeres during each cell cycle, or if there is some mechanism that regulates which telomeres are targeted for elongation. One possible explanation for how telomerase prevents the development of critically short telomeres is that it preferentially elongates short telomers. Again, our first insight into this question comes from the yeast model organism. The telomeres of *S. cerevisiae* are targeted for telomerase elongation by a protein counting mechanism, in which the number of Rif1 and Rif2 proteins bound to the telomere determine whether it will be extended or not (Levy and Blackburn, 2004; Teixeira et al., 2004). During one yeast cell cycle, the frequency of a telomeres being extended ranges from 6-8% when telomeres are long, to approximately 45% when telomeres are short (Teixeira et al., 2004). This indicates that in yeast, telomerase is preferentially recruited to short telomeres and that it this preference is mediated through interactions with telomere binding proteins (Teixeira et al., 2004). Other studies have implied that mammalian telomerase may be recruited to the shortest telomeres preferentially when telomere length is increasing faster than when telomere length is being maintained (Hemann et al., 2001a; Ouellette et al., 2000; Samper et al., 2001; Steinert et al., 2000; Zhu et al., 1998). Recently, it has been shown that nearly all telomeres are acted on by telomerase during each cell cycle when telomere length is being maintained (Zhao et al., 2009), suggesting that there is no preference for short telomeres in times where telomere length is not changing. It is still unclear what

mechanism human cancer cells use to allow for the preferential extension of critically short telomeres. The best insight we have into the difference between telomerase recruitment regulation under maintenance and lengthening conditions comes from recent data which shows that in a single cell cycle, telomeres being maintained at a baseline length are elongated by a single molecule of telomerase, while multiple molecules of telomerase perform multiple rounds of elongation of telomeres under conditions where telomeres are elongating (Zhao et al., 2011). This data suggests that human telomerase can act in both a processive manner, with a single telomerase molecule extending and translocating many times to elongate a single telomere, and also in a distributive manner, with many molecules of telomerase working to extend a telomere. It is conceivable that a telomerase positive cancer cell that is lengthening its telomeres (rather than maintaining telomere length) uses a combination of processive and distributive telomerase recruitment to ensure that the shortest telomeres in the cell are rapidly elongated by many telomerase molecules while the longer telomeres in the cell are extended by a single, processive telomerase molecule. There is little data available that distinguishes the rate of elongation of the shortest telomeres from the rate of elongation of the longest telomeres in a cell under non steady-state telomere length conditions.

We developed an experimental system in which we could utilize the high-resolution telomere length measurements obtained with STELA to determine

when telomerase acts on the G-rich strand, and to differentiate the timing of the elongation of the G-rich strand from the timing of fill-in of the C-rich strand. We also use Universal STELA to examine the rate of growth of the shortest telomeres in a cell population that is recovering from long-term telomerase inhibition treatment, providing insight into the dynamics of telomerase activity control in non-maintenance conditions.

RESULTS

Summary of experimental design

Telomerase-positive human cancer cells with short telomeres and relatively homogenous telomere length are treated with the telomerase inhibitor GRN163L (imetelstat) to shift the telomere length equilibrium away from maintenance conditions. In order to ensure robust telomerase activity, telomerase is transiently overexpressed using a retroviral system. These cells are then be synchronized at the G1/S interface, and samples are harvested throughout S phase. For each time point collected, STELA of the C-rich and G-rich strand is performed to determine the point in S phase which each strand is elongated. Cells that are expressing only homogenous telomerase are allowed to recover from GRN163L treatment for 30 population doublings, and samples are harvested every week. Universal STELA is performed and detailed telomere length

distribution analysis is conducted to determine the rate of growth of the shortest and longest telomeres during recovery from telomerase inhibition.

Developing a cell culture setting in which to study the temporal regulation of telomerase in human cancer cells

STELA and Universal STELA measure lengths of individual telomere molecules representing the entire distribution of telomere lengths in a cell population, providing high resolution telomere length data which can potentially detect very small changes in telomere length over time. In order to create a cell culture system that is capable of detecting the change in telomere length due to telomerase activity in one cell cycle, we chose cells which were derived from a clone with short telomeres. Telomere lengths are known to be heterogeneous within a cell, and a cell population derived from a clone will have a more uniform telomere length than the parent cell population. Additionally, a sample with a relatively shorter average telomere length will produce a more easily quantifiable change in telomere length following telomerase elongation. For this experiment, we chose a previously isolated clone of A549 lung carcinoma cells (called A549-C6) which had a shorter average telomere length than the parent population. A549-C6 had an average telomere length of approximately 3.5 kb as measured by TRF (unshown) and an average length of approximately 2.2 kb as measured by Universal STELA (Figure 4.2).

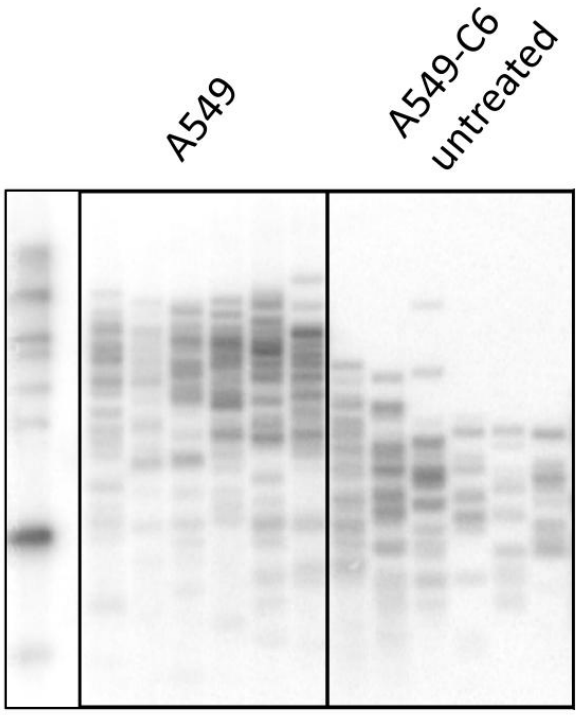

Figure 4.2: A549-C6 telomeres have a shorter average length than the telomeres of the parental A549 cell population. Universal STELA analysis of the parent A549 population as compared to a population derived from a clone of A549 ("A549-C6") that was selected for this study for its short average telomere length. Universal STELA analysis of approximately 100 telomere amplification products resulted in an average telomere length of approximately 4.1 kb for the parent population and approximately 2.2 kb for the A549-C6 clonally-derived population.

We next used the telomerase inhibitor GRN163L (Imetelstat) (Herbert et al., 2005) in order to cause the telomeres to shorten below the maintenance length of the clone. After treatment with 1 μM GRN163L for approximately 30 population doublings, average telomere length had shortened to approximately 2.5

kb as measured by TRF (unshown) and to approximately 1.9kb as measured by Universal STELA (Figure 4.3). This prolonged treatment with the telomerase inhibitor produced telomere shortening without affecting the rate of cell growth (Figure 4.4), indicating that the telomere shortening has not triggered replicative senescence. It is important to note that the telomere length measurements using Universal STELA produced shorter averages than measurements using TRF, and also indicated that there was a smaller average decrease in telomere length due to telomerase inhibition treatment. This could be attributed to the different biases of these respective assays: TRF is thought to be biased against the detection of short telomeres due to the fact that more probe hybridizes to longer telomeres than to shorter telomeres, while Universal STELA has a theoretical preference to amplify smaller telomeres over longer telomeres due to the nature of PCR. However, the range of telomere lengths being measured in these samples was well within the range of molecules that can be readily amplified by Universal STELA, and it is unlikely that the analysis excluded longer telomeres that were undetected. It is also curious that the length of GRN163L treatment did not induce replicative senescence or cause a greater magnitude of telomere shortening, since previous studies using the drug indicate that the rate of shortening should have been higher than that observed (Herbert et al., 2005). It is possible that the dosage and treatment schedule were not well-orchestrated to achieve continuous, complete telomerase inhibition. Without direct measurement of telomerase activity from

each cell passage using the TRAP assay, it is impossible to determine the level of telomerase inhibition over the course of treatment. However, it is clear from both TRF and Universal STELA data that telomeres were shortened beyond their maintenance length, which was the goal of this part of the experiment.

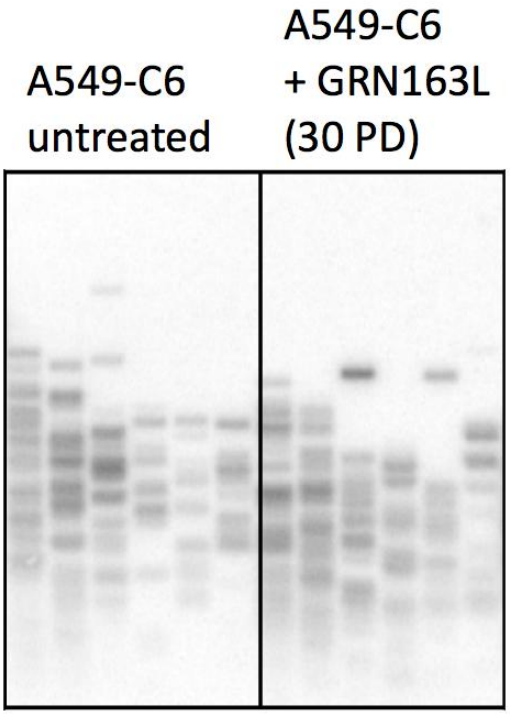

Figure 4.3: 30 PD of continuous telomerase inhibition causes average telomere length to become shorter than maintenance length. After approximately 30 population doublings in the presence of 1 μM GRN163L (Imetelstat) treatment, the average telomere length of A549-C6 declined from ~2.2 kb (untreated) to ~1.9 kb as measured by Universal STELA. Approximately 100 telomere amplification products were analyzed for each sample.

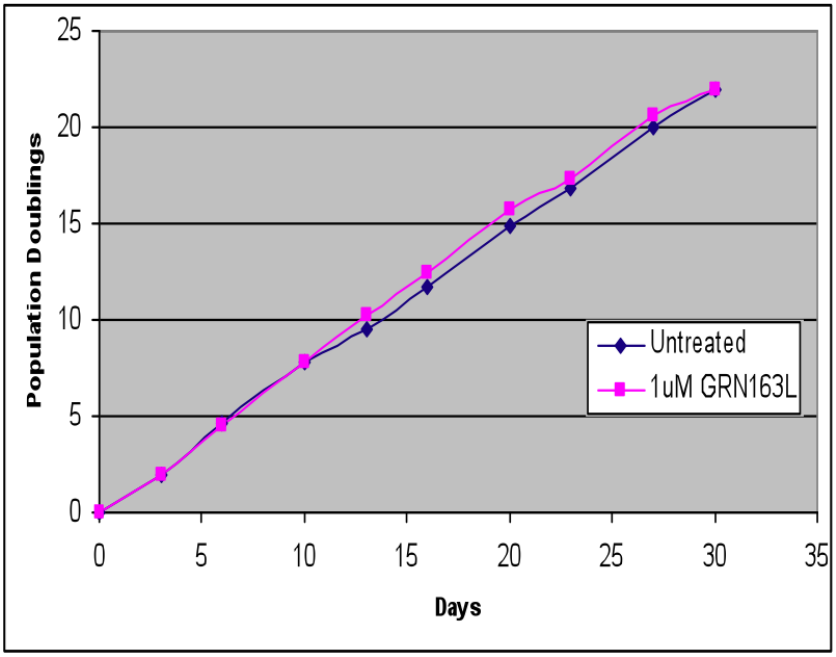

Figure 4.4: A549-C6 treated with 1 μM GRN163L for 30 PD have shortened telomeres but still actively divide at the same rate as untreated cells. Population doubling was calculated at each cell passage and days/PD was plotted to monitor the rate of growth of both untreated cells and cells treated with 1 μM GRN163L. A constant rate of growth indicates that the treated cells have not accumulated enough critically short telomeres as to initiate replicative senescence. Actively, dependably dividing cells are required for this experimental design.

To ensure that there was robust telomerase activity that would be detected during a single cell cycle, the GRN163L-treated A549-C6 cells were transduced with a retrovirus that overexpresses the hTERT catalytic subunit of human telomerase. Retroviral infection produced a significant increase in telomerase activity as determined qualitatively by TRAP assay (Figure 4.5). At the time of

infection, telomere length as measured by TRF was approximately 2.5 kb, and elongated at a calculated rate of approximately 500 bp per cell division as measured over the first 15 PD following infection (Figure 4.6).

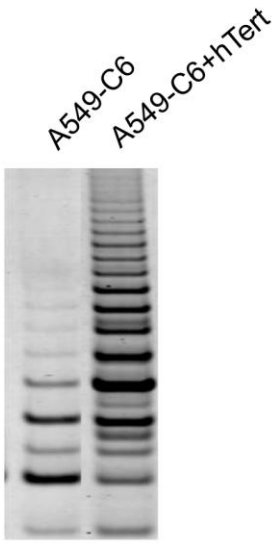

Figure 4.5: A549-C6 cells transduced with retrovirus overexpressing hTERT have increased telomerase activity. TRAP assay of A549-C6 cells expressing only endogenous levels of hTERT (left) and those that are expressing exogenous hTERT after being transduced with an hTERT-expressing retroviral vector and selection with puromycin (right).

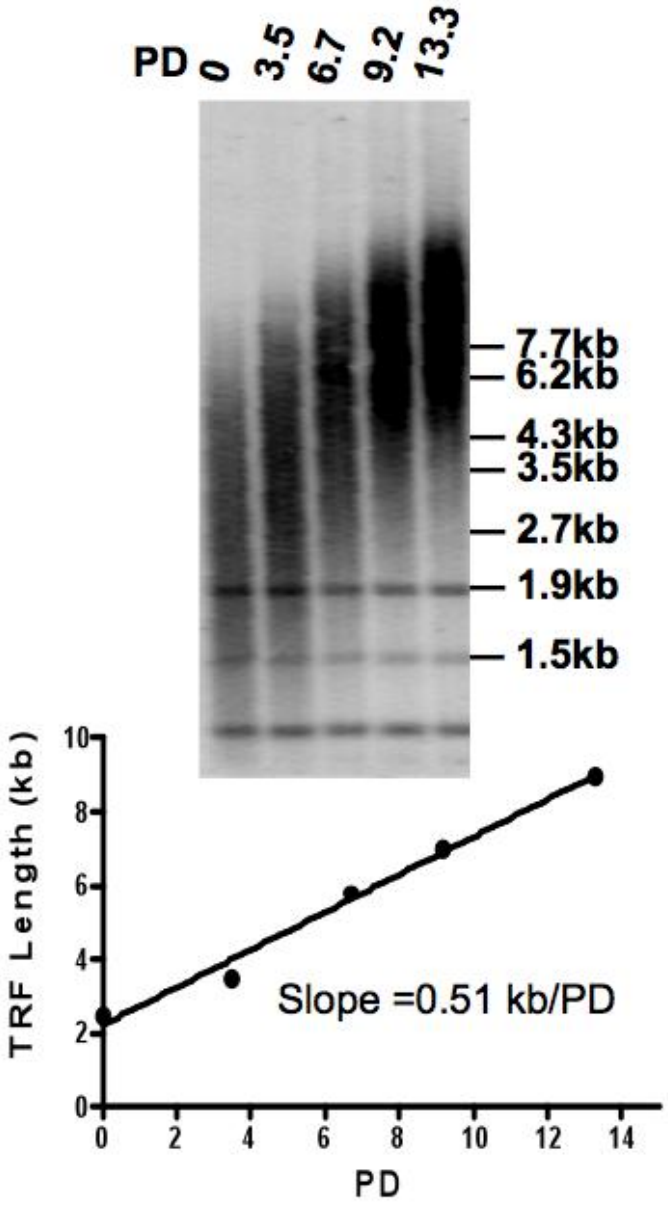

Figure 4.6: Overexpression of hTERT in GRN163L-treated A549-C6 cells causes rapid elongation of telomeres at a rate of approximately 500 bp per cell division. A549-C6+hTERT cells were harvested at each cell passage following transduction with the retroviral hTERT vector, and genomic DNA was analyzed using TRF analysis. The average rate of growth of telomeres was calculated to be approximately 500 bp per cell division.

Determining the timing of telomerase activity during one cell cycle

Immediately following selection for cells which were expressing the retroviral hTERT construct, cells were synchronized at the G1/S interface using a combined serum starvation/aphidicolin synchronization strategy. Cells were harvested at the time of release from Aphidicolin, and every two hours thereafter to extend through the duration of S phase. According to cell cycle analysis using FACS, approximately 50% of the cells that were synchronized entered S phase and DNA replication was completed between 6 and 8 hours following release (Figure 4.7).

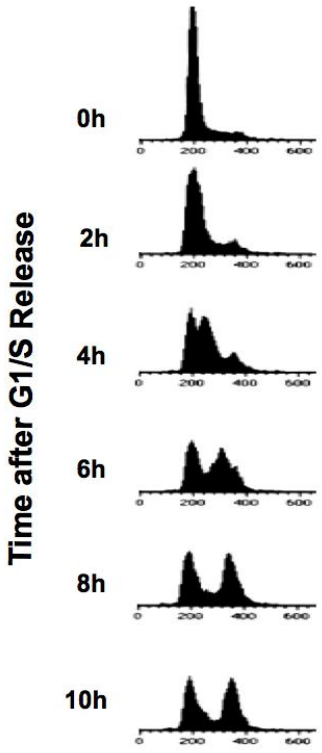

Figure 4.7: FACS analysis of synchronization shows that approximately 50% of synchronized A549-C6+hTERT cells entered S phase upon release.

Cells were fixed and stained with Propidium Iodide and flow cytometry was performed to analyze for DNA content. At release ("0h"), nearly all cells are in G0/G1, indicating effective synchronization. From 2h to 10h, cells with intermediate DNA concentrations can be observed which is indicative of DNA synthesis during S phase. Approximately 50% of cells never leave G0/G1, and 50% of cells move through S phase to G2/M.

Because STELA can determine the length of individual telomeres, it is possible to use this assay to determine the change in length of an individual telomere over the course of one cell cycle in this experimental system. In order to determine if telomerase extension is coupled to telomere replication as is found in yeast (Chandra et al., 2001; Diede and Gottschling, 1999; Fisher et al., 2004; Marcand et al., 2000; Taggart et al., 2002), the exact timing of the replication of individual telomeres must also be known. Although human telomeres replicate throughout S phase (Ten Hagen et al., 1990; Wright et al., 1999), each telomere on a particular chromosome end is known to have a characteristic replication time during S phase (Zou et al., 2004a). Previous studies using the ReDFISH technique (Bailey et al., 2004b; Zou et al., 2004a) had determined that most XpYp telomeres had replicated two to four hours into S phase (Zhao et al., 2009), which means that the XpYp telomere replicates earlier enough in S phase to be able to distinguish whether telomerase activity is coupled to replication (early S phase) or is programmed to be a late S phase event. In order to determine the timing of telomerase extension of the XpYp telomere, the size of the XpYp telomere was calculated using STELA for each timepoint harvested during a single S phase (Figure 4.8). Because the FACS data indicate that only 50% of the cells entered S phase (Figure 4.7), the assumption is made that the other 50% of cells neither replicated their DNA nor were available for telomerase extension. Approximately 100 telomere amplification products from STELA were analyzed at each time

point, and the measured increase of telomere length was approximately 250 nucleotide, which is roughly equivalent to what would be expected based on the estimated rate of growth of 500 bp/division (Figure 4.6) divided by 2 to account for the non-cycling cells. The 250 bp increase in telomere length occurs after six hours of release (Figure 4.8), which is significantly later in S phase than the majority of XpYp telomeres replicate (Zhao et al., 2009). It is important to note, however, that the original design of STELA measures the size of the C-rich strand of the telomere, which is not the strand that serves as the substrate for telomerase. It is therefore inaccurate to assume that telomerase extension occurs at the same time as the elongation of the C-rich strand. In order to accurately describe the timing of telomerase extension of the G-rich strand, a modification of STELA which measures the length of the G-rich strand was used (Sfeir et al., 2005) (Figure 4.9). The original STELA (Baird et al., 2003) uses the 3' overhang found naturally at linear telomeres as a platform which serves as a an annealing site for an oligonucleotide tag which is then ligated to the end of the C-rich strand; this tag serves as the unique site for the reverse primer while during PCR amplification (Figure 4.8). In order to use a similar strategy to measure the length of the G-rich telomeric strand, an artificial C-rich overhang is created by annealing a long, repetitive "platform" oligonucleotide to the G-rich telomere (Sfeir et al., 2005). This artificial overhang allows a similar oligonucleotide tag to be ligated to the end of the G-rich telomeric strand, and PCR amplification thus

amplifies the G-rich strand rather than the C-rich strand (Figure 4.9). When the samples were reanalyzed using the G-STELA modified assay, telomere length increased by a calculated 250 nucleotides over the course of one S phase, similar to the length increase calculated using the original C-STELA method. However, the increase in length of the G-rich strand of the telomere was observed between two and four hours after release into S phase (Figure 4.9). The calculated timing of the elongation of the G-rich strand is indicative of when telomerase is recruited to the telomere for extension, and coincides with the known replication timing of the XpYp telomere (Zhao et al., 2009). This suggests that telomerase recruitment is coupled to telomere replication in human cells, as has been suggested by *in situ* data from other studies (Jady et al., 2006; Tomlinson et al., 2006). Surprisingly, there is a significant delay between the elongation of the C-rich strand and the elongation of the G-rich strand, suggesting that telomerase extension of the G-rich telomere is uncoupled from the fill-in and end processing of the C-rich strand. This result was unexpected, and bolsters the need to better understand the mechanism and regulation of end-processing events that must occur on each C-rich strand (Bailey et al., 2001; Sfeir et al., 2005; Shore and Bianchi, 2009).

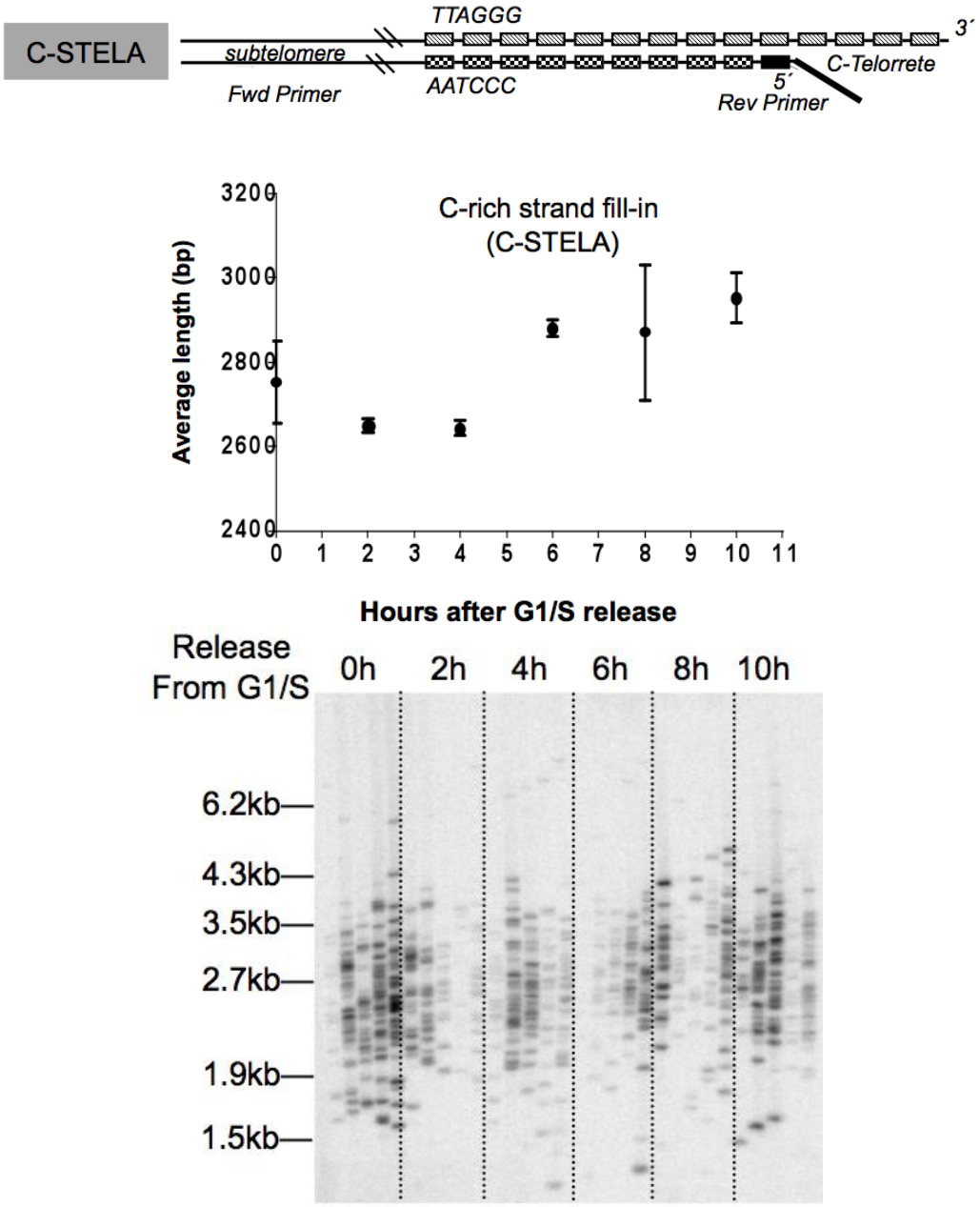

Figure 4.8: Elongation of the C-rich strand occurs in Late S phase.

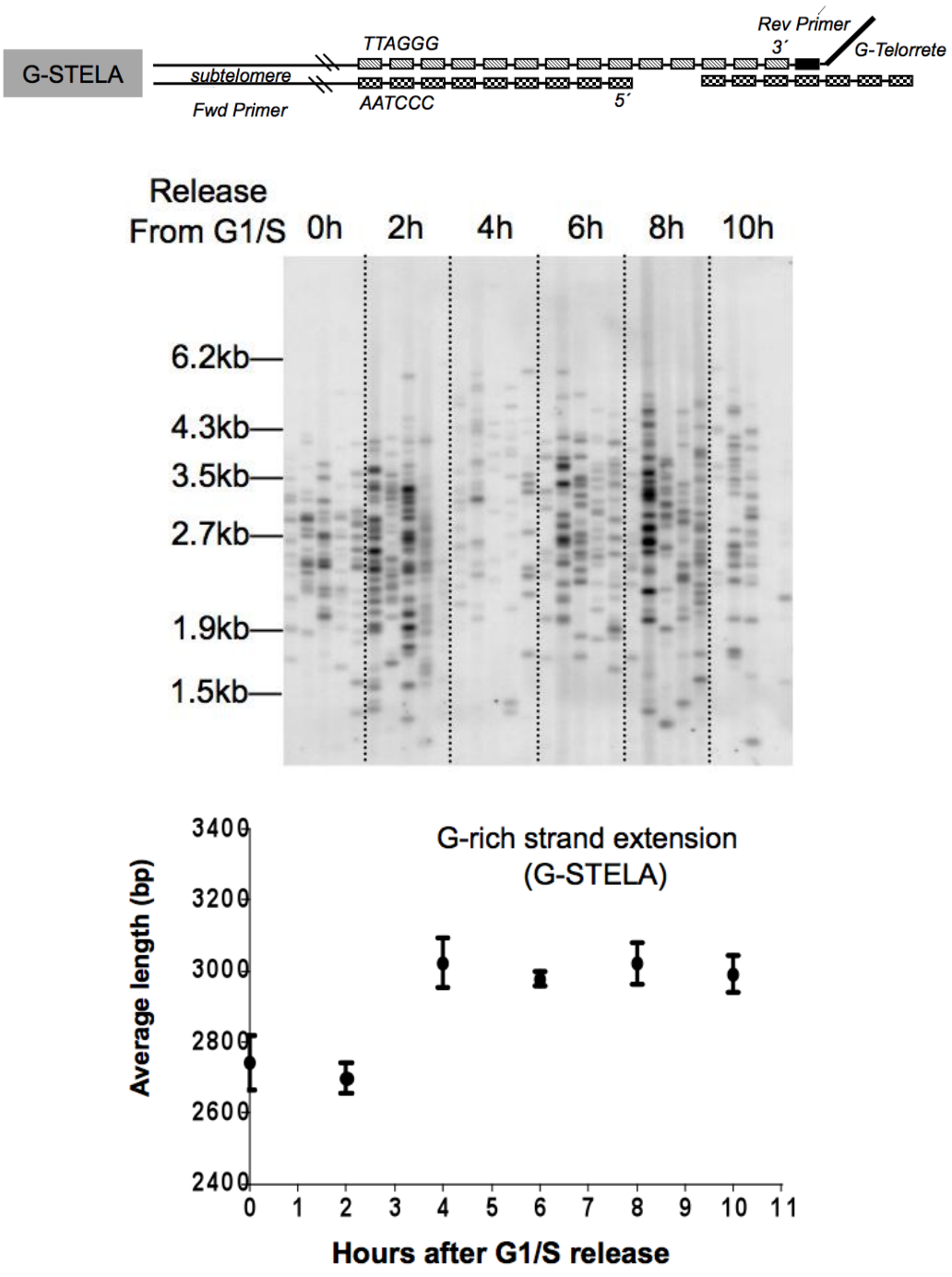

Figure 4.9: Elongation of the G-rich strand occurs in early S phase

Figure 4.8: Elongation of the C-rich strand occurs in Late S phase.
C-STELA is a PCR-based assay designed to amplify individual C-rich telomere molecules from a single chromosome. The site for the reverse primer is a tag that is annealed to the 3' G-rich telomeric overhang and ligated to the end of the C-rich strand, providing a unique sequence at the end of the otherwise repetitive telomere. The forward primer site is a sequence that is unique to the subtelomere of the XpYp chromosome and is located 421 bp away from the beginning of canonical telomere repeats. Each band on the Southern blot represents an individual telomere molecule that was amplified during PCR using these forward and reverse primers. Approximately 100 bands were analyzed at each time point to calculate the average telomere length. The C-rich strand is elongated by approximately 250 bp in late S phase (after 6 hours post-release).

Figure 4.9: Elongation of the G-rich strand occurs in early S phase.
G-STELA is a PCR-based assay designed to amplify individual G-rich telomere molecules from a single chromosome. To modify the C-STELA so that the G-rich strand can be amplified, an artificial 5' overhang is created by annealing a C-rich platform to the telomere. An oligonucleotide with a unique tag that is complementary to the artificial overhang is then ligated to the end of the G-rich telomere strand, serving as the reverse primer site. As in C-STELA, the forward primer site is a sequence that is unique to the subtelomere of the XpYp chromosome. Each band on the Southern blot represents an individual telomere molecule that was amplified during PCR using these forward and reverse primers. Approximately 100 bands were analyzed at each time point to calculate the average telomere length. The G-rich strand is elongated by approximately 250 bp in early S phase (between 2-4 hours after release into S phase).

Determining the rate of elongation of the shortest and longest telomeres in non-maintenance conditions

It is generally thought that telomerase is preferentially recruited to the shortest telomeres when telomeres are shorter than their normal maintenance length. Previous data suggests that when telomeres are artificially shortened after long-term telomerase inhibition, telomerase recruitment is distributive and many molecules act on a single telomere in a single cell cycle (Zhao et al., 2011). To compare the rate of elongation of the shortest and longest telomeres in conditions when telomere length is increasing, A549-C6 cells were treated with the telomerase inhibitor GRN163L (imetelstat) for 43 PDs, and were then released and allowed to grow in the absence of the telomerase inhibitor for 30 PDs. Cell samples were harvested at each passage after release from treatment, and genomic DNA was isolated for Universal STELA analysis (Figure 4.10). Telomere elongation could be observed on visual examination of the Universal STELA Southern blots. For each sample analyzed by Universal STELA, 150-300 individual telomere amplification products were analyzed for molecular weight and mean telomere length was computed. The average rate of telomere elongation after release from GRN163L telomerase inhibition was calculated to be approximately 60 bp per cell division (Figure 4.11), which notably is the same rate of telomere elongation previously calculated (using a different assay) in Hela cells that were in telomere length maintenance conditions (Zhao et al., 2009). However, Universal STELA allows for the examination of the full distribution of

telomere lengths rather than just the mean. Analyzing changes in the shape of the distribution of telomere lengths over the time course of release from telomerase inhibition allows for the calculation of a rate of change of telomeres by percentile. Thus, the rate of change of the shortest telomeres can be compared to the rate of change of the longest telomeres.

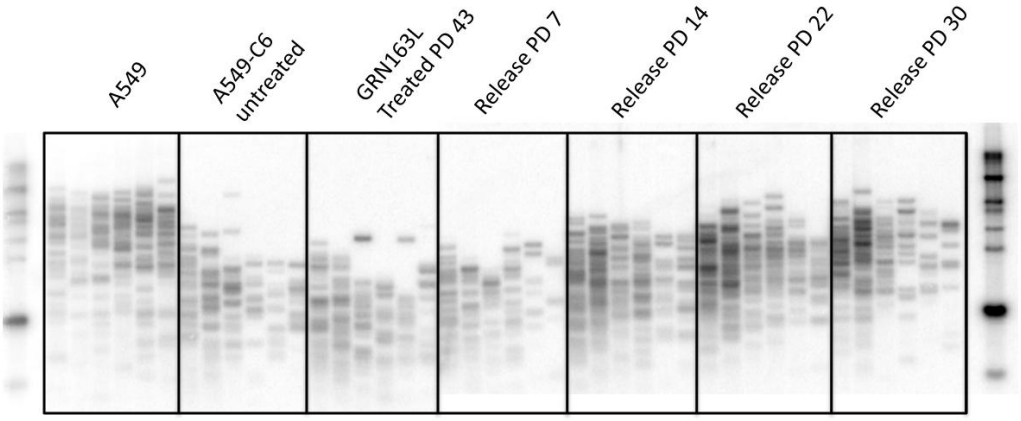

Figure 4.10 Universal STELA analysis of A549-C6 releasing from telomerase inhibtion therapy. Control samples show Universal STELA telomere length distribution of A549 parent cell line and the untreated A549-C6 clonally-derived cell population, which has a significantly shorter maintenance telomere length than the parent cell line. A549-C6 were treated with the telomerase inhibitor GRN163L for 43 PD and then released for 30 PD. Telomere length was measured by Universal STELA at 7, 14, 22 and 30 PD after release from telomerase inhibition to analyze the rate of telomeres that are recovering from being artificially shortened.

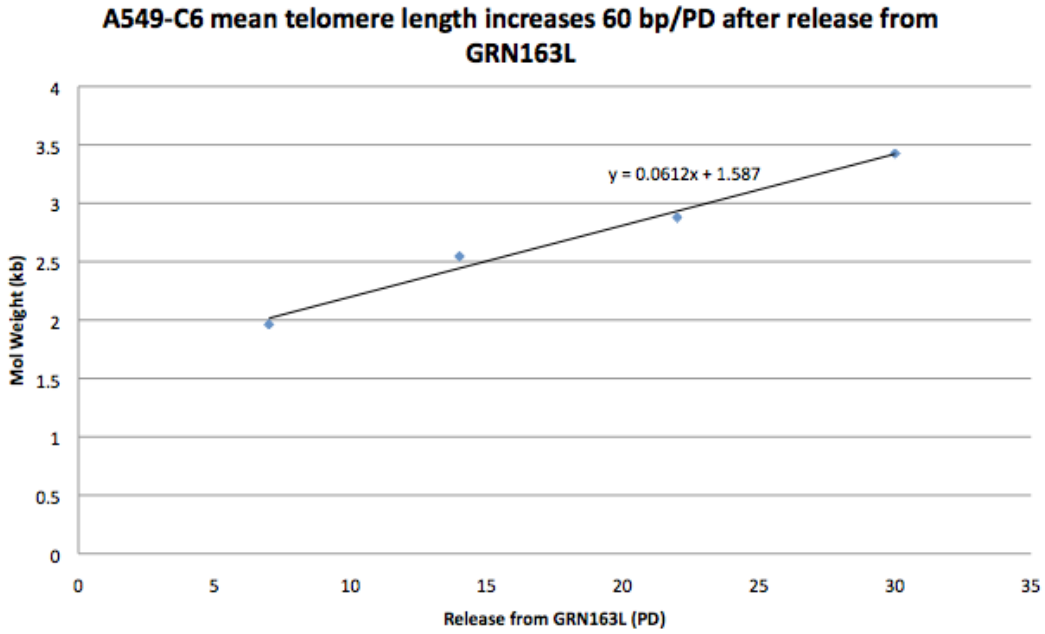

Figure 4.11 A549-C6 mean telomere length increases 60 bp per population doubling after release from GRN163L. Mean telomere length for each time point was calculated by averaging the molecular weights of 150-300 individual telomere amplification products from Universal STELA. A linear regression line was calculated to have a slope of approximately 60 bp per population doubling (R^2=0.98576), representing the average rate of telomere elongation.

To compare the rate of elongation of telomeres by percentile, the distribution of telomere lengths at each time point following release needed to be characterized. Telomere length distributions of the different samples were compared using quartile analysis (Figure 4.12). The minimum telomere length across all samples, including the A549 parent cell line, was similar (approximately 600 bp as measured by Universal STELA), suggesting that the presence of short telomeres is independent of mean telomere length or manipulation of telomere length via telomerase inhibition. Quartile analysis

(Figure 4.12) shows that the middle 50% of telomeres becomes tightly distributed around the median after telomerase inhibition, and gradually expands over the course of recovery/release. Notably, over the course of recovering from telomerase inhibition, the A549-C6 telomeres became longer than the telomeres from the untreated A549-C6 clonally-derived population. After 30 PD of release from telomerase inhibition, the telomere distribution more closely resembled that of the A549 parent cell line rather than that of the C6 clone. This was very surprising since the A549-C6 average telomere length had remained the same over many months of serial culture, suggesting that the clonally-derived population had an established maintenance telomere length. The comparison of telomere length distributions between the A549-C6 untreated, treated and release time course revealed that the longest telomeres, rather than the shortest, exhibited the greatest rate of change in telomere length upon release. In order to quantify this observation, the telomere length distributions for each time point after release were classified by percentile and the rate of change of telomere length across percentiles was calculated. In this analysis, the 5^{th} percentile of each timepoint represents the molecular weight cutoff at which only 5% of telomeres are shorter; similarly the 95^{th} percentile represents the molecular weight cutoff at which only 5% of telomeres are longer. Rates of change were calculated for the 5^{th}, 10^{th}, 20^{th}, 30^{th}, 40^{th}, 50^{th} (median), 75^{th}, and 95^{th} percentiles to allow for a comparison between the elongation of the shortest telomeres and the longest (Figure 4.13).

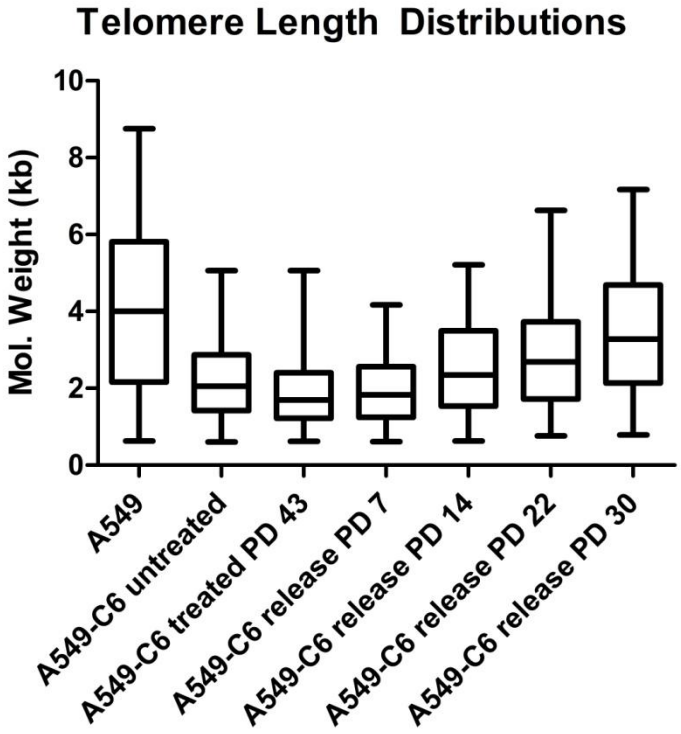

Figure 4.12 Telomere length distributions of A549-C6 after GRN163L treatment and 30 PD after release from treatment. For each timepoint, molecular weights of 150-300 individual telomere amplification products from Universal STELA were assessed and telomere length distribution was constructed. Box plot whiskers represent the maximum and minimum telomere lengths in each sample; the boxes represent the middle 50% of telomere lengths (25^{th} to 75^{th} percentile), with the median (50^{th} percentile) noted for each sample.

The calculated rate of change of the median (50^{th} percentile) of telomeres was approximately 60 bp per PD, correlating closely to the calculated average rate of telomere elongation. The greatest observed rate of change in telomere length was that of the longest telomeres, with the 95^{th} percentile of telomeres increasing in length at a rate of approximately 110 bp per PD. In stark contrast, the rate of

change of the shortest (5th percentile) telomeres was calculated at only ~17 bp per PD. The rate of change in telomere length over the release time course increases with percentile, with the shortest telomeres having the slowest rate of change and each subsequent higher percentile having a higher rate of change (Figure 4.13 and Table 4.1).

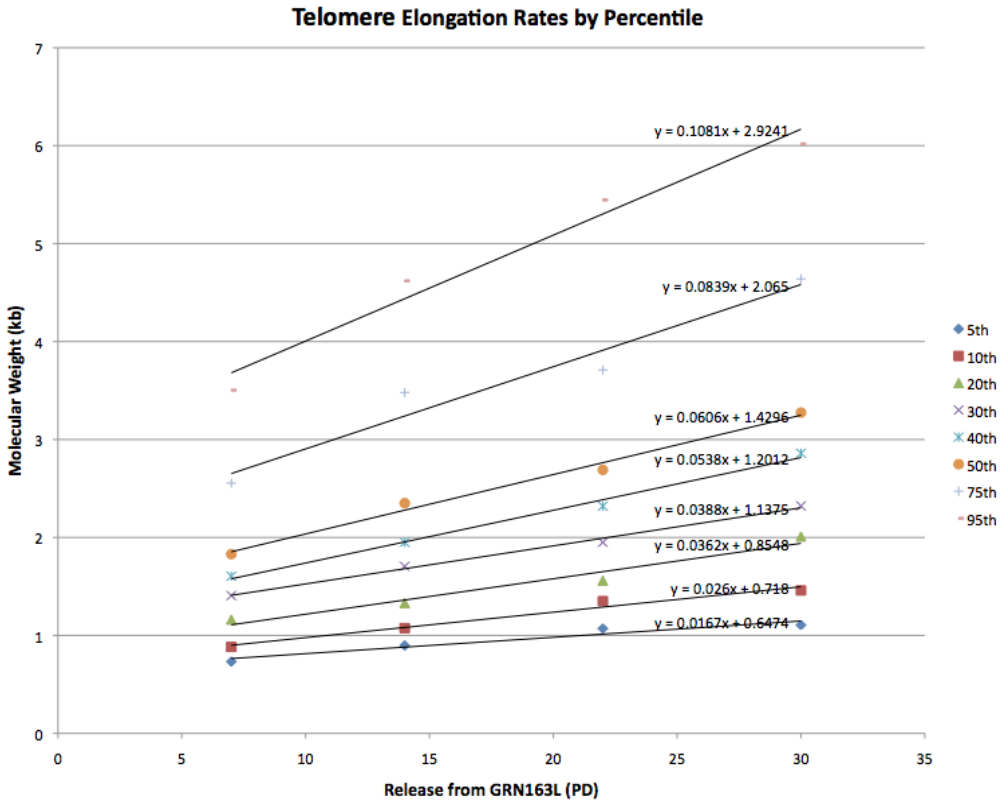

Figure 4.13 Rate of change in telomere length after release from GRN163L by percentile. Telomere length distributions for each time point following release from GRN163L telomerase inhibition were classified by percentile, and a linear regression line was calculated to describe the rate of change in telomere length for each percentile (5th to 95th). For each percentile, the linear regression model is displayed, and the slope of the line represents the rate of change in telomere length for that percentile class. R^2 values for each percentile are listed in Table 4.1.

Percentile	Calculated Rate of Change	Linear Regression Equation	R^2
5th	17 bp/PD	y=0.0167x + 0.6574	0.93126
10th	26 bp/PD	y=0.026x + 0.718	0.97344
20th	36 bp/PD	y=0.0362x + 0.8548	0.95812
30th	38 bp/PD	y=0.0388x + 1.1375	0.99399
40th	54 bp/PD	y=0.0538x + 1.2012	0.99203
50th	61 bp/PD	y=0.0606x + 1.4296	0.98930
75th	84 bp/PD	y=0.0839x + 2.065	0.94957
95th	108 bp/PD	y=0.1081x + 2.9241	0.97002

Table 4.1 Calculated rate of change in telomere length after release from GRN163L by percentile. A linear regression model was created for each percentile to model the rate of change in telomere length. The calculated rate of change is based on the slope of the linear regression equation for each percentile, with R^2 values reported for each regression model.

DISCUSSION

Telomerase extension of the G-rich telomeric strand occurs shortly after telomere replication, and is uncoupled from fill-in of the C-rich telomeric strand, which is a unique event that is delayed until S/G2

The ability to accurately measure changes in strand-specific telomere length over the course of a single cell cycle allowed for the first time to show that telomerase extension of the G-rich strand is coupled to telomere replication, while the extension of the C-rich strand is a separate step that occurs in late S/G2 phase. This was possible because C- and G-STELA are capable of measuring small, chromosome specific changes in telomere length, whereas the more traditional TRF method only provides information on changes in average telomere length over many PDs. Measuring both the changes in telomere length of both the C-

rich and the G-rich telomeric strands allowed us to observe that the two processes are uncoupled. G-STELA is not often used for telomere length measurement as it is more technically challenging than C-STELA while producing a nearly identical telomere length (taking into account the length of the G-rich 3' overhang). However, G-STELA has been used to learn detailed information about telomere biology such as the terminal nucleotide of the G-rich strand (Sfeir et al., 2005) and now, the timing of telomerase elongation of the G-rich strand. This exemplifies how telomere length studies can be used to examine molecular details of telomere biology that are otherwise complicated and difficult to study.

Our finding that telomerase extends the G-rich strand quickly after telomeres are replicated is consistent with previous studies in yeast (Diede and Gottschling, 1999; Marcand et al., 2000) as well as cytological evidence that telomerase co-localizes at small subsets of telomeres throughout S-phase in mammalian cells (Jady et al., 2006; Tomlinson et al., 2006). Because mammalian telomeres replicate throughout S-phase, relating the timing of telomere replication with telomerase extension required knowledge of the exact timing of replication of a specific telomere, as well as the ability of STELA to analyze changes in telomere length of a single telomere. In this study, the XpYp telomere was analyzed because the timing of XpYp replication was known and an XpYp-specific subtelomeric forward primer was available for STELA. The timing of telomerase extension could be similarly examined on other chromosomes for

which there are available subtelomere-specific forward STELA primers in order to confirm our findings. However, multiple assays have provided robust data supporting the finding that telomerase extension of the G-rich strand is coupled to telomere replication (Zhao et al., 2009), making this follow-up work using STELA largely unnecessary.

The finding that there is a delay between telomerase extension of the G-rich strand and the fill-in of the C-rich strand was unexpected and suggests that it is a unique regulatory step in telomere replication of telomerase positive cells. The C-STELA data indicated that fill-in of the C-rich strand occurs in late S phase/early G2 phase. Previous studies have shown that a localized DNA damage response is found at the telomeres at the end of S phase, with ChIP analysis showing co-localization of many DNA repair factors such as MRN, ATM, ATR, and Rad17 at telomeres (Verdun et al., 2005). This localized DNA damage response at telomeres at S/G2 could be in response to an unfoleded t-loop, leaving the telomeric ends free to be recognized as a double stranded break. Little is currently known about the dynamics of t-loop folding and unfolding, but it is clear they must unfold for telomere replication and that that the 3' G-rich overhang must be accessible (and thus the t-loop must be unfolded) for telomerase extension as well as C-strand fill-in. One possibility is that telomeres replicate asynchronously during S phase and immediately re-fold into t-loops, with all telomeres synchronously unfolding again at S/G2 for C-strand fill-in to occur.

The other possibility is that telomeres remain unfolded during the duration of S-phase until all have been asynchronously replicated and C-strand fill-in occurs at S/G2; this scenario would necessitate some regulatory function which must attenuate the DNA damage sensing machinery from recognizing the linear telomere ends as broken DNA during S phase. In either case, the DNA damage response at the end of S phase could be a signal that triggers both C-strand fill-in and subsequent t-loop folding. Importantly, the fact that we now know that C-strand fill-in is a distinct step in telomere replication and telomerase activity means that targeting this step could increase the efficiency of anti-telomerase cancer therapeutics.

Comparing the rate of telomerase elongation of the shortest, average, and longest telomeres after long-term GRN163L telomerase inhibition

There is a general consensus that telomerase preferentially targets short telomeres under conditions where telomere length is shorter than the set maintenance length (Hemann et al., 2001a; Ouellette et al., 2000; Samper et al., 2001; Steinert et al., 2000; Zhu et al., 1998). Recent data suggests that under conditions when telomerase must lengthen (rather than maintain) telomere length, multiple telomerase molecules are recruited for multiple rounds of elongation in a distributive manner (Zhao et al., 2011). In the present study, A549-C6 cells were treated with the telomerase inhibitor GRN163L for 43 PDs in order to artificially

shorten telomeres, and then allowed to recover from treatment in normal growth media for 30 PDs. Endogenous telomerase is known to elongate telomeres upon release from GRN163L treatment (Herbert et al., 1999), and when Universal STELA was performed on sequential samples after release, a mean average lengthening of ~60 bp per PD was measured. Because Universal STELA produces individual telomere amplification products that can be arranged in a distribution, it was possible to organize the measured telomeres from each release timepoint according to their percentile rank. This allowed for the calculation of the rate of change in telomere length according to percentile rank, and therefore the direct comparison of the rate of increase in telomere length of the shortest, average and longest telomeres from each release time point. When these rates were calculated, the data did not immediately support the hypothesis that the shortest telomeres are elongated more rapidly than the average and longer telomeres. In fact, the shortest (5^{th} percentile) telomeres had the slowest calculated rate of growth (only ~17 bp/PD), with each increasing percentile rank having a subsequently faster rate of growth, with the longest telomeres increasing in length at the highest rate (~110 bp/PD).

There are several issues that must be considered when interpreting this data. First of all, these calculated rates may accurately reflect a flawed experimental system. During the course of the treatment with GRN163L, routine assay of telomerase activity was not performed to confirm that telomerase activity

was completely inhibited. It is obvious that telomerase was inhibited enough to cause telomere shortening and induce telomere elongation upon release, but we cannot say with authority that there was no residual telomerase activity. If the cell system was truly telomerase deficient for many PD, one would expect the shortest telomeres to be the highest priority target of telomerase in a system that has been telomerase-deficient for many PD, and thus exhibit rapid elongation. However, if telomerase inhibition was not complete and there was even just 10% residual telomerase activity, it is reasonable to predict that the remaining active telomerase molecules would maintain the length of the shortest telomeres in the cells. Recent data indicates that in situations where telomerase is partly inhibited, and thus limiting, the fraction of extended ends is proportional to the number of active telomerase molecules available (Zhao et al., 2011). In this scenario, whatever active telomerase molecules are available could be targeted to elongate the shortest telomeres. This would imply that the shortest telomeres that were measured by Universal STELA would already be maintained at a stable length, and would not be in need of rapid elongation. This possibility could explain why we do not see a rapid rate of elongation of the shortest telomeres upon release, and could also explain why the minimum telomere length remains relatively constant (~600 bp) across all samples analyzed (including untreated samples). In order to test this possibility, this experiment could be repeated in replicate with multiple doses of telomerase inhibition (e.g. 50%, 75%, ~100%) before release.

However, there are additional practical limitations to the analysis of this data which may preclude the usefulness of this additional data.

A major drawback to the interpretation of this data is that it is impossible to derive a statistical model that lets us track how telomeres may change percentile rank over time. In other words, it is impossible to determine if a 5^{th} percentile telomere from the first release time point is elongated but stays a 5^{th} percentile telomere in subsequent time points, or if it is elongated enough relative to other telomeres that it jumps to a higher percentile rank in a subsequent time point. Alternatively, rapid telomere deletion events could occur which causes telomeres to drop to a lower percentile can rank over time. The analysis attempted in this study is only valid under the assumption that telomeres in a cell on average maintain a relative length in relationship to one another. This assumption is supported by previous studies which have shown that individual telomeres have set relative lengths that are inherited and maintained over a human lifetime (Graakjaer et al., 2003; Graakjaer et al., 2006). However, while telomeres may maintain their relative lengths over long periods of time, it is difficult to say what the short term length dynamics are as telomeres recover from a rapid telomere deletion event or – as in this study – artificial shortening by telomerase inhibition. Because the Universal STELA data shows an increasing expansion of the middle 50% of telomeres, and the greatest rate of elongation of the longest telomeres over time, it is reasonable to consider the possibility that the

shortest telomeres become elongated rapidly and extensively enough relative to average and long telomeres that they jump to higher percentile ranks in subsequent time points, thus causing the expansion of the distribution of average-to-long telomeres over the release time course. This does not, however, explain why such a large fraction of very short telomeres remain over the 30 PD of release from telomerase inhibition treatment. If the Universal STELA and calculated rates of elongation do reflect the reality of length dynamics in this experimental system, the slow rate of growth of the shortest telomeres may be reflective of data which indicates that the processivity of telomerase is impaired immediately following periods of long-term telomerase inhibition therapy (Zhao et al., 2011).

Long-term telomerase inhibition altered maintenance telomere length of a clonally-derived cell population

The A549-C6 cells used in this experimental setup were originally derived as a clone of A549 lung carcinoma that was picked because it had relatively short telomeres, and was expanded and subcultured for many months without a change in this relatively short average maintenance telomere length. After 43 PD of treatment with GRN163L, the recovering cells exhibited telomere elongation well beyond the original length of the clone, and at the latest time point analyzed (30 PD after release from treatment), the distribution was more similar to the length

and distribution of the parent A549 cell line. It is unclear what mechanism is responsible for the original A549-C6 having relatively shorter telomeres, or what caused the clone to revert to having relatively longer telomeres after extended GRN163L treatment. Subcloning the untreated and treated A549-C6 population and analyzing the subclones for telomerase activity and telomere length may give insight into this dynamic. This data which indicates that after release from telomerase inhibition, telomeres may extend beyond their original length may have important implications in telomerase inhibition cancer therapy, as incomplete inhibition or cessation of treatment may cause any residual cancer cells to extensively lengthen their telomeres, giving them a longer proliferative lifespan and making them less susceptible to induction of senescence by future rounds of telomerase inhibition treatment.

MATERIALS AND METHODS

Cell culture and Treatments

A population derived from a clone of A549 lung carcinoma cells with short telomeres, termed A549-C6, was cultured at 37°C in 5% CO_2 in medium containing 10% cosmic calf serum (HyClone, Logan, UT). During telomerase inhibition treatment, this media was supplemented with l µM GRN163L (Geron Corp, Menlo Park, CA) at every cell passage (approximately every three days) for one month. Treated cells were transduced with a retroviral vector pBabepuro-

hTERT that overexpresses hTERT. Puromycin selection was carried out over 10 days to yield A549-C6+hTERT cells. GRN163L-treated cells that expressed only endogenous hTERT were then grown in normal growth media in the absence of the telomerase inhibitor for approximately 30 PD. Cells were passaged every 3-4 days, and a sample was harvested for telomere length analysis at each cell passage

Cell cycle synchronization and FACS analysis

A549-C6+hTERT cells were synchronized by combining sequential serum starvation (to push cells into G0/G1) and then aphidicolin treatment (to inhibit DNA Polymerase and thus prevent progression through S phase, (Pedrali-Noy and Spadari, 1979)). First, cells were grown in DMEM with 0.1% cosmic calf serum and 20 mM HEPES, which is 1000-fold less serum than used in normal growth media, for two days. Then the cells were switched to fresh DMEM media containing 10% Cosmic Calf Serum that was treated with 4µg/ml aphidicolin for 24 hours. To release cells into S phase, cells were washed three times with pre-warmed PBS and placed in fresh growth serum (DMEM + 10% CCS) for zero to 10 hours. Cells were harvested every 2 hours after release into S phase. From each timepoint, cells were collected for FACS analysis of DNA content to monitor progression through S phase. At each timepoint, cells were harvested and fixed in ice cold 70% ethanol overnight. Cells were then washed with 10 mL PBS, passed through a nylon mesh to disrupt any cell aggregations and ensure a uniform suspension, and incubated with a propidium iodide solution (Sigma) for

30-60 minutes in the dark at room temperature. Flow cytometry on a FacscaliburII (BD Biosciences) machine was performed to analyze for DNA content using the CellQuest program (BD Bioscience).

Measurement of telomerase activity

The telomere repeat amplification protocol (TRAP) was used to measure telomerase activity in A549-C6 and A549-C6+hTERT cells. An aliquot of 100 thousand cells was harvested for TRAP analysis, and the TRAPexe (Intergen) kit was used according to the protocol.

Genomic DNA isolation

Genomic DNA for TRF and all variations of STELA was isolated from harvested cell pellets using the DNEasy Blood and Tissue Kit (Qiagen) according to kit instructions with a few modifications: After adding the cell lysis buffer, RNA was digested by adding 4 ul of 100 mg/ml RNaseA (Ambion) and incubating at room temperature for 15 minutes. ProteinaseK treatment was carried out at 55° C for 30-60 minutes to maximize degradation of cellular proteins. ProteinaseK was then heat inactivated at 70° C for 10 minutes. Kit protocol was used to bind and wash spin columns. Genomic DNA was eluted twice in DEPC-treated H_2O (Ambion).

TRF analysis

TRF analysis was used as a simple way to quickly measure mean telomere length. Genomic DNA isolated as described above was digested with a

mixture of six frequently-cutting, four base cutter restriction enzymes (Alu I, Cfo I, Hae III, Hinf I, Msp I and Rsa I) at 37° C for one-two hours and resolved on a 0.7% agarose gel overnight. The gel was denatured in a 0.5M NaOH, 1.5 M NaCl solution for 20 minutes at room temperature, and then rinsed in dH_2O for 10 minutes. The gel was then dried on a slab gel dryer at 55° C for approximately two hours, or until the gel was paper thin. The dried and denatured gel was neutralized in 1.5 M NaCl, 0.5 M Tris (pH=8.0) for 15 minutes at room temperature. The gel was then incubated with a ^{32}P-labeled telomere-specific [$(TTAGGG)_4$] oligonucleotide probe in a hybridization oven at 42 ^{o}C for at least four hours. The gel was then washed once with low-stringency buffer (2x SSC) and twice with high stringency wash (0.1x SSC, 0.1% SDS) for 15 minutes each at 42° C. The gel was then exposed to a PhosphorImager screen and scanned on a Typhoon biomolecular imager (GE Healthcare Life Science) and weighted mean telomere length was calculated as described (Ouellette et al., 2000) using ImageQuant (GE Healthcare Life Science) software.

C-STELA and G-STELA

C-STELA protocol was developed from previously reported protocols (Baird et al., 2003; Sfeir et al., 2005) and optimized for this experimental setting. 960 ng of purified genomic DNA was digested with EcoRI at 37° C for 60 minutes. 320ng of the EcoRI digested genomic DNA was incubated in a 20ul ligation reaction containing 50 U T4 DNA ligase (NEB), 1x ligase buffer, and 1

μM of a mixture of all six C-telorettes (making the final concentration of each telorette 0.16 μM) at 17° C for at least 15 hours. 28 cycles of PCR amplification (95°C for 15 s, 62°C for 20 s, and 68°C for 10 min) were performed using the Extensor Hi-Fidelity PCR Master Mix 1 (ABgene, Thermo Scientific) in a 25 μl reaction which contained 2 ng of ligated DNA and 0.5 μM primers (forward: XpYpE2; reverse: C-Teltail). Telomere amplification products were transferred to positively charged membrane (Hybond N+, GE Healthcare Life Science) by capillary action, and DNA was fixed to the membrane by baking at 85° for two hours. A probe specific to the subtelomeric region of the XpYp telomere was generated by amplifying the region of the XpYp subtelomere that lies between the XpYpE2 forward and XpYpB2 reverse primers and labeling the product using the RadPrime DNA labeling system (Invitrogen). The membrane was incubated with the labeled subtelomeric probe in RapidHyb buffer (Amersham) at 65° overnight, washed once with low-stringency buffer (2x SSC) and twice with high stringency wash (0.1x SSC, 0.1% SDS) for 15 minutes each at 65° C. The gel was then exposed to a PhosphorImager screen and scanned on a Typhoon biomolecular imager (GE Healthcare Life Science). Molecular weight of the individual telomere amplification products was determined using AlphaEaseFC Software (Alpha Innotech), and average telomere lengths were determined using Microsoft Excel and Graphpad Prism software.

G-STELA follows a very similar protocol to C-STELA, with the following modifications: genomic DNA digested with EcoRI is first incubated with a C-rich platform oligonucleotide $(AATCCC)_{10}$ at 1 nM final concentragion at room temperature for 3 hours. Conditions for the ligation and PCR are the same, except that a mixture of six G-telorettes is used for G-STELA, and the reverse primer used during PCR amplification is the G-Teltail reverse primer. All other steps are identical to C-STELA. A listing of all primers used for C- and G-STELA and their sequences is found in Table 3.1 and 3.2.

Universal STELA

Universal STELA was performed using a strategy modified from that previously described (Bendix et al.). 500 ng purified DNA was digested for 1 hour at 37°C with the restriction enzyme NlaIII (New England Biolabs). An NlaIII restriction site-specific panhandle linker was designed and created by incubating two oligonucleotides ("long" and "short") in a 1:2 ratio at 95°C for 5 minutes and cooling to room temperature over one hour in 50 mM NaCl. 100 ng of digested genomic DNA was incubated in a10 μl ligation reaction containing 1x ligase buffer, 50 U T4 DNA ligase (NEB), 10^{-2} μM of a mixture of all six C-telorettes (0.16×10^{-2} μM each) and 10 μM NlaIII-specific panhandle for 15 hours at 17°C. Multiple PCR reactions were performed (Initial melt of 94°C for 30 s followed by 22 cycles of 94°C for 15 s + 68°C for 12 min) using Extensor Hi-

Fidelity PCR Master Mix 1 (ABGene, Thermo Scientific) in 25 µl reaction containing 100 pg ligated DNA, 0.5 µM primers (Adapter forward primer and C-Teltail reverse primer) and supplemented with 5% DMSO. Telomere amplification products were resolved on a 0.7% agarose gel, and subject to in-gel hybridization using a ^{32}P-labeled telomere-specific [$(TTAGGG)_4$] oligonucleotide probe in a hybridization oven at 42 ^{o}C for at least four hours. The gel was then washed once with low-stringency buffer (2x SSC) and twice with high stringency wash (0.1x SSC, 0.1% SDS) for 15 minutes each at 42° C. The gel was then exposed to a PhosphorImager screen and scanned on a Typhoon biomolecular imager (GE Healthcare Life Science). Universal STELA telomere amplification products were analyzed for molecular weight using AlphaEaseFC (AlphaInnotech) software and all statistical analyses was carried out using Microsoft Excel and GraphPad Prism. A listing of all primers used for Universal STELA and their sequences is found in Table 3.3

Table 3.2 Primers used in C-STELA

Name	Function	Sequence
XpYp E2	Forward Primer (subtelomeric)	5'-TTGTCTCAGGGTCCTAGTG-3'
XpYp B2	Reverse Primer (subtelomeric)	5'-TCTGAAAGTGGACC(A/T)ATCAG-3
C-telorette 1	C-telomere tag	5' TGCTCCGTGCATCTGGCATCCCCTAAC-3'
C-telorette 2	C-telomere tag	5'-TGCTCCGTGCATCTGGCATCTAACCCT-3'
C-telorette 3	C-telomere tag	5'-TGCTCCGTGCATCTGGCATCCCTAACC-3'
C-telorette 4	C-telomere tag	5'-TGCTCCGTGCATCTGGCATCCTAACCC-3'
C-telorette 5	C-telomere tag	5'-TGCTCCGTGCATCTGGCATCAACCCTA-3'
C-telorette 6	C-telomere tag	5'-TGCTCCGTGCATCTGGCATCACCCTAA-3
C-teltail	Reverse Primer	5'-TGCTCCGTGCATCTGGCATC-3'

Table 3.3 Primers used in G-STELA

Name	Function	Sequence
Platform	Artificial 5' overhang	$(5'\ AATCCC\ 3')_{10}$
XpYp E2	Forward Primer (subtelomeric)	5'-TTGTCTCAGGGTCCTAGTG-3'
XpYp B2	Reverse Primer (subtelomeric)	5'-TCTGAAAGTGGACC(A/T)ATCAG-3'
G-telorette 1	G-telomere tag	5' P-GTTAGGGCTACGGTCTACGTGCCTCGT-3'
G-telorette 2	G-telomere tag	5' P-TTAGGGTCTACGGTCTACGTGCCTCGT-3'
G-telorette 3	G-telomere tag	5' P-TAGGGTTCTACGGTCTACGTGCCTCGT-3'
G-telorette 4	G-telomere tag	5'P-AGGGTTACTACGGTCTACGTGCCTCGT-3'
G-telorette 5	G-telomere tag	5'P-GGGTTAGCTACGGTCTACGTGCCTCGT-3'
G-telorette 6	G-telomere tag	5'P-GGTTAGGCTACGGTCTACGTGCCTCGT-3'
G-teltail	Reverse Primer	5'-ACGAGGCACGTAGACCGTAG-3'

Table 3.4 Primers used in Universal STELA

Name	Function	Sequence
Adapter	Forward Primer	5′- TGT AGC GTG AAG ACG ACA GAA - 3′
Long	Panhandle linker	5’TGTAGCGTGAAGACGACAGAAAGGGCGTGGT GCGGACGCGGGCATG 3’
Short	Panhandle linker	5’ CCCGCGTCCGC 3’
C-telorette 1	C-telomere tag	5' TGCTCCGTGCATCTGGCATCCCCTAAC-3'
C-telorette 2	C-telomere tag	5'-TGCTCCGTGCATCTGGCATCTAACCCT-3'
C-telorette 3	C-telomere tag	5'-TGCTCCGTGCATCTGGCATCCCTAACC-3'
C-telorette 4	C-telomere tag	5'-TGCTCCGTGCATCTGGCATCCTAACCC-3'
C-telorette 5	C-telomere tag	5'-TGCTCCGTGCATCTGGCATCAACCCTA-3'
C-telorette 6	C-telomere tag	5'-TGCTCCGTGCATCTGGCATCACCCTAA-3
C-teltail	Reverse Primer	5'-TGCTCCGTGCATCTGGCATC-3'

CHAPTER FIVE

FUTURE DIRECTIONS

The major advantage of the Universal STELA assay is that it is capable of directly measuring the full distribution of lengths of individual telomere molecules in a cell population, including the shortest telomeres. This is the first assay that can detect any short telomeres that are located on any chromosome, because the assay is not telomere specific (like the original STELA method, (Baird et al., 2003)). The ability to detect short telomeres and describe the distribution of all telomere lengths in a cell makes the assay very valuable in experimental settings where induction of replicative senescence is of concern. A few short telomeres are thought to be sufficient to induce replicative senescence (Abdallah et al., 2009; Hemann et al., 2001b; Zou et al., 2004b), and there is not a good way to predict which chromosome these critically short telomeres will first appear. While Universal STELA will not be able to provide any information about which specific telomere has become critically short, the ability to correlate the presence of ultra-short telomeres with physiologic signs of cellular aging and senescence. This has applications in cell biology, aging biology and cancer biology.

Critically short telomeres in response to oxidative stress. It has been observed that oxidative stress can enhance telomere attrition rates and cause rapid telomere deletion events (Chen et al., 1995; Martin-Ruiz et al., 2004; Richter and Zglinicki, 2007; von Zglinicki, 2000, 2002). In order to study the dynamics of oxidative damage induced telomere shortening, an experimental system could be derived in which cells with a narrow telomere length distribution were grown in normal or high oxygen concentrations over the course of many PDs. In order to decrease the natural telomere length heterogeneity normally found in cell populations, these cells could either be clonally derived, or express a deletion mutant of the shelterin component protein hRap1, which is known to decrease telomere length heterogeneity (Li and de Lange, 2003). Cells would be harvested at each passage and analyzed by Universal STELA in order to track the change in the shape of the telomere length distribution. Starting with cells that had a more uniform telomere length would facilitate the detection of a gradual accumulation of shorter telomeres in response to the high oxygen stress, versus the sudden occurrence of very short telomeres due to rapid telomere deletion events. Changes in the telomere length distribution could be correlated to other indicators of cellular stress and senescence. Because oxidative damage is one of the known causes of telomere shortening, it is important to better understand how telomeres actually respond to high oxygen stress. Universal STELA would allow us to directly measure this stress response.

Telomerase inhibition therapy. In the present study, Universal STELA was used to investigate whether cancer stem cells were susceptible to telomerase inhibition therapy because they have either a large fraction of short telomeres, or a shorter mean baseline telomere length. Universal STELA was also used to investigate the rate of telomere elongation after prolonged telomerase inhibition. Telomerase inhibition therapy is currently in a variety of phase 2 clinical trials, and has the potential to work in combination with other cancer debulking therapies (such as traditional chemotherapies and radiation therapy) or as a maintenance therapy following tumor debulking therapies in order to produce a more durable disease response. While clinical trials are progressing, preclinical trials examining the effects of telomerase inhibition on cell lines, primary tumor cells, cancer stem cells and xenograft models are abundant. Universal STELA will be a useful assay in the toolkit for studying telomerase inhibition. Not only does it measure the short telomeres which telomerase inhibition seeks to generate, but it also requires very small amounts of DNA starting material, which is perfect for clinical and preclinical experimental settings where a sample might be anything from a small number of isolated circulating tumor cells to a small fraction of sorted CSCs to a small tissue biopsy. Universal STELA can help provide routine data pertinent to telomerase inhibition, such as determining the required duration of telomerase inhibition therapy that produces critically short telomeres and induces cell senescence. It can also be used to investigate how the

distribution of telomere lengths in a sample predicts response to telomerase inhibition therapy.

Short telomeres and aging biology. The ability to measure short telomeres has potential uses in clinical and epidemiological studies of aging related diseases. A recent study used the Q-PCR telomere length measurement method to look for an association between telomere length and a variety of disease states in centenarians (Atzmon et al., 2010). Their study hypothesizes that longer telomeres is indicative of general genomic integrity, and is associated with a longer life and better health outcomes. Universal STELA could be applied to experimental settings in which diseased versus healthy samples or old versus young samples are being compared, and the telomere length distributions would help us to understand the role that critically short telomeres play in long term health outcomes. Universal STELA is superior to the Q-PCR method for measuring telomere lengths because it provides a direct length measurement and allows for the construction of length distributions that includes even the shortest of telomeres. One potential drawback to using Universal STELA for this kind of experiment is that some cells have quite long telomeres which are difficult to analyze. While Universal STELA is sufficiently time consuming as an assay to preclude it from routine epidemiologic screening of thousands of samples, it is quite possible to analyze smaller numbers of samples in clinical studies and smaller case control and cohort epidemiology studies.

Telomere biology: Universal STELA can measure the X-region. One aspect of telomere biology that is generally accepted yet not well understood is the nature of the so-called "X-region," the portion of the subtelomere that is resistant to restriction digestion (Steinert et al., 2004). This region is of particular importance to telomere length measurements obtained from measuring telomere restriction fragments, such as Universal STELA and the standard TRF analysis. While the X-region is presumed to influence the lengths of these telomere restriction fragments, a direct way to measure the X-region and thus determine the degree to which it influences measured telomere lengths has not previously been developed. The nature of the design of Univesal STELA allows for the detection of the length of the X-region, and is going to be a valuable tool for learning more about this aspect of telomere biology that has been so elusive. Universal STELA involves digestion of genomic DNA with restriction enzymes to create an overhang that can be ligated with the proximal panhandle linker. In a complete digestion, it can be assumed that all available restriction sites will be digested, up to the restriction site that is closest to the telomere that is not protected by the X region. These digested telomere restriction fragments are then amplified using PCR. While we do not know the mechanism that confers the X-region protection against restriction digestion, it is certain that PCR amplified products will not retain the protective capacity. Thus, the telomere amplification products from Universal STELA can be redigested with the same enzyme(s) used to originally

digest the genomic DNA, and any restriction sites which were previously protected from digestion should now be digested. Comparing the lengths of the undigested PCR products (which represent the size of the telomere plus the X region) and the digested PCR products (which have had the X region removed) will allow for the determination of the size of the X region. Because Universal STELA measures all telomeres in a cell population, this will tell us average size of the X region in an actual cell population as opposed to on an artificial telomere in a manipulated experimental system (Steinert et al., 2004). This will allow many questions about the X region to be answered, such as whether the size of the X region changes as a function of telomere length, if all cell lines have an X region and if so, is it the same length in all cells. Ultimately, we must elucidate the mechanism that confers the protective property of the X region. Gaining more data to characterize the nature of the X region will allow us to form better hypotheses as to the origin and function of the X region.

Summary. Studies of telomere length have practical and theoretical implications in a wide variety of fields, from evolutionary biology to medicine and epidemiology to molecular and cellular biology. Universal STELA serves as an important tool to study issues of telomere length that cannot be studied using other methods. We continue to work to improve the assay by utilizing additional molecular strategies which will make the assay more robust.

BIBLIOGRAPHY

Abdallah, P., Luciano, P., Runge, K.W., Lisby, M., Geli, V., Gilson, E., and Teixeira, M.T. (2009). A two-step model for senescence triggered by a single critically short telomere. Nat Cell Biol *11*, 988-993.

Akiyama, M., Hideshima, T., Shammas, M.A., Hayashi, T., Hamasaki, M., Tai, Y.T., Richardson, P., Gryaznov, S., Munshi, N.C., and Anderson, K.C. (2003). Effects of oligonucleotide N3'-->P5' thio-phosphoramidate (GRN163) targeting telomerase RNA in human multiple myeloma cells. Cancer Res *63*, 6187-6194.

Al-Hajj, M., and Clarke, M.F. (2004). Self-renewal and solid tumor stem cells. Oncogene *23*, 7274-7282.

Allan, A.L., Vantyghem, S.A., Tuck, A.B., and Chambers, A.F. (2006). Tumor dormancy and cancer stem cells: implications for the biology and treatment of breast cancer metastasis. Breast Dis *26*, 87-98.

Allen, N.D., and Baird, D.M. (2009). Telomere length maintenance in stem cell populations. Biochim Biophys Acta *1792*, 324-328.

Allsopp, R.C., Chang, E., Kashefi-Aazam, M., Rogaev, E.I., Piatyszek, M.A., Shay, J.W., and Harley, C.B. (1995a). Telomere Shortening Is Associated with Cell Division in Vitro and in Vivo. Experimental Cell Research *220*, 194-200.

Allsopp, R.C., Chang, E., Kashefi-Aazam, M., Rogaev, E.I., Piatyszek, M.A., Shay, J.W., and Harley, C.B. (1995b). Telomere shortening is associated with cell division in vitro and in vivo. Exp Cell Res *220*, 194-200.

Allsopp, R.C., and Harley, C.B. (1995). Evidence for a critical telomere length in senescent human fibroblasts. Exp Cell Res *219*, 130-136.

Allsopp, R.C., Vaziri, H., Patterson, C., Goldstein, S., Younglai, E.V., Futcher, A.B., Greider, C.W., and Harley, C.B. (1992). Telomere length predicts replicative capacity of human fibroblasts. Proc Natl Acad Sci U S A *89*, 10114-10118.

Amiard, S., Doudeau, M., Pinte, S., Poulet, A., Lenain, C., Faivre-Moskalenko, C., Angelov, D., Hug, N., Vindigni, A., Bouvet, P., *et al.* (2007). A topological mechanism for TRF2-enhanced strand invasion. Nat Struct Mol Biol *14*, 147-154.

Ancelin, K., Brunori, M., Bauwens, S., Koering, C.E., Brun, C., Ricoul, M., Pommier, J.P., Sabatier, L., and Gilson, E. (2002). Targeting assay to study the cis functions of human telomeric proteins: evidence for inhibition of telomerase by TRF1 and for activation of telomere degradation by TRF2. Mol Cell Biol *22*, 3474-3487.

Arai, K., Masutomi, K., Khurts, S., Kaneko, S., Kobayashi, K., and Murakami, S. (2002). Two independent regions of human telomerase reverse transcriptase are important for its oligomerization and telomerase activity. J Biol Chem *277*, 8538-8544.

Armanios, M.Y., Chen, J.J., Cogan, J.D., Alder, J.K., Ingersoll, R.G., Markin, C., Lawson, W.E., Xie, M., Vulto, I., Phillips, J.A., 3rd, *et al.* (2007). Telomerase mutations in families with idiopathic pulmonary fibrosis. N Engl J Med *356*, 1317-1326.

Arnoult, N., Saintome, C., Ourliac-Garnier, I., Riou, J.F., and Londono-Vallejo, A. (2009). Human POT1 is required for efficient telomere C-rich strand replication in the absence of WRN. Genes Dev *23*, 2915-2924.

Asai, A., Oshima, Y., Yamamoto, Y., Uochi, T.A., Kusaka, H., Akinaga, S., Yamashita, Y., Pongracz, K., Pruzan, R., Wunder, E., *et al.* (2003). A novel telomerase template antagonist (GRN163) as a potential anticancer agent. Cancer Res *63*, 3931-3939.

Attwooll, C.L., Akpinar, M., and Petrini, J.H. (2009). The mre11 complex and the response to dysfunctional telomeres. Mol Cell Biol *29*, 5540-5551.

Atzmon, G., Cho, M., Cawthon, R.M., Budagov, T., Katz, M., Yang, X., Siegel, G., Bergman, A., Huffman, D.M., Schechter, C.B., *et al.* (2010). Evolution in health and medicine Sackler colloquium: Genetic variation in human telomerase is associated with telomere length in Ashkenazi centenarians. Proc Natl Acad Sci U S A *107 Suppl 1*, 1710-1717.

Austad, S.N. (2010). Methusaleh's Zoo: how nature provides us with clues for extending human health span. J Comp Pathol *142 Suppl 1*, S10-21.

Bae, N.S., and Baumann, P. (2007). A RAP1/TRF2 complex inhibits nonhomologous end-joining at human telomeric DNA ends. Mol Cell *26*, 323-334.

Baerlocher, G.M., Mak, J., Tien, T., and Lansdorp, P.M. (2002). Telomere length measurement by fluorescence in situ hybridization and flow cytometry: tips and pitfalls. Cytometry *47*, 89-99.

Bailey, S.M., Brenneman, M.A., and Goodwin, E.H. (2004a). Frequent recombination in telomeric DNA may extend the proliferative life of telomerase-negative cells. Nucleic Acids Res *32*, 3743-3751.

Bailey, S.M., Cornforth, M.N., Kurimasa, A., Chen, D.J., and Goodwin, E.H. (2001). Strand-specific postreplicative processing of mammalian telomeres. Science *293*, 2462-2465.

Bailey, S.M., Goodwin, E.H., and Cornforth, M.N. (2004b). Strand-specific fluorescence in situ hybridization: the CO-FISH family. Cytogenet Genome Res *107*, 14-17.

Baird, D.M. (2008). Mechanisms of telomeric instability. Cytogenet Genome Res *122*, 308-314.

Baird, D.M., Britt-Compton, B., Rowson, J., Amso, N.N., Gregory, L., and Kipling, D. (2006). Telomere instability in the male germline. Hum Mol Genet *15*, 45-51.

Baird, D.M., Jeffreys, A.J., and Royle, N.J. (1995). Mechanisms underlying telomere repeat turnover, revealed by hypervariable variant repeat distribution patterns in the human Xp/Yp telomere. EMBO J *14*, 5433-5443.

Baird, D.M., and Kipling, D. (2004). The extent and significance of telomere loss with age. Ann N Y Acad Sci *1019*, 265-268.

Baird, D.M., Rowson, J., Wynford-Thomas, D., and Kipling, D. (2003). Extensive allelic variation and ultrashort telomeres in senescent human cells. Nat Genet *33*, 203-207.

Barrientos, K.S., Kendellen, M.F., Freibaum, B.D., Armbruster, B.N., Etheridge, K.T., and Counter, C.M. (2008). Distinct functions of POT1 at telomeres. Mol Cell Biol *28*, 5251-5264.

Baumann, P., and Cech, T.R. (2001). Pot1, the putative telomere end-binding protein in fission yeast and humans. Science *292*, 1171-1175.

Baumann, P., and Price, C. (2010). Pot1 and telomere maintenance. FEBS Lett.

Bechter, O.E., Zou, Y., Walker, W., Wright, W.E., and Shay, J.W. (2004). Telomeric recombination in mismatch repair deficient human colon cancer cells after telomerase inhibition. Cancer Res *64*, 3444-3451.

Bendix, L., Horn, P.B., Jensen, U.B., Rubelj, I., and Kolvraa, S. The load of short telomeres, estimated by a new method, Universal STELA, correlates with number of senescent cells. Aging Cell *9*, 383-397.

Bendix, L., Horn, P.B., Jensen, U.B., Rubelj, I., and Kolvraa, S. (2010). The load of short telomeres, estimated by a new method, Universal STELA, correlates with number of senescent cells. Aging Cell.

Benetti, R., Schoeftner, S., Munoz, P., and Blasco, M.A. (2008). Role of TRF2 in the assembly of telomeric chromatin. Cell Cycle *7*, 3461-3468.

Bertuch, A.A. (2002). Telomeres: the molecular events driving end-to-end fusions. Curr Biol *12*, R738-740.

Bianchi, A., and Shore, D. (2008). How telomerase reaches its end: mechanism of telomerase regulation by the telomeric complex. Mol Cell *31*, 153-165.

Bianchi, A., Smith, S., Chong, L., Elias, P., and de Lange, T. (1997). TRF1 is a dimer and bends telomeric DNA. EMBO J *16*, 1785-1794.

Bianchi, A., Stansel, R.M., Fairall, L., Griffith, J.D., Rhodes, D., and de Lange, T. (1999). TRF1 binds a bipartite telomeric site with extreme spatial flexibility. EMBO J *18*, 5735-5744.

Bilaud, T., Brun, C., Ancelin, K., Koering, C.E., Laroche, T., and Gilson, E. (1997). Telomeric localization of TRF2, a novel human telobox protein. Nat Genet *17*, 236-239.

Bjerkvig, R., Tysnes, B.B., Aboody, K.S., Najbauer, J., and Terzis, A.J. (2005). Opinion: the origin of the cancer stem cell: current controversies and new insights. Nat Rev Cancer *5*, 899-904.

Blackburn, E.H. (1990). Telomeres and their synthesis. Science *249*, 489-490.

Blackburn, E.H. (2005). Telomeres and telomerase: their mechanisms of action and the effects of altering their functions. FEBS Letters *579*, 859-862.

Blackburn, E.H. (2006). History of Telomere Biology. In Telomeres, T. de Lange, Lundblad, V., and Blackburn, E.H., ed. (Cold Spring Harbor, New York, Cold Spring Harbor Press), pp. 1-20.

Blackburn, E.H. (2006b). A Personal Account of the Discovery of Telomerase. In Telomeres, T. de Lange, Lundblad, V., and Blackburn, E.H., ed. (Cold Spring Harbor, New York, Cold Spring Harbor Press), pp. 551-563.

Blackburn, E.H., and Chiou, S.S. (1981). Non-nucleosomal packaging of a tandemly repeated DNA sequence at termini of extrachromosomal DNA coding for rRNA in Tetrahymena. Proc Natl Acad Sci U S A *78*, 2263-2267.

Blackburn, E.H., and Gall, J.G. (1978). A tandemly repeated sequence at the termini of the extrachromosomal ribosomal RNA genes in Tetrahymena. J Mol Biol *120*, 33-53.

Blasco, M.A. (2007). Telomere length, stem cells and aging. Nat Chem Biol *3*, 640-649.

Bodnar, A.G., Ouellette, M., Frolkis, M., Holt, S.E., Chiu, C.P., Morin, G.B., Harley, C.B., Shay, J.W., Lichtsteiner, S., and Wright, W.E. (1998). Extension of life-span by introduction of telomerase into normal human cells. Science *279*, 349-352.

Bollmann, F.M. (2008). The many faces of telomerase: emerging extratelomeric effects. BioEssays *30*, 728-732.

Bonnet, D., and Dick, J.E. (1997). Human acute myeloid leukemia is organized as a hierarchy that originates from a primitive hematopoietic cell. Nat Med *3*, 730-737.

Bradshaw, P.S., Stavropoulos, D.J., and Meyn, M.S. (2005). Human telomeric protein TRF2 associates with genomic double-strand breaks as an early response to DNA damage. Nat Genet *37*, 193-197.

Brennan, S.K., Wang, Q., Tressler, R., Harley, C., Go, N., Bassett, E., Huff, C.A., Jones, R.J., and Matsui, W. (2010). Telomerase inhibition targets clonogenic multiple myeloma cells through telomere length-dependent and independent mechanisms. PLoS One *5*.

Britt-Compton, B., and Baird, D.M. (2006). Intra-allelic mutation at human telomeres. Biochem Soc Trans *34*, 581-582.

Broccoli, D., Chong, L., Oelmann, S., Fernald, A.A., Marziliano, N., van Steensel, B., Kipling, D., Le Beau, M.M., and de Lange, T. (1997a). Comparison of the human and mouse genes encoding the telomeric protein, TRF1: chromosomal localization, expression and conserved protein domains. Hum Mol Genet *6*, 69-76.

Broccoli, D., Smogorzewska, A., Chong, L., and de Lange, T. (1997b). Human telomeres contain two distinct Myb-related proteins, TRF1 and TRF2. Nat Genet *17*, 231-235.

Bryan, T.M., Englezou, A., Dalla-Pozza, L., Dunham, M.A., and Reddel, R.R. (1997). Evidence for an alternative mechanism for maintaining telomere length in human tumors and tumor-derived cell lines. Nat Med *3*, 1271-1274.

Bryan, T.M., Goodrich, K.J., and Cech, T.R. (2000). Telomerase RNA bound by protein motifs specific to telomerase reverse transcriptase. Mol Cell *6*, 493-499.

Buchman, A.R., Kimmerly, W.J., Rine, J., and Kornberg, R.D. (1988). Two DNA-binding factors recognize specific sequences at silencers, upstream activating sequences, autonomously replicating sequences, and telomeres in Saccharomyces cerevisiae. Mol Cell Biol *8*, 210-225.

Burnett, M. (1974). Intrinsic Mutagenesis (Lancaster, Medical and Technical Publishing Co.).

Calado, R.T., and Young, N.S. (2009). Telomere diseases. N Engl J Med *361*, 2353-2365.

Canela, A., Klatt, P., and Blasco, M.A. (2007). Telomere length analysis. Methods Mol Biol *371*, 45-72.

Carrel, A., and Ebeling, A.H. (1921). The Multiplication of Fibroblasts in Vitro. J Exp Med *34*, 317-337.

Castelo-Branco, P., Zhang, C., Lipman, T., Fujitani, M., Hansford, L., Clarke, I., Harley, C.B., Tressler, R., Malkin, D., Walker, E., *et al.* (2011). Neural Tumor-Initiating Cells Have Distinct Telomere Maintenance and Can be Safely Targeted for Telomerase Inhibition. Clin Cancer Res *17*, 111-121.

Cawthon, R.M. (2002). Telomere measurement by quantitative PCR. Nucleic Acids Res *30*, e47.

Cech, T.R., Nakamura, T.M., and Lingner, J. (1997). Telomerase is a true reverse transcriptase. A review. Biochemistry (Mosc) *62*, 1202-1205.

Celli, G.B., and de Lange, T. (2005). DNA processing is not required for ATM-mediated telomere damage response after TRF2 deletion. Nat Cell Biol *7*, 712-718.

Celli, G.B., Denchi, E.L., and de Lange, T. (2006). Ku70 stimulates fusion of dysfunctional telomeres yet protects chromosome ends from homologous recombination. Nat Cell Biol *8*, 885-890.

Cesare, A.J., Quinney, N., Willcox, S., Subramanian, D., and Griffith, J.D. (2003). Telomere looping in P. sativum (common garden pea). Plant J *36*, 271-279.

Chai, W., Du, Q., Shay, J.W., and Wright, W.E. (2006a). Human telomeres have different overhang sizes at leading versus lagging strands. Mol Cell *21*, 427-435.

Chai, W., Sfeir, A.J., Hoshiyama, H., Shay, J.W., and Wright, W.E. (2006b). The involvement of the Mre11/Rad50/Nbs1 complex in the generation of G-overhangs at human telomeres. EMBO Rep *7*, 225-230.

Chai, W., Shay, J.W., and Wright, W.E. (2005). Human telomeres maintain their overhang length at senescence. Mol Cell Biol *25*, 2158-2168.

Chandra, A., Hughes, T.R., Nugent, C.I., and Lundblad, V. (2001). Cdc13 both positively and negatively regulates telomere replication. Genes Dev *15*, 404-414.

Chen, J.L., and Greider, C.W. (2003). Template boundary definition in mammalian telomerase. Genes Dev *17*, 2747-2752.

Chen, J.L., and Greider, C.W. (2004). An emerging consensus for telomerase RNA structure. Proc Natl Acad Sci U S A *101*, 14683-14684.

Chen, L.Y., Liu, D., and Songyang, Z. (2007). Telomere maintenance through spatial control of telomeric proteins. Mol Cell Biol *27*, 5898-5909.

Chen, Q., Fischer, A., Reagan, J.D., Yan, L.J., and Ames, B.N. (1995). Oxidative DNA damage and senescence of human diploid fibroblast cells. Proc Natl Acad Sci U S A *92*, 4337-4341.

Chen, Y., Yang, Y., van Overbeek, M., Donigian, J.R., Baciu, P., de Lange, T., and Lei, M. (2008). A shared docking motif in TRF1 and TRF2 used for differential recruitment of telomeric proteins. Science *319*, 1092-1096.

Chiang, Y.J., Kim, S.H., Tessarollo, L., Campisi, J., and Hodes, R.J. (2004). Telomere-associated protein TIN2 is essential for early embryonic development through a telomerase-independent pathway. Mol Cell Biol *24*, 6631-6634.

Chin, L., Artandi, S.E., Shen, Q., Tam, A., Lee, S.L., Gottlieb, G.J., Greider, C.W., and DePinho, R.A. (1999). p53 deficiency rescues the adverse effects of telomere loss and cooperates with telomere dysfunction to accelerate carcinogenesis. Cell *97*, 527-538.

Chong, L., van Steensel, B., Broccoli, D., Erdjument-Bromage, H., Hanish, J., Tempst, P., and de Lange, T. (1995). A human telomeric protein. Science *270*, 1663-1667.

Cimino-Reale, G., Pascale, E., Battiloro, E., Starace, G., Verna, R., and D'Ambrosio, E. (2001). The length of telomeric G-rich strand 3'-overhang measured by oligonucleotide ligation assay. Nucleic Acids Res *29*, E35.

Clark, A.J., Ferrier, P., Aslam, S., Burl, S., Denning, C., Wylie, D., Ross, A., de Sousa, P., Wilmut, I., and Cui, W. (2003). Proliferative lifespan is conserved after nuclear transfer. Nat Cell Biol *5*, 535-538.

Clarke, M.F., Dick, J.E., Dirks, P.B., Eaves, C.J., Jamieson, C.H., Jones, D.L., Visvader, J., Weissman, I.L., and Wahl, G.M. (2006). Cancer stem cells--perspectives on current status and future directions: AACR Workshop on cancer stem cells. Cancer Res *66*, 9339-9344.

Cohen, S.B., Graham, M.E., Lovrecz, G.O., Bache, N., Robinson, P.J., and Reddel, R.R. (2007). Protein composition of catalytically active human telomerase from immortal cells. Science *315*, 1850-1853.

Colgin, L.M., Baran, K., Baumann, P., Cech, T.R., and Reddel, R.R. (2003). Human POT1 facilitates telomere elongation by telomerase. Curr Biol *13*, 942-946.

Collado, M., Blasco, M.A., and Serrano, M. (2007). Cellular senescence in cancer and aging. Cell *130*, 223-233.

Cong, Y.S., Wright, W.E., and Shay, J.W. (2002). Human telomerase and its regulation. Microbiol Mol Biol Rev *66*, 407-425, table of contents.

Conrad, M.N., Wright, J.H., Wolf, A.J., and Zakian, V.A. (1990). RAP1 protein interacts with yeast telomeres in vivo: overproduction alters telomere structure and decreases chromosome stability. Cell *63*, 739-750.

Cooke, H.J., and Smith, B.A. (1986). Variability at the telomeres of the human X/Y pseudoautosomal region. Cold Spring Harb Symp Quant Biol *51 Pt 1*, 213-219.

Counter, C.M., Avilion, A.A., LeFeuvre, C.E., Stewart, N.G., Greider, C.W., Harley, C.B., and Bacchetti, S. (1992). Telomere shortening associated with chromosome

instability is arrested in immortal cells which express telomerase activity. Embo J *11*, 1921-1929.

Court, R., Chapman, L., Fairall, L., and Rhodes, D. (2005). How the human telomeric proteins TRF1 and TRF2 recognize telomeric DNA: a view from high-resolution crystal structures. EMBO Rep *6*, 39-45.

Creighton, H.B., and McClintock, B. (1931). A Correlation of Cytological and Genetical Crossing-Over in Zea Mays. Proc Natl Acad Sci U S A *17*, 492-497.

Cristofari, G., and Lingner, J. (2006). Telomere length homeostasis requires that telomerase levels are limiting. EMBO J *25*, 565-574.

Cristofari, G., Sikora, K., and Lingner, J. (2007). Telomerase unplugged. ACS Chem Biol *2*, 155-158.

Croker, A.K., and Allan, A.L. (2008). Cancer stem cells: implications for the progression and treatment of metastatic disease. J Cell Mol Med *12*, 374-390.

d'Adda di Fagagna, F., Reaper, P.M., Clay-Farrace, L., Fiegler, H., Carr, P., Von Zglinicki, T., Saretzki, G., Carter, N.P., and Jackson, S.P. (2003). A DNA damage checkpoint response in telomere-initiated senescence. Nature *426*, 194-198.

De Boeck, G., Forsyth, R.G., Praet, M., and Hogendoorn, P.C. (2009). Telomere-associated proteins: cross-talk between telomere maintenance and telomere-lengthening mechanisms. J Pathol *217*, 327-344.

de Lange, T. (2002). Protection of mammalian telomeres. Oncogene *21*, 532-540.

de Lange, T. (2004). T-loops and the origin of telomeres. Nat Rev Mol Cell Biol *5*, 323-329.

de Lange, T. (2005). Shelterin: the protein complex that shapes and safeguards human telomeres. Genes Dev *19*, 2100-2110.

de Lange, T. (2009). How telomeres solve the end-protection problem. Science *326*, 948-952.

de Lange, T., Shiue, L., Myers, R.M., Cox, D.R., Naylor, S.L., Killery, A.M., and Varmus, H.E. (1990). Structure and variability of human chromosome ends. Mol Cell Biol *10*, 518-527.

Dean, M., Fojo, T., and Bates, S. (2005). Tumour stem cells and drug resistance. Nat Rev Cancer *5*, 275-284.

Denchi, E.L., and de Lange, T. (2007). Protection of telomeres through independent control of ATM and ATR by TRF2 and POT1. Nature *448*, 1068-1071.

Deng, Y., Guo, X., Ferguson, D.O., and Chang, S. (2009). Multiple roles for MRE11 at uncapped telomeres. Nature *460*, 914-918.

Dez, C., Henras, A., Faucon, B., Lafontaine, D., Caizergues-Ferrer, M., and Henry, Y. (2001). Stable expression in yeast of the mature form of human telomerase RNA depends on its association with the box H/ACA small nucleolar RNP proteins Cbf5p, Nhp2p and Nop10p. Nucleic Acids Res *29*, 598-603.

Dick, J.E. (2009). Looking ahead in cancer stem cell research. Nat Biotechnol *27*, 44-46.

Diede, S.J., and Gottschling, D.E. (1999). Telomerase-mediated telomere addition in vivo requires DNA primase and DNA polymerases alpha and delta. Cell *99*, 723-733.

Dikmen, Z.G., Gellert, G.C., Jackson, S., Gryaznov, S., Tressler, R., Dogan, P., Wright, W.E., and Shay, J.W. (2005). In vivo inhibition of lung cancer by GRN163L: a novel human telomerase inhibitor. Cancer Res *65*, 7866-7873.

Dikmen, Z.G., Wright, W.E., Shay, J.W., and Gryaznov, S.M. (2008). Telomerase targeted oligonucleotide thio-phosphoramidates in T24-luc bladder cancer cells. J Cell Biochem *104*, 444-452.

Dimitrova, N., Chen, Y.C., Spector, D.L., and de Lange, T. (2008). 53BP1 promotes non-homologous end joining of telomeres by increasing chromatin mobility. Nature *456*, 524-528.

Dimitrova, N., and de Lange, T. (2009). Cell cycle-dependent role of MRN at dysfunctional telomeres: ATM signaling-dependent induction of nonhomologous end joining (NHEJ) in G1 and resection-mediated inhibition of NHEJ in G2. Mol Cell Biol *29*, 5552-5563.

Djojosubroto, M.W., Chin, A.C., Go, N., Schaetzlein, S., Manns, M.P., Gryaznov, S., Harley, C.B., and Rudolph, K.L. (2005). Telomerase antagonists GRN163 and GRN163L inhibit tumor growth and increase chemosensitivity of human hepatoma. Hepatology *42*, 1127-1136.

Donnenberg, V.S., and Donnenberg, A.D. (2005). Multiple drug resistance in cancer revisited: the cancer stem cell hypothesis. J Clin Pharmacol *45*, 872-877.

Ducrest, A.L., Szutorisz, H., Lingner, J., and Nabholz, M. (2002). Regulation of the human telomerase reverse transcriptase gene. Oncogene *21*, 541-552.

Eickbush, T.H. (1997). Telomerase and retrotransposons: which came first? Science *277*, 911-912.

Espejel, S., Franco, S., Sgura, A., Gae, D., Bailey, S.M., Taccioli, G.E., and Blasco, M.A. (2002). Functional interaction between DNA-PKcs and telomerase in telomere length maintenance. EMBO J *21*, 6275-6287.

Espejel, S., Martin, M., Klatt, P., Martin-Caballero, J., Flores, J.M., and Blasco, M.A. (2004). Shorter telomeres, accelerated ageing and increased lymphoma in DNA-PKcs-deficient mice. EMBO Rep *5*, 503-509.

Fagagna, F.d.A.d., Reaper, P.M., Clay-Farrace, L., Fiegler, H., Carr, P., von Zglinicki, T., Saretzki, G., Carter, N.P., and Jackson, S.P. (2003). A DNA damage checkpoint response in telomere-initiated senescence. Nature *426*, 194-198.

Fairall, L., Chapman, L., Moss, H., de Lange, T., and Rhodes, D. (2001). Structure of the TRFH dimerization domain of the human telomeric proteins TRF1 and TRF2. Mol Cell *8*, 351-361.

Farnie, G., and Clarke, R.B. (2006). Breast stem cells and cancer. Ernst Schering Found Symp Proc *5*, 141-153.

Feng, J., Funk, W.D., Wang, S.S., Weinrich, S.L., Avilion, A.A., Chiu, C.P., Adams, R.R., Chang, E., Allsopp, R.C., Yu, J., *et al.* (1995). The RNA component of human telomerase. Science *269*, 1236-1241.

Ferenac, M., Polancec, D., Huzak, M., Pereira-Smith, O.M., and Rubelj, I. (2005). Early-senescing human skin fibroblasts do not demonstrate accelerated telomere shortening. J Gerontol A Biol Sci Med Sci *60*, 820-829.

Fillmore, C.M., and Kuperwasser, C. (2008). Human breast cancer cell lines contain stem-like cells that self-renew, give rise to phenotypically diverse progeny and survive chemotherapy. Breast Cancer Res *10*, R25.

Fisher, T.S., Taggart, A.K., and Zakian, V.A. (2004). Cell cycle-dependent regulation of yeast telomerase by Ku. Nat Struct Mol Biol *11*, 1198-1205.

Flores, I., Cayuela, M.L., and Blasco, M.A. (2005). Effects of telomerase and telomere length on epidermal stem cell behavior. Science *309*, 1253-1256.

Fouche, N., Cesare, A.J., Willcox, S., Ozgur, S., Compton, S.A., and Griffith, J.D. (2006). The basic domain of TRF2 directs binding to DNA junctions irrespective of the presence of TTAGGG repeats. J Biol Chem *281*, 37486-37495.

Frackman, S., Kobs, G., Simpson, D., and Storts, D. (1998). Betaine and DMSO: Enhancing Agents for PCR. Promega Notes *65*, 27-30.

Gavory, G., Symmons, M.F., Krishnan Ghosh, Y., Klenerman, D., and Balasubramanian, S. (2006). Structural analysis of the catalytic core of human telomerase RNA by FRET and molecular modeling. Biochemistry *45*, 13304-13311.

Gellert, G.C., Dikmen, Z.G., Wright, W.E., Gryaznov, S., and Shay, J.W. (2006). Effects of a novel telomerase inhibitor, GRN163L, in human breast cancer. Breast Cancer Res Treat *96*, 73-81.

Gil, M.E., and Coetzer, T.L. (2004). Real-time quantitative PCR of telomere length. Mol Biotechnol *27*, 169-172.

Gilson, E., and Londono-Vallejo, A. (2007). Telomere length profiles in humans: all ends are not equal. Cell Cycle *6*, 2486-2494.

Gomez-Millan, J., Goldblatt, E.M., Gryaznov, S.M., Mendonca, M.S., and Herbert, B.S. (2007). Specific telomere dysfunction induced by GRN163L increases radiation sensitivity in breast cancer cells. Int J Radiat Oncol Biol Phys *67*, 897-905.

Gottschling, D.E., and Zakian, V.A. (1986). Telomere proteins: specific recognition and protection of the natural termini of Oxytricha macronuclear DNA. Cell *47*, 195-205.

Graakjaer, J., Bischoff, C., Korsholm, L., Holstebroe, S., Vach, W., Bohr, V.A., Christensen, K., and Kolvraa, S. (2003). The pattern of chromosome-specific variations in telomere length in humans is determined by inherited, telomere-near factors and is maintained throughout life. Mech Ageing Dev *124*, 629-640.

Graakjaer, J., Der-Sarkissian, H., Schmitz, A., Bayer, J., Thomas, G., Kolvraa, S., and Londono-Vallejo, J.A. (2006). Allele-specific relative telomere lengths are inherited. Hum Genet *119*, 344-350.

Graakjaer, J., Pascoe, L., Der-Sarkissian, H., Thomas, G., Kolvraa, S., Christensen, K., and Londoño-Vallejo, J.-A. (2004a). The relative lengths of individual telomeres are defined in the zygote and strictly maintained during life. Aging Cell *3*, 97-102.

Graakjaer, J., Pascoe, L., Der-Sarkissian, H., Thomas, G., Kolvraa, S., Christensen, K., and Londono-Vallejo, J.A. (2004b). The relative lengths of individual telomeres are defined in the zygote and strictly maintained during life. Aging Cell *3*, 97-102.

Greider, C.W. (1999). Telomeres do D-loop-T-loop. Cell *97*, 419-422.

Greider, C.W., and Blackburn, E.H. (1985). Identification of a specific telomere terminal transferase activity in Tetrahymena extracts. Cell *43*, 405-413.

Greider, C.W., and Blackburn, E.H. (1987). The telomere terminal transferase of Tetrahymena is a ribonucleoprotein enzyme with two kinds of primer specificity. Cell *51*, 887-898.

Greider, C.W., and Blackburn, E.H. (1989). A telomeric sequence in the RNA of Tetrahymena telomerase required for telomere repeat synthesis. Nature *337*, 331-337.

Griffith, J., Bianchi, A., and de Lange, T. (1998). TRF1 promotes parallel pairing of telomeric tracts in vitro. J Mol Biol *278*, 79-88.

Griffith, J.D., Comeau, L., Rosenfield, S., Stansel, R.M., Bianchi, A., Moss, H., and de Lange, T. (1999). Mammalian telomeres end in a large duplex loop. Cell *97*, 503-514.

Gryaznov, S., Pongracz, K., Matray, T., Schultz, R., Pruzan, R., Aimi, J., Chin, A., Harley, C., Shea-Herbert, B., Shay, J., *et al.* (2001). Telomerase inhibitors--oligonucleotide phosphoramidates as potential therapeutic agents. Nucleosides Nucleotides Nucleic Acids *20*, 401-410.

Gryaznov, S.M., Jackson, S., Dikmen, G., Harley, C., Herbert, B.S., Wright, W.E., and Shay, J.W. (2007). Oligonucleotide conjugate GRN163L targeting human telomerase as potential anticancer and antimetastatic agent. Nucleosides Nucleotides Nucleic Acids *26*, 1577-1579.

Guo, X., Deng, Y., Lin, Y., Cosme-Blanco, W., Chan, S., He, H., Yuan, G., Brown, E.J., and Chang, S. (2007). Dysfunctional telomeres activate an ATM-ATR-dependent DNA damage response to suppress tumorigenesis. EMBO J *26*, 4709-4719.

Hamilton, S.E., Pitts, A.E., Katipally, R.R., Jia, X., Rutter, J.P., Davies, B.A., Shay, J.W., Wright, W.E., and Corey, D.R. (1997). Identification of determinants for inhibitor binding within the RNA active site of human telomerase using PNA scanning. Biochemistry *36*, 11873-11880.

Hanahan, D., and Weinberg, R.A. (2000). The hallmarks of cancer. Cell *100*, 57-70.

Hanaoka, S., Nagadoi, A., Yoshimura, S., Aimoto, S., Li, B., de Lange, T., and Nishimura, Y. (2001). NMR structure of the hRap1 Myb motif reveals a canonical three-helix bundle lacking the positive surface charge typical of Myb DNA-binding domains. J Mol Biol *312*, 167-175.

Harley, C.B. (1991). Telomere loss: mitotic clock or genetic time bomb? Mutat Res *256*, 271-282.

Harley, C.B., Futcher, A.B., and Greider, C.W. (1990). Telomeres shorten during ageing of human fibroblasts. Nature *345*, 458-460.

Harrington, L., McPhail, T., Mar, V., Zhou, W., Oulton, R., Bass, M.B., Arruda, I., and Robinson, M.O. (1997a). A mammalian telomerase-associated protein. Science *275*, 973-977.

Harrington, L., Zhou, W., McPhail, T., Oulton, R., Yeung, D.S., Mar, V., Bass, M.B., and Robinson, M.O. (1997b). Human telomerase contains evolutionarily conserved catalytic and structural subunits. Genes Dev *11*, 3109-3115.

Harrison, R.G., Greenman, M.J., Mall, F.P., and Jackson, C.M. (1907). Observations of the living developing nerve fiber. The Anatomical Record *1*, 116-128.

Hastie, N.D., Dempster, M., Dunlop, M.G., Thompson, A.M., Green, D.K., and Allshire, R.C. (1990). Telomere reduction in human colorectal carcinoma and with ageing. Nature *346*, 866-868.

Hayflick, L. (1965). The Limited in Vitro Lifetime of Human Diploid Cell Strains. Exp Cell Res *37*, 614-636.

Hayflick, L. (1998). How and why we age. Exp Gerontol *33*, 639-653.

Hayflick, L., and Moorhead, P.S. (1961). The serial cultivation of human diploid cell strains. Exp Cell Res *25*, 585-621.

Hemann, M.T., and Greider, C.W. (1999). G-strand overhangs on telomeres in telomerase-deficient mouse cells. Nucleic Acids Res *27*, 3964-3969.

Hemann, M.T., Strong, M.A., Hao, L.-Y., and Greider, C.W. (2001a). The Shortest Telomere, Not Average Telomere Length, Is Critical for Cell Viability and Chromosome Stability. Cell *107*, 67-77.

Hemann, M.T., Strong, M.A., Hao, L.Y., and Greider, C.W. (2001b). The shortest telomere, not average telomere length, is critical for cell viability and chromosome stability. Cell *107*, 67-77.

Herbert, B., Pitts, A.E., Baker, S.I., Hamilton, S.E., Wright, W.E., Shay, J.W., and Corey, D.R. (1999). Inhibition of human telomerase in immortal human cells leads to progressive telomere shortening and cell death. Proc Natl Acad Sci U S A *96*, 14276-14281.

Herbert, B.S., Gellert, G.C., Hochreiter, A., Pongracz, K., Wright, W.E., Zielinska, D., Chin, A.C., Harley, C.B., Shay, J.W., and Gryaznov, S.M. (2005). Lipid modification of GRN163, an N3'-->P5' thio-phosphoramidate oligonucleotide, enhances the potency of telomerase inhibition. Oncogene *24*, 5262-5268.

Herbert, B.S., Pongracz, K., Shay, J.W., Gryaznov, S.M., and Shea-Herbert, B. (2002). Oligonucleotide N3'-->P5' phosphoramidates as efficient telomerase inhibitors. Oncogene *21*, 638-642.

Herbig, U., Jobling, W.A., Chen, B.P., Chen, D.J., and Sedivy, J.M. (2004). Telomere shortening triggers senescence of human cells through a pathway involving ATM, p53, and p21(CIP1), but not p16(INK4a). Mol Cell *14*, 501-513.

Hermann, P.C., Huber, S.L., Herrler, T., Aicher, A., Ellwart, J.W., Guba, M., Bruns, C.J., and Heeschen, C. (2007). Distinct Populations of Cancer Stem Cells Determine Tumor Growth and Metastatic Activity in Human Pancreatic Cancer. Cell Stem Cell *1*, 313-323.

Hochreiter, A.E., Xiao, H., Goldblatt, E.M., Gryaznov, S.M., Miller, K.D., Badve, S., Sledge, G.W., and Herbert, B.S. (2006). Telomerase template antagonist GRN163L disrupts telomere maintenance, tumor growth, and metastasis of breast cancer. Clin Cancer Res *12*, 3184-3192.

Hockemeyer, D., Daniels, J.P., Takai, H., and de Lange, T. (2006). Recent expansion of the telomeric complex in rodents: Two distinct POT1 proteins protect mouse telomeres. Cell *126*, 63-77.

Hockemeyer, D., Palm, W., Else, T., Daniels, J.P., Takai, K.K., Ye, J.Z., Keegan, C.E., de Lange, T., and Hammer, G.D. (2007). Telomere protection by mammalian Pot1 requires interaction with Tpp1. Nat Struct Mol Biol *14*, 754-761.

Hockemeyer, D., Sfeir, A.J., Shay, J.W., Wright, W.E., and de Lange, T. (2005). POT1 protects telomeres from a transient DNA damage response and determines how human chromosomes end. EMBO J *24*, 2667-2678.

Houghtaling, B.R., Cuttonaro, L., Chang, W., and Smith, S. (2004). A dynamic molecular link between the telomere length regulator TRF1 and the chromosome end protector TRF2. Curr Biol *14*, 1621-1631.

Hsu, H.L., Gilley, D., Galande, S.A., Hande, M.P., Allen, B., Kim, S.H., Li, G.C., Campisi, J., Kohwi-Shigematsu, T., and Chen, D.J. (2000). Ku acts in a unique way at the mammalian telomere to prevent end joining. Genes Dev *14*, 2807-2812.

Huang, P., Wang, C.Y., Gou, S.M., Wu, H.S., Liu, T., and Xiong, J.X. (2008). Isolation and biological analysis of tumor stem cells from pancreatic adenocarcinoma. World J Gastroenterol *14*, 3903-3907.

Huda, N., Tanaka, H., Mendonca, M.S., and Gilley, D. (2009). DNA damage-induced phosphorylation of TRF2 is required for the fast pathway of DNA double-strand break repair. Mol Cell Biol *29*, 3597-3604.

Huffman, K.E., Levene, S.D., Tesmer, V.M., Shay, J.W., and Wright, W.E. (2000). Telomere shortening is proportional to the size of the G-rich telomeric 3'-overhang. J Biol Chem *275*, 19719-19722.

Hultdin, M., Gronlund, E., Norrback, K., Eriksson-Lindstrom, E., Just, T., and Roos, G. (1998). Telomere analysis by fluorescence in situ hybridization and flow cytometry. Nucleic Acids Res *26*, 3651-3656.

Ishikawa, F. (1998). FISH goes with the flow. Nat Biotechnol *16*, 723-724.

Iwano, T., Tachibana, M., Reth, M., and Shinkai, Y. (2004). Importance of TRF1 for functional telomere structure. J Biol Chem *279*, 1442-1448.

Jackson, S.R., Zhu, C.H., Paulson, V., Watkins, L., Dikmen, Z.G., Gryaznov, S.M., Wright, W.E., and Shay, J.W. (2007). Antiadhesive effects of GRN163L--an oligonucleotide N3'->P5' thio-phosphoramidate targeting telomerase. Cancer Res *67*, 1121-1129.

Jady, B.E., Richard, P., Bertrand, E., and Kiss, T. (2006). Cell cycle-dependent recruitment of telomerase RNA and Cajal bodies to human telomeres. Mol Biol Cell *17*, 944-954.

Joseph, I., Tressler, R., Bassett, E., Harley, C., Buseman, C.M., Pattamatta, P., Wright, W.E., Shay, J.W., and Go, N.F. (2010). The telomerase inhibitor imetelstat depletes cancer stem cells in breast and pancreatic cancer cell lines. Cancer Res *70*, 9494-9504.

Ju, Z., and Rudolph, K.L. (2006). Telomeres and telomerase in cancer stem cells. Eur J Cancer *42*, 1197-1203.

Karlseder, J., Broccoli, D., Dai, Y., Hardy, S., and de Lange, T. (1999). p53- and ATM-dependent apoptosis induced by telomeres lacking TRF2. Science *283*, 1321-1325.

Karlseder, J., Hoke, K., Mirzoeva, O.K., Bakkenist, C., Kastan, M.B., Petrini, J.H., and de Lange, T. (2004). The telomeric protein TRF2 binds the ATM kinase and can inhibit the ATM-dependent DNA damage response. PLoS Biol *2*, E240.

Karlseder, J., Kachatrian, L., Takai, H., Mercer, K., Hingorani, S., Jacks, T., and de Lange, T. (2003). Targeted deletion reveals an essential function for the telomere length regulator Trf1. Mol Cell Biol *23*, 6533-6541.

Kelleher, C., Kurth, I., and Lingner, J. (2005). Human protection of telomeres 1 (POT1) is a negative regulator of telomerase activity in vitro. Mol Cell Biol *25*, 808-818.

Kelleher, C., Teixeira, M.T., Forstemann, K., and Lingner, J. (2002). Telomerase: biochemical considerations for enzyme and substrate. Trends Biochem Sci *27*, 572-579.

Kendellen, M.F., Barrientos, K.S., and Counter, C.M. (2009). POT1 association with TRF2 regulates telomere length. Mol Cell Biol *29*, 5611-5619.

Khan, S.J., Yanez, G., Seldeen, K., Wang, H., Lindsay, S.M., and Fletcher, T.M. (2007). Interactions of TRF2 with model telomeric ends. Biochem Biophys Res Commun *363*, 44-50.

Kim, H., Lee, O.H., Xin, H., Chen, L.Y., Qin, J., Chae, H.K., Lin, S.Y., Safari, A., Liu, D., and Songyang, Z. (2009). TRF2 functions as a protein hub and regulates telomere maintenance by recognizing specific peptide motifs. Nat Struct Mol Biol *16*, 372-379.

Kim, N.K., Zhang, Q., Zhou, J., Theimer, C.A., Peterson, R.D., and Feigon, J. (2008). Solution structure and dynamics of the wild-type pseudoknot of human telomerase RNA. J Mol Biol *384*, 1249-1261.

Kim, N.W., Piatyszek, M.A., Prowse, K.R., Harley, C.B., West, M.D., Ho, P.L., Coviello, G.M., Wright, W.E., Weinrich, S.L., and Shay, J.W. (1994). Specific association of human telomerase activity with immortal cells and cancer. Science *266*, 2011-2015.

Kim, S.H., Beausejour, C., Davalos, A.R., Kaminker, P., Heo, S.J., and Campisi, J. (2004). TIN2 mediates functions of TRF2 at human telomeres. J Biol Chem *279*, 43799-43804.

Kim, S.H., Kaminker, P., and Campisi, J. (1999). TIN2, a new regulator of telomere length in human cells. Nat Genet *23*, 405-412.

Kimura, M., Hjelmborg, J.V., Gardner, J.P., Bathum, L., Brimacombe, M., Lu, X., Christiansen, L., Vaupel, J.W., Aviv, A., and Christensen, K. (2008). Telomere length and mortality: a study of leukocytes in elderly Danish twins. Am J Epidemiol *167*, 799-806.

Kipling, D., and Cooke, H.J. (1990). Hypervariable ultra-long telomeres in mice. Nature *347*, 400-402.

Konishi, A., and de Lange, T. (2008). Cell cycle control of telomere protection and NHEJ revealed by a ts mutation in the DNA-binding domain of TRF2. Genes Dev *22*, 1221-1230.

Krauskopf, A., and Blackburn, E.H. (1996). Control of telomere growth by interactions of RAP1 with the most distal telomeric repeats. Nature *383*, 354-357.

Lansdorp, P., Verwoerd, N., van de Rijke, F., Dragowska, V., Little, M., Dirks, R., Raap, A., and Tanke, H. (1996a). Heterogeneity in telomere length of human chromosomes. Hum Mol Genet *5*, 685-691.

Lansdorp, P.M., Verwoerd, N.P., van de Rijke, F.M., Dragowska, V., Little, M.T., Dirks, R.W., Raap, A.K., and Tanke, H.J. (1996b). Heterogeneity in telomere length of human chromosomes. Hum Mol Genet *5*, 685-691.

Lark, K.G. (1969). Initiation and control of DNA synthesis. Annu Rev Biochem *38*, 569-604.

Larrivee, M., LeBel, C., and Wellinger, R.J. (2004). The generation of proper constitutive G-tails on yeast telomeres is dependent on the MRX complex. Genes Dev *18*, 1391-1396.

Latrick, C.M., and Cech, T.R. (2010). POT1-TPP1 enhances telomerase processivity by slowing primer dissociation and aiding translocation. EMBO J *29*, 924-933.

Lauzon, W., Sanchez Dardon, J., Cameron, D.W., and Badley, A.D. (2000). Flow cytometric measurement of telomere length. Cytometry *42*, 159-164.

Lavoie, J., Bronsard, M., Lebel, M., and Drouin, R. (2003). Mouse telomere analysis using an optimized primed in situ (PRINS) labeling technique. Chromosoma *111*, 438-444.

Lei, M., Podell, E.R., Baumann, P., and Cech, T.R. (2003). DNA self-recognition in the structure of Pot1 bound to telomeric single-stranded DNA. Nature *426*, 198-203.

Lei, M., Podell, E.R., and Cech, T.R. (2004). Structure of human POT1 bound to telomeric single-stranded DNA provides a model for chromosome end-protection. Nat Struct Mol Biol *11*, 1223-1229.

Lei, M., Zaug, A.J., Podell, E.R., and Cech, T.R. (2005). Switching human telomerase on and off with hPOT1 protein in vitro. J Biol Chem *280*, 20449-20456.

Levy, D.L., and Blackburn, E.H. (2004). Counting of Rif1p and Rif2p on Saccharomyces cerevisiae telomeres regulates telomere length. Mol Cell Biol *24*, 10857-10867.

Levy, M.Z., Allsopp, R.C., Futcher, A.B., Greider, C.W., and Harley, C.B. (1992). Telomere end-replication problem and cell aging. J Mol Biol *225*, 951-960.

Li, B., and de Lange, T. (2003). Rap1 affects the length and heterogeneity of human telomeres. Mol Biol Cell *14*, 5060-5068.

Li, B., Espinal, A., and Cross, G.A. (2005). Trypanosome telomeres are protected by a homologue of mammalian TRF2. Mol Cell Biol *25*, 5011-5021.

Li, B., Oestreich, S., and de Lange, T. (2000). Identification of human Rap1: implications for telomere evolution. Cell *101*, 471-483.

Li, C., Heidt, D.G., Dalerba, P., Burant, C.F., Zhang, L., Adsay, V., Wicha, M., Clarke, M.F., and Simeone, D.M. (2007). Identification of pancreatic cancer stem cells. Cancer Res *67*, 1030-1037.

Lieber, M.R., Ma, Y., Pannicke, U., and Schwarz, K. (2003). Mechanism and regulation of human non-homologous DNA end-joining. Nat Rev Mol Cell Biol *4*, 712-720.

Lin, J.J., and Zakian, V.A. (1996). The Saccharomyces CDC13 protein is a single-strand TG1-3 telomeric DNA-binding protein in vitro that affects telomere behavior in vivo. Proc Natl Acad Sci U S A *93*, 13760-13765.

Lin, K.W., and Yan, J. (2005). The telomere length dynamic and methods of its assessment. J Cell Mol Med *9*, 977-989.

Lindsey, J., McGill, N.I., Lindsey, L.A., Green, D.K., and Cooke, H.J. (1991). In vivo loss of telomeric repeats with age in humans. Mutat Res *256*, 45-48.

Lingner, J., Hughes, T.R., Shevchenko, A., Mann, M., Lundblad, V., and Cech, T.R. (1997). Reverse transcriptase motifs in the catalytic subunit of telomerase. Science *276*, 561-567.

Liu, D., Safari, A., O'Connor, M.S., Chan, D.W., Laegeler, A., Qin, J., and Songyang, Z. (2004). PTOP interacts with POT1 and regulates its localization to telomeres. Nat Cell Biol *6*, 673-680.

Loayza, D., and De Lange, T. (2003). POT1 as a terminal transducer of TRF1 telomere length control. Nature *423*, 1013-1018.

Loayza, D., Parsons, H., Donigian, J., Hoke, K., and de Lange, T. (2004). DNA binding features of human POT1: a nonamer 5'-TAGGGTTAG-3' minimal binding site, sequence specificity, and internal binding to multimeric sites. J Biol Chem *279*, 13241-13248.

Londono-Vallejo, J.A. (2004). Telomere length heterogeneity and chromosome instability. Cancer Lett *212*, 135-144.

Londono-Vallejo, J.A., DerSarkissian, H., Cazes, L., and Thomas, G. (2001). Differences in telomere length between homologous chromosomes in humans. Nucleic Acids Res *29*, 3164-3171.

Lundblad, V., and Szostak, J.W. (1989). A mutant with a defect in telomere elongation leads to senescence in yeast. Cell *57*, 633-643.

Lustig, A.J., Kurtz, S., and Shore, D. (1990). Involvement of the silencer and UAS binding protein RAP1 in regulation of telomere length. Science *250*, 549-553.

Ly, H., Blackburn, E.H., and Parslow, T.G. (2003). Comprehensive structure-function analysis of the core domain of human telomerase RNA. Mol Cell Biol *23*, 6849-6856.

Makarov, V.L., Hirose, Y., and Langmore, J.P. (1997). Long G tails at both ends of human chromosomes suggest a C strand degradation mechanism for telomere shortening. Cell *88*, 657-666.

Makarov, V.L., Lejnine, S., Bedoyan, J., and Langmore, J.P. (1993). Nucleosomal organization of telomere-specific chromatin in rat. Cell *73*, 775-787.

Mao, Z., Seluanov, A., Jiang, Y., and Gorbunova, V. (2007). TRF2 is required for repair of nontelomeric DNA double-strand breaks by homologous recombination. Proc Natl Acad Sci U S A *104*, 13068-13073.

Marcand, S., Brevet, V., Mann, C., and Gilson, E. (2000). Cell cycle restriction of telomere elongation. Curr Biol *10*, 487-490.

Marcand, S., Wotton, D., Gilson, E., and Shore, D. (1997). Rap1p and telomere length regulation in yeast. Ciba Found Symp *211*, 76-93; discussion 93-103.

Marian, C.O., Cho, S.K., McEllin, B.M., Maher, E.A., Hatanpaa, K.J., Madden, C.J., Mickey, B.E., Wright, W.E., Shay, J.W., and Bachoo, R.M. (2010a). The telomerase antagonist, imetelstat, efficiently targets glioblastoma tumor-initiating cells leading to decreased proliferation and tumor growth. Clin Cancer Res *16*, 154-163.

Marian, C.O., Wright, W.E., and Shay, J.W. (2010b). The effects of telomerase inhibition on prostate tumor-initiating cells. Int J Cancer *127*, 321-331.

Martens, U.M., Chavez, E.A., Poon, S.S., Schmoor, C., and Lansdorp, P.M. (2000). Accumulation of short telomeres in human fibroblasts prior to replicative senescence. Exp Cell Res *256*, 291-299.

Martens, U.M., Zijlmans, J.M., Poon, S.S., Dragowska, W., Yui, J., Chavez, E.A., Ward, R.K., and Lansdorp, P.M. (1998). Short telomeres on human chromosome 17p. Nat Genet *18*, 76-80.

Martin-Ruiz, C., Saretzki, G., Petrie, J., Ladhoff, J., Jeyapalan, J., Wei, W., Sedivy, J., and von Zglinicki, T. (2004). Stochastic variation in telomere shortening rate causes heterogeneity of human fibroblast replicative life span. J Biol Chem *279*, 17826-17833.

Martinez, P., and Blasco, M.A. (2010). Role of shelterin in cancer and aging. Aging Cell.

McCarroll, R.M., and Fangman, W.L. (1988). Time of replication of yeast centromeres and telomeres. Cell *54*, 505-513.

McClintock, B. (1939). The Behavior in Successive Nuclear Divisions of a Chromosome Broken at Meiosis. Proc Natl Acad Sci U S A *25*, 405-416.

McClintock, B. (1941). The Stability of Broken Ends of Chromosomes in Zea Mays. Genetics *26*, 234-282.

McElligott, R., and Wellinger, R.J. (1997). The terminal DNA structure of mammalian chromosomes. EMBO J *16*, 3705-3714.

Meeker, A.K., Gage, W.R., Hicks, J.L., Simon, I., Coffman, J.R., Platz, E.A., March, G.E., and De Marzo, A.M. (2002). Telomere length assessment in human archival tissues: combined telomere fluorescence in situ hybridization and immunostaining. Am J Pathol *160*, 1259-1268.

Meyne, J., Ratliff, R.L., and Moyzis, R.K. (1989). Conservation of the human telomere sequence (TTAGGG)n among vertebrates. Proc Natl Acad Sci U S A *86*, 7049-7053.

Molckovsky, A., and Siu, L.L. (2008). First-in-class, first-in-human phase I results of targeted agents: highlights of the 2008 American society of clinical oncology meeting. J Hematol Oncol *1*, 20.

Morgan, T.H. (1911). Random Segregation Versus Coupling in Mendelian Inheritance. Science *34*, 384.

Morin, G.B. (1989). The human telomere terminal transferase enzyme is a ribonucleoprotein that synthesizes TTAGGG repeats. Cell *59*, 521-529.

Moyzis, R.K., Buckingham, J.M., Cram, L.S., Dani, M., Deaven, L.L., Jones, M.D., Meyne, J., Ratliff, R.L., and Wu, J.R. (1988). A highly conserved repetitive DNA sequence, (TTAGGG)n, present at the telomeres of human chromosomes. Proc Natl Acad Sci U S A *85*, 6622-6626.

Muller, H.J. (1938). The remaking of chromosomes. The Collecting Net *8*, 182-195.

Munoz-Jordan, J.L., Cross, G.A., de Lange, T., and Griffith, J.D. (2001). t-loops at trypanosome telomeres. EMBO J *20*, 579-588.

Murti, K.G., and Prescott, D.M. (1999). Telomeres of polytene chromosomes in a ciliated protozoan terminate in duplex DNA loops. Proc Natl Acad Sci U S A *96*, 14436-14439.

Mushiroda, T., Wattanapokayakit, S., Takahashi, A., Nukiwa, T., Kudoh, S., Ogura, T., Taniguchi, H., Kubo, M., Kamatani, N., and Nakamura, Y. (2008). A genome-wide association study identifies an association of a common variant in TERT with susceptibility to idiopathic pulmonary fibrosis. J Med Genet *45*, 654-656.

Nakamura, T.M., and Cech, T.R. (1998). Reversing time: origin of telomerase. Cell *92*, 587-590.

Nakamura, T.M., Morin, G.B., Chapman, K.B., Weinrich, S.L., Andrews, W.H., Lingner, J., Harley, C.B., and Cech, T.R. (1997). Telomerase catalytic subunit homologs from fission yeast and human. Science *277*, 955-959.

Nakamura, Y., Hirose, M., Matsuo, H., Tsuyama, N., Kamisango, K., and Ide, T. (1999). Simple, rapid, quantitative, and sensitive detection of telomere repeats in cell lysate by a hybridization protection assay. Clin Chem *45*, 1718-1724.

Nikitina, T., and Woodcock, C.L. (2004). Closed chromatin loops at the ends of chromosomes. J Cell Biol *166*, 161-165.

Njajou, O.T., Cawthon, R.M., Damcott, C.M., Wu, S.H., Ott, S., Garant, M.J., Blackburn, E.H., Mitchell, B.D., Shuldiner, A.R., and Hsueh, W.C. (2007). Telomere length is paternally inherited and is associated with parental lifespan. Proc Natl Acad Sci U S A *104*, 12135-12139.

Nobelprize.org. The Nobel Prize in Physiology or Medicine 2009.

Nora, G.J., Buncher, N.A., and Opresko, P.L. (2010). Telomeric protein TRF2 protects Holliday junctions with telomeric arms from displacement by the Werner syndrome helicase. Nucleic Acids Res.

Norton, J.C., Piatyszek, M.A., Wright, W.E., Shay, J.W., and Corey, D.R. (1996). Inhibition of human telomerase activity by peptide nucleic acids. Nat Biotechnol *14*, 615-619.

Nugent, C.I., Hughes, T.R., Lue, N.F., and Lundblad, V. (1996). Cdc13p: a single-strand telomeric DNA-binding protein with a dual role in yeast telomere maintenance. Science *274*, 249-252.

O'Connor, M.S., Safari, A., Xin, H., Liu, D., and Songyang, Z. (2006). A critical role for TPP1 and TIN2 interaction in high-order telomeric complex assembly. Proc Natl Acad Sci U S A *103*, 11874-11879.

Oexle, K. (1998). Telomere length distribution and Southern blot analysis. J Theor Biol *190*, 369-377.

Okamoto, K., and Shinkai, Y. (2009). TRFH domain is critical for TRF1-mediated telomere stabilization. Cell Struct Funct *34*, 71-76.

Olovnikov, A.M. (1971). [Principle of marginotomy in template synthesis of polynucleotides]. Dokl Akad Nauk SSSR *201*, 1496-1499.

Olovnikov, A.M. (1973). A theory of marginotomy. The incomplete copying of template margin in enzymic synthesis of polynucleotides and biological significance of the phenomenon. J Theor Biol *41*, 181-190.

Olovnikov, A.M. (1996). Telomeres, telomerase, and aging: origin of the theory. Exp Gerontol *31*, 443-448.

Ouellette, M.M., and Choi, K.H. (2007). Telomeres and Telomerase in Ageing and Cancer. In Encyclopedia of Life Sciences (http://wwwelsnet/) (Chichester, UK, John Wiley & Sons Ltd).

Ouellette, M.M., Liao, M., Herbert, B.S., Johnson, M., Holt, S.E., Liss, H.S., Shay, J.W., and Wright, W.E. (2000). Subsenescent telomere lengths in fibroblasts immortalized by limiting amounts of telomerase. J Biol Chem *275*, 10072-10076.

Ouellette, M.M., Wright, W.E., and Shay, J.W. (2011). Targeting Telomerase-Expressing Cancer Cells. J Cell Mol Med.

Ozawa, T., Gryaznov, S.M., Hu, L.J., Pongracz, K., Santos, R.A., Bollen, A.W., Lamborn, K.R., and Deen, D.F. (2004). Antitumor effects of specific telomerase inhibitor GRN163 in human glioblastoma xenografts. Neuro Oncol *6*, 218-226.

Palm, W., and de Lange, T. (2008). How shelterin protects mammalian telomeres. Annu Rev Genet *42*, 301-334.

Palm, W., Hockemeyer, D., Kibe, T., and de Lange, T. (2009). Functional dissection of human and mouse POT1 proteins. Mol Cell Biol *29*, 471-482.

Park, J.I., Venteicher, A.S., Hong, J.Y., Choi, J., Jun, S., Shkreli, M., Chang, W., Meng, Z., Cheung, P., Ji, H., *et al.* (2009). Telomerase modulates Wnt signalling by association with target gene chromatin. Nature *460*, 66-72.

Parkinson, E.K., Fitchett, C., and Cereser, B. (2008). Dissecting the non-canonical functions of telomerase. Cytogenet Genome Res *122*, 273-280.

Passos, J.F., Saretzki, G., and von Zglinicki, T. (2007). DNA damage in telomeres and mitochondria during cellular senescence: is there a connection? Nucleic Acids Res *35*, 7505-7513.

Pedrali-Noy, G., and Spadari, S. (1979). Effect of aphidicolin on viral and human DNA polymerases. Biochem Biophys Res Commun *88*, 1194-1202.

Pogacic, V., Dragon, F., and Filipowicz, W. (2000). Human H/ACA small nucleolar RNPs and telomerase share evolutionarily conserved proteins NHP2 and NOP10. Mol Cell Biol *20*, 9028-9040.

Portugal, R.D., Land, M.G., and Svaiter, B.F. (2008). A computational model for telomere-dependent cell-replicative aging. Biosystems *91*, 262-267.

Poulet, A., Buisson, R., Faivre-Moskalenko, C., Koelblen, M., Amiard, S., Montel, F., Cuesta-Lopez, S., Bornet, O., Guerlesquin, F., Godet, T., *et al.* (2009). TRF2 promotes, remodels and protects telomeric Holliday junctions. EMBO J *28*, 641-651.

Raices, M., Verdun, R.E., Compton, S.A., Haggblom, C.I., Griffith, J.D., Dillin, A., and Karlseder, J. (2008). C. elegans telomeres contain G-strand and C-strand overhangs that are bound by distinct proteins. Cell *132*, 745-757.

Rando, T.A. (2006). Prognostic value of telomere length: the long and short of it. Ann Neurol *60*, 155-157.

Richardson, C.C. (1969). Enzymes in DNA metabolism. Annu Rev Biochem *38*, 795-840.

Richter, T., and Zglinicki, T.v. (2007). A continuous correlation between oxidative stress and telomere shortening in fibroblasts. Experimental Gerontology *42*, 1039-1042.

Rodriguez-Brenes, I.A., and Peskin, C.S. (2010). Quantitative theory of telomere length regulation and cellular senescence. Proc Natl Acad Sci U S A *107*, 5387-5392.

Rubelj, I., Huzak, M., Brdar, B., and Pereira-Smith, O.M. (2002). A single-stage mechanism controls replicative senescence through Sudden Senescence Syndrome. Biogerontology *3*, 213-222.

Rubelj, I., and Vondracek, Z. (1999). Stochastic mechanism of cellular aging--abrupt telomere shortening as a model for stochastic nature of cellular aging. J Theor Biol *197*, 425-438.

Rufer, N., Dragowska, W., Thornbury, G., Roosnek, E., and Lansdorp, P.M. (1998). Telomere length dynamics in human lymphocyte subpopulations measured by flow cytometry. Nat Biotechnol *16*, 743-747.

Samper, E., Flores, J.M., and Blasco, M.A. (2001). Restoration of telomerase activity rescues chromosomal instability and premature aging in Terc-/- mice with short telomeres. EMBO Rep *2*, 800-807.

Sarin, K.Y., Cheung, P., Gilison, D., Lee, E., Tennen, R.I., Wang, E., Artandi, M.K., Oro, A.E., and Artandi, S.E. (2005). Conditional telomerase induction causes proliferation of hair follicle stem cells. Nature *436*, 1048-1052.

Sarraf, S.A., and Harper, J.W. (2010). Telomeric TuRF1 wars. Dev Cell *18*, 167-168.

Sarthy, J., Bae, N.S., Scrafford, J., and Baumann, P. (2009). Human RAP1 inhibits non-homologous end joining at telomeres. EMBO J *28*, 3390-3399.

Scherthan, H., Jerratsch, M., Li, B., Smith, S., Hulten, M., Lock, T., and de Lange, T. (2000). Mammalian meiotic telomeres: protein composition and redistribution in relation to nuclear pores. Mol Biol Cell *11*, 4189-4203.

Schmid, I., Dagarag, M.D., Hausner, M.A., Matud, J.L., Just, T., Effros, R.B., and Jamieson, B.D. (2002). Simultaneous flow cytometric analysis of two cell surface markers, telomere length, and DNA content. Cytometry *49*, 96-105.

Schnapp, G., Rodi, H.P., Rettig, W.J., Schnapp, A., and Damm, K. (1998). One-step affinity purification protocol for human telomerase. Nucleic Acids Res *26*, 3311-3313.

Seluanov, A., Chen, Z., Hine, C., Sasahara, T.H., Ribeiro, A.A., Catania, K.C., Presgraves, D.C., and Gorbunova, V. (2007). Telomerase activity coevolves with body mass not lifespan. Aging Cell *6*, 45-52.

Serra, V., Grune, T., Sitte, N., Saretzki, G., and von Zglinicki, T. (2000). Telomere length as a marker of oxidative stress in primary human fibroblast cultures. Ann N Y Acad Sci *908*, 327-330.

Sfeir, A., Kabir, S., van Overbeek, M., Celli, G.B., and de Lange, T. (2010). Loss of Rap1 induces telomere recombination in the absence of NHEJ or a DNA damage signal. Science *327*, 1657-1661.

Sfeir, A., Kosiyatrakul, S.T., Hockemeyer, D., MacRae, S.L., Karlseder, J., Schildkraut, C.L., and de Lange, T. (2009). Mammalian telomeres resemble fragile sites and require TRF1 for efficient replication. Cell *138*, 90-103.

Sfeir, A.J., Chai, W., Shay, J.W., and Wright, W.E. (2005). Telomere-end processing the terminal nucleotides of human chromosomes. Mol Cell *18*, 131-138.

Shammas, M.A., Koley, H., Bertheau, R.C., Neri, P., Fulciniti, M., Tassone, P., Blotta, S., Protopopov, A., Mitsiades, C., Batchu, R.B., *et al.* (2008a). Telomerase inhibitor GRN163L inhibits myeloma cell growth in vitro and in vivo. Leukemia *22*, 1410-1418.

Shammas, M.A., Qazi, A., Batchu, R.B., Bertheau, R.C., Wong, J.Y., Rao, M.Y., Prasad, M., Chanda, D., Ponnazhagan, S., Anderson, K.C., *et al.* (2008b). Telomere maintenance in laser capture microdissection-purified Barrett's adenocarcinoma cells and effect of telomerase inhibition in vivo. Clin Cancer Res *14*, 4971-4980.

Shampay, J., Szostak, J.W., and Blackburn, E.H. (1984). DNA sequences of telomeres maintained in yeast. Nature *310*, 154-157.

Shay, J.W., and Keith, W.N. (2008). Targeting telomerase for cancer therapeutics. Br J Cancer *98*, 677-683.

Shay, J.W., Pereira-Smith, O.M., and Wright, W.E. (1991). A role for both RB and p53 in the regulation of human cellular senescence. Exp Cell Res *196*, 33-39.

Shay, J.W., and Wright, W.E. (1996). Telomerase activity in human cancer. Curr Opin Oncol *8*, 66-71.

Shay, J.W., and Wright, W.E. (2000). Hayflick, his limit, and cellular ageing. Nat Rev Mol Cell Biol *1*, 72-76.

Shay, J.W., and Wright, W.E. (2002). Telomerase: a target for cancer therapeutics. Cancer Cell *2*, 257-265.

Shay, J.W., and Wright, W.E. (2005). Mechanism-based combination telomerase inhibition therapy. Cancer Cell *7*, 1-2.

Shay, J.W., and Wright, W.E. (2006). Telomerase therapeutics for cancer: challenges and new directions. Nat Rev Drug Discov *5*, 577-584.

Shay, J.W., and Wright, W.E. (2007). Hallmarks of telomeres in ageing research. J Pathol *211*, 114-123.

Shay, J.W., Wright, W.E., Brasiskyte, D., and Van der Haegen, B.A. (1993). E6 of human papillomavirus type 16 can overcome the M1 stage of immortalization in human mammary epithelial cells but not in human fibroblasts. Oncogene *8*, 1407-1413.

Shechter, D., Costanzo, V., and Gautier, J. (2004). Regulation of DNA replication by ATR: signaling in response to DNA intermediates. DNA Repair (Amst) *3*, 901-908.

Shervington, A., Lu, C., Patel, R., and Shervington, L. (2009). Telomerase downregulation in cancer brain stem cell. Mol Cell Biochem *331*, 153-159.

Shippen-Lentz, D., and Blackburn, E.H. (1989). Telomere terminal transferase activity from Euplotes crassus adds large numbers of TTTTGGGG repeats onto telomeric primers. Mol Cell Biol *9*, 2761-2764.

Shore, D., and Bianchi, A. (2009). Telomere length regulation: coupling DNA end processing to feedback regulation of telomerase. EMBO J *28*, 2309-2322.

Silverman, J., Takai, H., Buonomo, S.B., Eisenhaber, F., and de Lange, T. (2004). Human Rif1, ortholog of a yeast telomeric protein, is regulated by ATM and 53BP1 and functions in the S-phase checkpoint. Genes Dev *18*, 2108-2119.

Slagboom, P.E., Droog, S., and Boomsma, D.I. (1994). Genetic determination of telomere size in humans: a twin study of three age groups. Am J Hum Genet *55*, 876-882.

Slijepcevic, P. (2001). Telomere length measurement by Q-FISH. Methods Cell Sci *23*, 17-22.

Smith, S., and de Lange, T. (2000). Tankyrase promotes telomere elongation in human cells. Curr Biol *10*, 1299-1302.

Smogorzewska, A., and de Lange, T. (2004). Regulation of telomerase by telomeric proteins. Annu Rev Biochem *73*, 177-208.

Smogorzewska, A., Karlseder, J., Holtgreve-Grez, H., Jauch, A., and de Lange, T. (2002). DNA ligase IV-dependent NHEJ of deprotected mammalian telomeres in G1 and G2. Curr Biol *12*, 1635-1644.

Smogorzewska, A., van Steensel, B., Bianchi, A., Oelmann, S., Schaefer, M.R., Schnapp, G., and de Lange, T. (2000). Control of human telomere length by TRF1 and TRF2. Mol Cell Biol *20*, 1659-1668.

Sonoda, E., Sasaki, M.S., Morrison, C., Yamaguchi-Iwai, Y., Takata, M., and Takeda, S. (1999). Sister chromatid exchanges are mediated by homologous recombination in vertebrate cells. Mol Cell Biol *19*, 5166-5169.

Southern, E.M. (1975). Detection of specific sequences among DNA fragments separated by gel electrophoresis. J Mol Biol *98*, 503-517.

Stansel, R.M., de Lange, T., and Griffith, J.D. (2001). T-loop assembly in vitro involves binding of TRF2 near the 3' telomeric overhang. EMBO J *20*, 5532-5540.

Stansel, R.M., Subramanian, D., and Griffith, J.D. (2002). p53 binds telomeric single strand overhangs and t-loop junctions in vitro. J Biol Chem *277*, 11625-11628.

Starling, J.A., Maule, J., Hastie, N.D., and Allshire, R.C. (1990). Extensive telomere repeat arrays in mouse are hypervariable. Nucleic Acids Res *18*, 6881-6888.

Steinert, S., Shay, J.W., and Wright, W.E. (2000). Transient expression of human telomerase extends the life span of normal human fibroblasts. Biochem Biophys Res Commun *273*, 1095-1098.

Steinert, S., Shay, J.W., and Wright, W.E. (2004). Modification of subtelomeric DNA. Mol Cell Biol *24*, 4571-4580.

Szostak, J.W., and Blackburn, E.H. (1982). Cloning yeast telomeres on linear plasmid vectors. Cell *29*, 245-255.

Taggart, A.K., Teng, S.C., and Zakian, V.A. (2002). Est1p as a cell cycle-regulated activator of telomere-bound telomerase. Science *297*, 1023-1026.

Tahara, H., Kusunoki, M., Yamanaka, Y., Matsumura, S., and Ide, T. (2005). G-tail telomere HPA: simple measurement of human single-stranded telomeric overhangs. Nat Methods *2*, 829-831.

Takai, H., Smogorzewska, A., and de Lange, T. (2003). DNA damage foci at dysfunctional telomeres. Curr Biol *13*, 1549-1556.

Takai, K.K., Hooper, S., Blackwood, S., Gandhi, R., and de Lange, T. (2010). In vivo stoichiometry of shelterin components. J Biol Chem *285*, 1457-1467.

Takakura, M., Kyo, S., Kanaya, T., Tanaka, M., and Inoue, M. (1998). Expression of human telomerase subunits and correlation with telomerase activity in cervical cancer. Cancer Res *58*, 1558-1561.

Tang, J., Kan, Z.Y., Yao, Y., Wang, Q., Hao, Y.H., and Tan, Z. (2008). G-quadruplex preferentially forms at the very 3' end of vertebrate telomeric DNA. Nucleic Acids Res *36*, 1200-1208.

Teixeira, M.T., Arneric, M., Sperisen, P., and Lingner, J. (2004). Telomere length homeostasis is achieved via a switch between telomerase- extendible and -nonextendible states. Cell *117*, 323-335.

Ten Hagen, K.G., Gilbert, D.M., Willard, H.F., and Cohen, S.N. (1990). Replication timing of DNA sequences associated with human centromeres and telomeres. Mol Cell Biol *10*, 6348-6355.

Theimer, C.A., and Feigon, J. (2006). Structure and function of telomerase RNA. Curr Opin Struct Biol *16*, 307-318.

Therkelsen, A.J., Nielsen, A., Koch, J., Hindkjaer, J., and Kolvraa, S. (1995). Staining of human telomeres with primed in situ labeling (PRINS). Cytogenet Cell Genet *68*, 115-118.

Tomaska, L., Makhov, A.M., Griffith, J.D., and Nosek, J. (2002). t-Loops in yeast mitochondria. Mitochondrion *1*, 455-459.

Tomlinson, R.L., Ziegler, T.D., Supakorndej, T., Terns, R.M., and Terns, M.P. (2006). Cell cycle-regulated trafficking of human telomerase to telomeres. Mol Biol Cell *17*, 955-965.

Tsakiri, K.D., Cronkhite, J.T., Kuan, P.J., Xing, C., Raghu, G., Weissler, J.C., Rosenblatt, R.L., Shay, J.W., and Garcia, C.K. (2007). Adult-onset pulmonary fibrosis caused by mutations in telomerase. Proc Natl Acad Sci U S A *104*, 7552-7557.

Ulbert, S., Eide, L., Seeberg, E., and Borst, P. (2004). Base J, found in nuclear DNA of Trypanosoma brucei, is not a target for DNA glycosylases. DNA Repair (Amst) *3*, 145-154.

van Steensel, B., and de Lange, T. (1997). Control of telomere length by the human telomeric protein TRF1. Nature *385*, 740-743.

van Steensel, B., Smogorzewska, A., and de Lange, T. (1998). TRF2 protects human telomeres from end-to-end fusions. Cell *92*, 401-413.

Varela, E., and Blasco, M.A. (2010). 2009 nobel prize in physiology or medicine: telomeres and telomerase. Oncogene *29*, 1561-1565.

Vaziri, H., Dragowska, W., Allsopp, R.C., Thomas, T.E., Harley, C.B., and Lansdorp, P.M. (1994). Evidence for a mitotic clock in human hematopoietic stem cells: loss of telomeric DNA with age. Proc Natl Acad Sci U S A *91*, 9857-9860.

Veldman, T., Etheridge, K.T., and Counter, C.M. (2004). Loss of hPot1 function leads to telomere instability and a cut-like phenotype. Curr Biol *14*, 2264-2270.

Verdun, R.E., Crabbe, L., Haggblom, C., and Karlseder, J. (2005). Functional human telomeres are recognized as DNA damage in G2 of the cell cycle. Mol Cell *20*, 551-561.

von Zglinicki, T. (2000). Role of oxidative stress in telomere length regulation and replicative senescence. Ann N Y Acad Sci *908*, 99-110.

von Zglinicki, T. (2002). Oxidative stress shortens telomeres. Trends Biochem Sci *27*, 339-344.

von Zglinicki, T., Pilger, R., and Sitte, N. (2000). Accumulation of single-strand breaks is the major cause of telomere shortening in human fibroblasts. Free Radic Biol Med *28*, 64-74.

von Zglinicki, T., Saretzki, G., Docke, W., and Lotze, C. (1995). Mild hyperoxia shortens telomeres and inhibits proliferation of fibroblasts: a model for senescence? Exp Cell Res *220*, 186-193.

Vulliamy, T.J., Knight, S.W., Mason, P.J., and Dokal, I. (2001). Very short telomeres in the peripheral blood of patients with X-linked and autosomal dyskeratosis congenita. Blood Cells Mol Dis *27*, 353-357.

Wang, E.S., Wu, K., Chin, A.C., Chen-Kiang, S., Pongracz, K., Gryaznov, S., and Moore, M.A. (2004a). Telomerase inhibition with an oligonucleotide telomerase template antagonist: in vitro and in vivo studies in multiple myeloma and lymphoma. Blood *103*, 258-266.

Wang, F., Podell, E.R., Zaug, A.J., Yang, Y., Baciu, P., Cech, T.R., and Lei, M. (2007). The POT1-TPP1 telomere complex is a telomerase processivity factor. Nature *445*, 506-510.

Wang, R.C., Smogorzewska, A., and de Lange, T. (2004b). Homologous recombination generates T-loop-sized deletions at human telomeres. Cell *119*, 355-368.

Watson, J.D. (1972). Origin of concatemeric T7 DNA. Nat New Biol *239*, 197-201.

Watson, J.D., and Crick, F.H. (1953). The structure of DNA. Cold Spring Harb Symp Quant Biol *18*, 123-131.

Wei, C., and Price, C.M. (2004). Cell cycle localization, dimerization, and binding domain architecture of the telomere protein cPot1. Mol Cell Biol *24*, 2091-2102.

Weinrich, S.L., Pruzan, R., Ma, L., Ouellette, M., Tesmer, V.M., Holt, S.E., Bodnar, A.G., Lichtsteiner, S., Kim, N.W., Trager, J.B., *et al.* (1997). Reconstitution of human telomerase with the template RNA component hTR and the catalytic protein subunit hTRT. Nat Genet *17*, 498-502.

Wellinger, R.J., Ethier, K., Labrecque, P., and Zakian, V.A. (1996). Evidence for a new step in telomere maintenance. Cell *85*, 423-433.

Wellinger, R.J., Wolf, A.J., and Zakian, V.A. (1993a). Origin activation and formation of single-strand TG1-3 tails occur sequentially in late S phase on a yeast linear plasmid. Mol Cell Biol *13*, 4057-4065.

Wellinger, R.J., Wolf, A.J., and Zakian, V.A. (1993b). Saccharomyces telomeres acquire single-strand TG1-3 tails late in S phase. Cell *72*, 51-60.

White, L.K., Wright, W.E., and Shay, J.W. (2001). Telomerase inhibitors. Trends Biotechnol *19*, 114-120.

Williams, E.S., Stap, J., Essers, J., Ponnaiya, B., Luijsterburg, M.S., Krawczyk, P.M., Ullrich, R.L., Aten, J.A., and Bailey, S.M. (2007). DNA double-strand breaks are not sufficient to initiate recruitment of TRF2. Nat Genet *39*, 696-698; author reply 698-699.

Wright, W.E., and Hayflick, L. (1975). Nuclear control of cellular aging demonstrated by hybridization of anucleate and whole cultured normal human fibroblasts. Exp Cell Res *96*, 113-121.

Wright, W.E., Pereira-Smith, O.M., and Shay, J.W. (1989). Reversible cellular senescence: implications for immortalization of normal human diploid fibroblasts. Mol Cell Biol *9*, 3088-3092.

Wright, W.E., Piatyszek, M.A., Rainey, W.E., Byrd, W., and Shay, J.W. (1996). Telomerase activity in human germline and embryonic tissues and cells. Dev Genet *18*, 173-179.

Wright, W.E., and Shay, J.W. (1992). The two-stage mechanism controlling cellular senescence and immortalization. Exp Gerontol *27*, 383-389.

Wright, W.E., and Shay, J.W. (2005). Telomere biology in aging and cancer. J Am Geriatr Soc *53*, S292-294.

Wright, W.E., Tesmer, V.M., Huffman, K.E., Levene, S.D., and Shay, J.W. (1997). Normal human chromosomes have long G-rich telomeric overhangs at one end. Genes Dev *11*, 2801-2809.

Wright, W.E., Tesmer, V.M., Liao, M.L., and Shay, J.W. (1999). Normal human telomeres are not late replicating. Exp Cell Res *251*, 492-499.

Wu, L., Multani, A.S., He, H., Cosme-Blanco, W., Deng, Y., Deng, J.M., Bachilo, O., Pathak, S., Tahara, H., Bailey, S.M., *et al.* (2006). Pot1 deficiency initiates DNA damage checkpoint activation and aberrant homologous recombination at telomeres. Cell *126*, 49-62.

Wu, X., Amos, C.I., Zhu, Y., Zhao, H., Grossman, B.H., Shay, J.W., Luo, S., Hong, W.K., and Spitz, M.R. (2003). Telomere dysfunction: a potential cancer predisposition factor. J Natl Cancer Inst *95*, 1211-1218.

Xin, H., Liu, D., Wan, M., Safari, A., Kim, H., Sun, W., O'Connor, M.S., and Songyang, Z. (2007). TPP1 is a homologue of ciliate TEBP-beta and interacts with POT1 to recruit telomerase. Nature *445*, 559-562.

Xu, L., and Blackburn, E.H. (2007). Human cancer cells harbor T-stumps, a distinct class of extremely short telomeres. Mol Cell *28*, 315-327.

Xu, Y., Sato, H., Shinohara, K., Komiyama, M., and Sugiyama, H. (2007). T-loop formation by human telomeric G-quadruplex. Nucleic Acids Symp Ser (Oxf), 243-244.

Yamaguchi, H., Baerlocher, G.M., Lansdorp, P.M., Chanock, S.J., Nunez, O., Sloand, E., and Young, N.S. (2003). Mutations of the human telomerase RNA gene (TERC) in aplastic anemia and myelodysplastic syndrome. Blood *102*, 916-918.

Yamaguchi, H., Calado, R.T., Ly, H., Kajigaya, S., Baerlocher, G.M., Chanock, S.J., Lansdorp, P.M., and Young, N.S. (2005). Mutations in TERT, the gene for telomerase reverse transcriptase, in aplastic anemia. N Engl J Med *352*, 1413-1424.

Yang, Q., Zheng, Y.L., and Harris, C.C. (2005). POT1 and TRF2 cooperate to maintain telomeric integrity. Mol Cell Biol *25*, 1070-1080.

Ye, J.Z., and de Lange, T. (2004). TIN2 is a tankyrase 1 PARP modulator in the TRF1 telomere length control complex. Nat Genet *36*, 618-623.

Ye, J.Z., Donigian, J.R., van Overbeek, M., Loayza, D., Luo, Y., Krutchinsky, A.N., Chait, B.T., and de Lange, T. (2004a). TIN2 binds TRF1 and TRF2 simultaneously and stabilizes the TRF2 complex on telomeres. J Biol Chem *279*, 47264-47271.

Ye, J.Z., Hockemeyer, D., Krutchinsky, A.N., Loayza, D., Hooper, S.M., Chait, B.T., and de Lange, T. (2004b). POT1-interacting protein PIP1: a telomere length regulator that recruits POT1 to the TIN2/TRF1 complex. Genes Dev *18*, 1649-1654.

Yeoman, J.A., Orte, A., Ashbridge, B., Klenerman, D., and Balasubramanian, S. (2010). RNA conformation in catalytically active human telomerase. J Am Chem Soc *132*, 2852-2853.

Yu, G.L., Bradley, J.D., Attardi, L.D., and Blackburn, E.H. (1990). In vivo alteration of telomere sequences and senescence caused by mutated Tetrahymena telomerase RNAs. Nature *344*, 126-132.

Zahler, A.M., and Prescott, D.M. (1988). Telomere terminal transferase activity in the hypotrichous ciliate Oxytricha nova and a model for replication of the ends of linear DNA molecules. Nucleic Acids Res *16*, 6953-6972.

Zaug, A.J., Podell, E.R., Nandakumar, J., and Cech, T.R. (2010). Functional interaction between telomere protein TPP1 and telomerase. Genes Dev *24*, 613-622.

Zeng, Z., Wang, W., Yang, Y., Chen, Y., Yang, X., Diehl, J.A., Liu, X., and Lei, M. (2010). Structural basis of selective ubiquitination of TRF1 by SCFFbx4. Dev Cell *18*, 214-225.

Zhao, Y., Abreu, E.B., Kim, J., Stadler, G., Terns, M.P., Terns, R.M., Shay, J.W., and Wright, W.E. (2011). Processive and Distributive Extension of Human Telomeres by Telomerase Under Homeostatic
and Non-equilibrium Conditions. Molecular Cell *In press*.

Zhao, Y., Hoshiyama, H., Shay, J.W., and Wright, W.E. (2008). Quantitative telomeric overhang determination using a double-strand specific nuclease. Nucleic Acids Res *36*, e14.

Zhao, Y., Sfeir, A.J., Zou, Y., Buseman, C.M., Chow, T.T., Shay, J.W., and Wright, W.E. (2009). Telomere extension occurs at most chromosome ends and is uncoupled from fill-in in human cancer cells. Cell *138*, 463-475.

Zhong, Z., Shiue, L., Kaplan, S., and de Lange, T. (1992). A mammalian factor that binds telomeric TTAGGG repeats in vitro. Mol Cell Biol *12*, 4834-4843.

Zhu, L., Hathcock, K.S., Hande, P., Lansdorp, P.M., Seldin, M.F., and Hodes, R.J. (1998). Telomere length regulation in mice is linked to a novel chromosome locus. Proc Natl Acad Sci U S A *95*, 8648-8653.

Zou, Y., Gryaznov, S.M., Shay, J.W., Wright, W.E., and Cornforth, M.N. (2004a). Asynchronous replication timing of telomeres at opposite arms of mammalian chromosomes. Proc Natl Acad Sci U S A *101*, 12928-12933.

Zou, Y., Sfeir, A., Gryaznov, S.M., Shay, J.W., and Wright, W.E. (2004b). Does a sentinel or a subset of short telomeres determine replicative senescence? Mol Biol Cell *15*, 3709-3718.